5-2008

Establishment of a Structure-Activity Relationship in Heterogeneous Titanosilicate Catalysts for Olefin Epoxidation via a Building Block Method

Geoffrey T. Eldridge
University of Tennessee - Knoxville

To the Graduate Council:

I am submitting herewith a dissertation written by Geoffrey T. Eldridge entitled "Establishment of a Structure-Activity Relationship in Heterogeneous Titanosilicate Catalysts for Olefin Epoxidation via a Building Block Method." I have examined the final electronic copy of this dissertation for form and content and recommend that it be accepted in partial fulfillment of the requirements for the degree of Doctor of Philosophy, with a major in Chemistry.

Craig E. Barnes, Major Professor

We have read this dissertation and recommend its acceptance:

Jamie L. Adcock, Edmund Perfect, Bin Zhao

Accepted for the Council:

Carolyn R. Hodges

Vice Provost and Dean of the Graduate School

(Original signatures are on file with official student records.)

To the Graduate Council:

I am submitting herewith a dissertation written by Geoffrey Thomas Eldridge entitled “Establishment of a Structure-Activity Relationship in Heterogeneous Titanosilicate Catalysts for Olefin Epoxidation via a Building Block Method.” I have examined the final electronic copy of this dissertation for form and content and, recommend that it be accepted in partial fulfillment of the requirements for the degree of Doctor of Philosophy, with a major in Chemistry.

Craig E. Barnes

Major Professor

We have read this dissertation

And recommend its acceptance:

Jamie L. Adcock

Edmund Perfect

Bin Zhao

Accepted for the Council:

Carolyn R. Hodges

Vice Provost and Dean of the

Graduate School

(Original signatures are on file with official student records.)

Establishment of a Structure-Activity Relationship in Heterogeneous Titanosilicate Catalysts for Olefin Epoxidation via a Building Block Method

A Dissertation

Presented for the

Doctor of Philosophy

Degree

The University of Tennessee, Knoxville

Geoffrey Thomas Eldridge

May 2008

Dedication

For my daughter, Leanna

In loving memory of my uncle, Bradley Alexander Hodge

March 26, 1951 – March 12, 2008

a Green Beret

Abstract

The non-aqueous building block (NABB) method is a synthetic method that has the goal of producing atomically dispersed, well-defined, single-site heterogeneous catalysts. The active sites of these catalysts are able to be structured on the nanometer scale using the process of *sequential additions*. The method is designed in such a manner that it should be able to produce a series of catalysts each with a unique, well-defined, single active site. This series of catalysts can then be used to elucidate the structure-activity relationship for the active site in a particular chemical reaction.

In this dissertation a new building block, butyltin cube, is developed for the NABB method. The preparation of the butyltin cube uses reagents that are less toxic and costly than the reagents used to prepare the previous methyltin cube starting material. A series of titanium NABB materials containing different active sites was prepared. The local structure around the active site of these materials was then probed using quantitative NMR, FT-IR, Raman, XANES, and EXAFS. The activity and selectivity of these materials in the epoxidation of cyclohexene with *tert*-butylhydroperoxide was then measured. The information was then used to propose a structure-activity relationship for olefin epoxidation and comparisons were made with structure-activity relationships noted in the literature.

Table of Contents

List of Tables

List of Figures

Chapter 1. Introduction

Importance of Catalysts

Catalysts are “mandatory in the manufacture of a vast array of chemicals and fuels, and as such contribute significantly to our economy” and high standard of living.[1,2] This concisely states the fact that catalysts currently touch nearly every aspect of modern life. They are used in the production of gasoline, diesel, and kerosene from petroleum, as well as important chemical feedstocks such as ethylene oxide, propylene, and styrene.[3] Many of the plastics that now are ubiquitous in consumer products owe their existence to catalytic processes. These plastics are found in product packaging, drink bottles, electronic devices, and even car bumpers.

Catalysis also makes important contributions to agriculture. Eighty-five percent of the 98 million tons of nitrogen fixed by the Haber-Bosch process annually are used in agricultural fertilizer, and one-half of all the nitrogen consumed in agriculture today is provided by this important catalytic process.[4,5] Most of the world’s population depends upon nitrogen obtained from the Haber-Bosch process to produce at least some of their sustenance, and this dependence is projected to increase over time.[4]

Environmental remediation is another field heavily impacted by catalysis. The three-way catalysts used to reduce automobile emissions may be the most visible catalysts used to protect our environment.[1] These catalysts are used to reduce the amount of nitrogen oxides, carbon monoxide, and hydrocarbons

released into the lower atmosphere by vehicles. Recently, catalysts have also been commercialized for the deep oxidation of volatile organic compounds, dioxin destruction, and carbon monoxide removal.[3]

With a 1999 U.S. market that approached $3 billion in sales, the production of catalysts is a significant business.[2] A recent publication indicates that 130 new catalytic technologies were commercialized in the 1990s in the United States alone, and that number includes only catalysts the companies surveyed were willing to publicize.[3] The ongoing development of catalysts reflects the need for better, more efficient catalysts.

Theory of Catalysis and Applicable Terminology

A catalyst can be defined as a substance that increases the rate of a chemical reaction while not being consumed in the reaction, and without modifying the overall standard Gibbs energy change in the reaction (Figure 1-1).[6] When used on an industrial scale catalysts save significant amounts of energy. This results from the lowering of the activation energy of the reaction relative to that of the uncatalyzed reaction.

A second property of catalysts is their ability to influence what products are produced in a reaction if they selectively influence the rate of formation of one product over other products. This selectivity can extend to stereochemical reactions. Catalysts have been used successfully to preferentially produce certain enantiomers of compounds.[7,8]

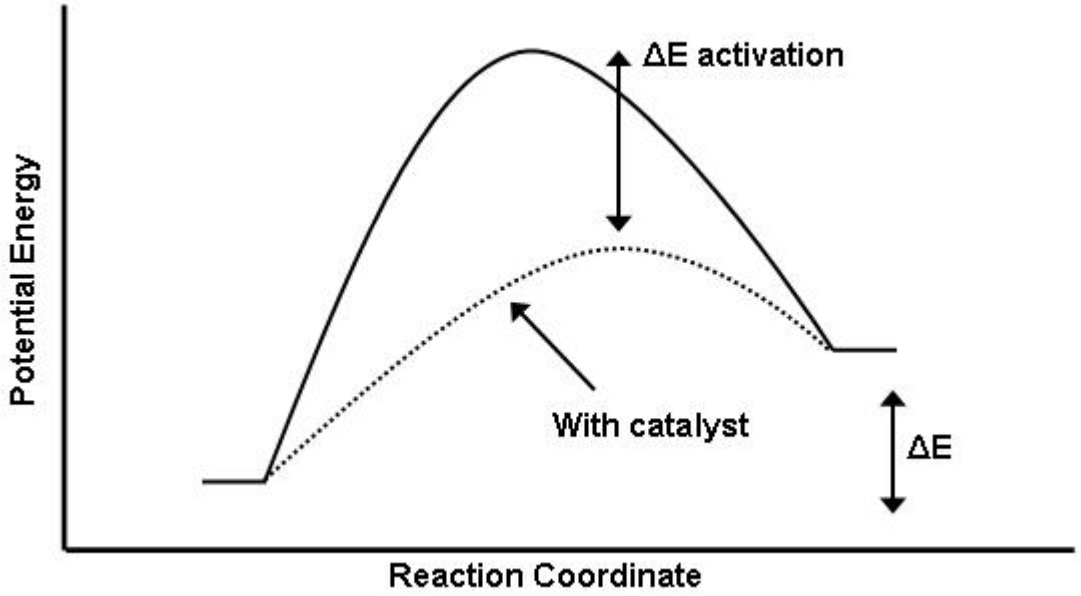

Figure 1-1. Reaction coordinate diagram illustrating the effect of a catalyst upon a chemical reaction.

Selectivity and Activity

The effect of a catalyst is usually described in terms of selectivity and activity. The term *selectivity* describes the amount of a specific reagent converted to a desired product when more than one product is possible.[9] To prevent the activity of the catalyst from affecting selectivity calculations of the selectivity are based upon the amount of substrate consumed when the reaction is ended, and is calculated as shown in the equation below.

$$\text{Selectivity (\%)} = 100 \times [\text{desired product}]/([\text{reagent}]_0 - [\text{reagent}])$$

Unfortunately, expressing the activity of a catalyst is not as straightforward as expressing the selectivity. Quantitative comparison of catalysts between

different research facilities is difficult as reactant concentrations, temperature, and even the type of reactor used vary widely.[10,11] While activity can be expressed in raw percent conversion, turnover frequency, TOF, is commonly used in academic descriptions of catalysts. Turnover frequency is defined as the amount of product (frequently moles) produced per mole of catalyst metal per unit time, as expressed in the equation below.[10]

$$TOF = [product]/([catalyst] \times time)$$

However, the presentation of turnover frequency at a single time does not provide information about the stability of a catalyst over time.[10] Turnover number, TON, is the amount of moles of product produced per mole of catalyst metal.[10] When presented as a function of time, a series of turnover numbers provide more revealing information about the stability of a catalyst through the course of a reaction. For example, as long as reactant concentrations are sufficient to maintain a constant rate in a batch-type reaction, the slope of a plot of turnover number versus time will be equal to one if the rate of reaction remains constant.

Finally, an important industrial measurement describing catalysts is productivity. The productivity relates the mass of catalyst to the mass of product produced as shown in the equation below.[10] Productivity aids the comparison between the cost of a catalyst and the value of the product it yields.

$$Productivity = (mass\ of\ product)/(mass\ of\ catalyst)$$

The Active Site

In a simple sense the active site of a catalyst is the atom or ensemble of atoms where the transformation from reactant to product takes place. The breaking and formation of bonds takes place at the active site, and as such the nature of an active site may vary for different chemical processes and products.[12] Information describing the active site, its identity, should describe the properties of the site that influence its reactivity and selectivity in a chemical reaction. The oxidation state of the metal, its coordination number, the coordination geometry, and the electronic and steric nature of its ligands are a number of important characteristics of the active site of a catalyst.[13]

In order to reveal the most information about what is happening in a given reaction the active site should be a description of the activated complex that forms during the transformation of the substrate to product. However, the transient nature of these species can make them difficult to characterize. Furthermore, since one material may be used to catalyze many reactions or even multiple classes of reactions it makes sense to describe the active site in terms of its structure before use in a reaction. This structure is commonly referred to as the active site precursor or active precursor. Thus it can be said that chemists often loosely distinguish between the active site and the active site precursor.[14] In this dissertation references to the active site will actually describe the active precursor to the catalyst. Of particular interest in describing the active precursor

will be the oxidation state of the metal, its coordination number and geometry, and the number of bonds from the metal to the heterogeneous support.

Description and Importance of Single-Site Catalysts

"The atomic architecture of a homogeneous catalyst is usually very well defined, and in many cases precisely known."[13] When a pure active precursor is dissolved in solution, it is generally assumed that all the resulting metal containing species are identical, and therefore react identically. Thus, homogeneous catalysts are frequently described as **single-site** catalysts. The essence of the single-site catalyst is that each active site is identical. This implies that each active site produces product at the same rate and with the same selectivity. The low product selectivity of some traditional heterogeneous catalysts has been attributed to presence of multiple sites in those catalysts. Figure 1-2 shows the multiple sites formed in a traditionally synthesized gold on titania catalyst. The synthesis of single-site catalysts is generally considered to be a critical factor for high product selectivity, and is a current challenge in the science of heterogeneous catalysts.

Advantages of Heterogeneous Catalysts

The terms homogeneous and heterogeneous refer to two families of catalysts based upon the phase of the catalyst as compared to the phase in which the reactants and products exist. Homogeneous catalysts are in the same phase as the solvents and substrates of the reactions which they catalyze. On the other hand, heterogeneous catalysts are in a phase other than that of the

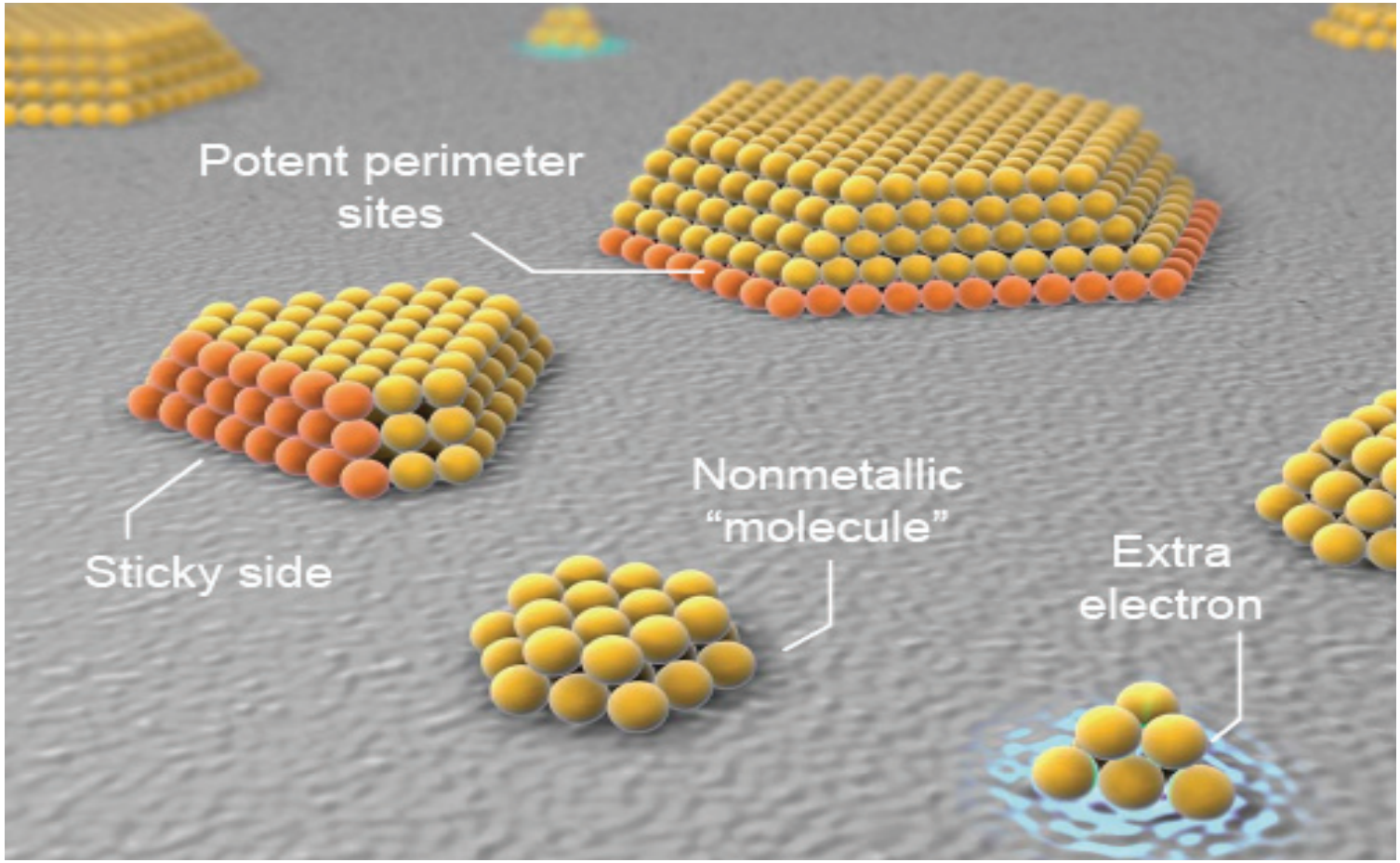

Figure 1-2. Depiction of the various sites possible when gold is deposited on titania. From Cho, Science, 299:1684 (3/14/2003). Illustration: Cameron Slayden. Reprinted with permission from AAAS.

reactions which they catalyze. Both fields of catalysis share many of the same goals and challenges such as: 1) understanding the reaction mechanism, 2) knowing what the active site is and characterizing it, 3) determining how the electronic and steric properties of the active site impact the activity, and 4) using the information above to optimize the activity of the catalyst in terms of rate and selectivity. However, there are also significant differences between the two fields.

The different properties of homogeneous and heterogeneous catalysts lead to trade-offs to be considered when choosing which family of catalysts to employ. Although homogeneous catalysts generally both allow the use of more mild reaction conditions and are more active and selective then their heterogeneous counterparts[15], their stability becomes an issue above 150 °C. Therefore, reactions involving homogeneous catalysts are conducted at lower temperatures.[16,17]

The major drawback to homogeneous catalysts is the difficulty associated with the separation of the catalyst from the product mixture.[18-21] In most cases homogeneous catalysts must be separated from the reaction mixture via distillation[21] or extraction into a different phase.[22] These means of separation prevent the reaction from being continuous, add costs to the process, and expose the catalyst and products to conditions which may cause them to decompose or lose activity.[21] The expense of the catalytically active metals and their associated ligands in a homogeneous catalyst means any loss of catalyst or

decreases in activity can raise process costs significantly. Furthermore, the presence of residual catalyst in the product can negatively impact the desired properties of the product.[23,24]

The properties of heterogeneous catalysts make them an obvious solution to some of these concerns. Heterogeneous catalysts may simply be removed from the reaction mixture via filtration. This makes them amenable to use in fixed-bed reactors or in gas phase reactions which allows the reaction to be carried out continuously.[21,25] Product contamination is also less of an issue when heterogeneous catalysts are used, especially when steps are taken to prevent the leaching of species from the catalyst. Finally, the greater thermal stability of heterogeneous catalysts compared to their homogeneous counterparts allows them to be used when "forcing" reaction conditions are required.

Leaching

In order for the benefits of a heterogeneous catalyst to be realized in application it is important that the catalyst remain truly heterogeneous throughout the reaction period. Leaching refers to the desorption of a metal site from a heterogeneous catalyst during the reaction.[26] Should leaching occur, it is possible that the resultant free metal species in solution could contribute to the observed activity of the catalyst. Thus, it is important to confirm that a heterogeneous catalyst retains the same amount of active metal after use.

Major Research Areas in Heterogeneous Catalysis

The many themes of research in heterogeneous catalysis have the underlying goal of producing “next generation”, highly selective heterogeneous catalysts. Ideally, these catalysts will be 100 percent selective and produce the product at rates that equal or exceed their homogeneous counterparts. With the aim of achieving this goal, a great deal of effort has been put into establishing a relationship between the structure of the active site and its catalytic activity. Unfortunately, the techniques that have been used to characterize homogeneous catalysts so well (e.g. NMR spectroscopy and X-ray diffraction) cannot definitively characterize the vast majority of heterogeneous catalysts. Further complicating the matter is the fact that methodologies commonly employed for the synthesis of heterogeneous catalysts frequently yield materials that have multiple types of metal sites.

Within this context, even without rigorous proof of the identity of the active site, the synthesis of nanostructured heterogeneous catalysts has fallen into vogue. Ultimately, nanostructured catalysts will have to be structured on three levels. First, they must be structured on the scale of the active site to maximize rate of reaction and product selectivity of a given reaction. For many catalysts and the work herein, this structuring is on the atomic scale. Second, the dispersion of the active sites must be controlled. This level of structure is likely to be on the nanometer scale. Spatial dispersion of the sites is important in order to keep them from interacting with one another and to prevent aggregation or phase

separation of the catalyst from a support under reaction conditions. Finally, the structural morphology of the catalyst must be controlled in order to maximize reaction rates and catalyst efficiency. Reactions occur at the surface of a heterogeneous catalyst. Producing materials with high surface areas allows for the placement of a high density of active sties at the surface which leads to catalysts with high activity per unit weight. Reaction rates can be increased by facilitating mass transport of reagents to the active site when pore diameters of the material are in the mesopore range (> 2nm). Additionally, product shape selectivity can be influenced by controlling the shape of the pore structure.

Meeting the design requirements for these nanostructured catalysts is still quite challenging. Each part of the design hierarchy is important in the preparation of catalysts if maximum activities are to be obtained. However, the limited knowledge about the relationship between the structure of current heterogeneous catalysts and their activity gives the construction of catalysts containing only one single nanostructured active site preeminent importance. Consequently, we decided to focus on the development of a synthetic method for well-dispersed single-site heterogeneous catalysts that would be generally applicable to the transition metals. The remainder of this chapter describes common synthetic methodologies for silica supported heterogeneous catalysts, and then goes on to introduce the building block method developed by our research.

Traditional Methods of Heterogeneous Catalyst Synthesis

Incipient Wetness and Grafting

One of the earliest and most simple and direct methods for the synthesis of heterogeneous catalysts is the incipient wetness method. This method involves dissolving a metal compound in a solvent (frequently water) and applying an amount of solution equal to the pore volume of a porous support. Capillary action will then draw the solution into the pores. Following evaporation of the solvent, the metal remains within the pores of the support adsorbed on the surface in various manners. A schematic diagram of an incipient wetness material is shown in Figure 1-3.

Grafting catalysts onto the surfaces of a support is procedurally similar to the incipient wetness method, with the significant difference being a lack of emphasis on drawing the metal complex into the pore structure of the support through capillary action. Another significant difference is the use of non-aqueous and aprotic solvents in the grafting technique, which allows the use of moisture sensitive metal compounds. Perhaps the most widely cited use of the grafting technique is the work of Thomas and Maschmeyer wherein titanium was applied to the surface of the mesoporous material MCM-41 (Figure 1-4).[27]

While procedurally simple, the chemistry behind the incipient wetness and grafting techniques is somewhat more complex. The metal sites produced depend upon what metal complex or complexes are formed in solution and their interaction with the surface of the metal oxide support.[28] In the case of silica, the

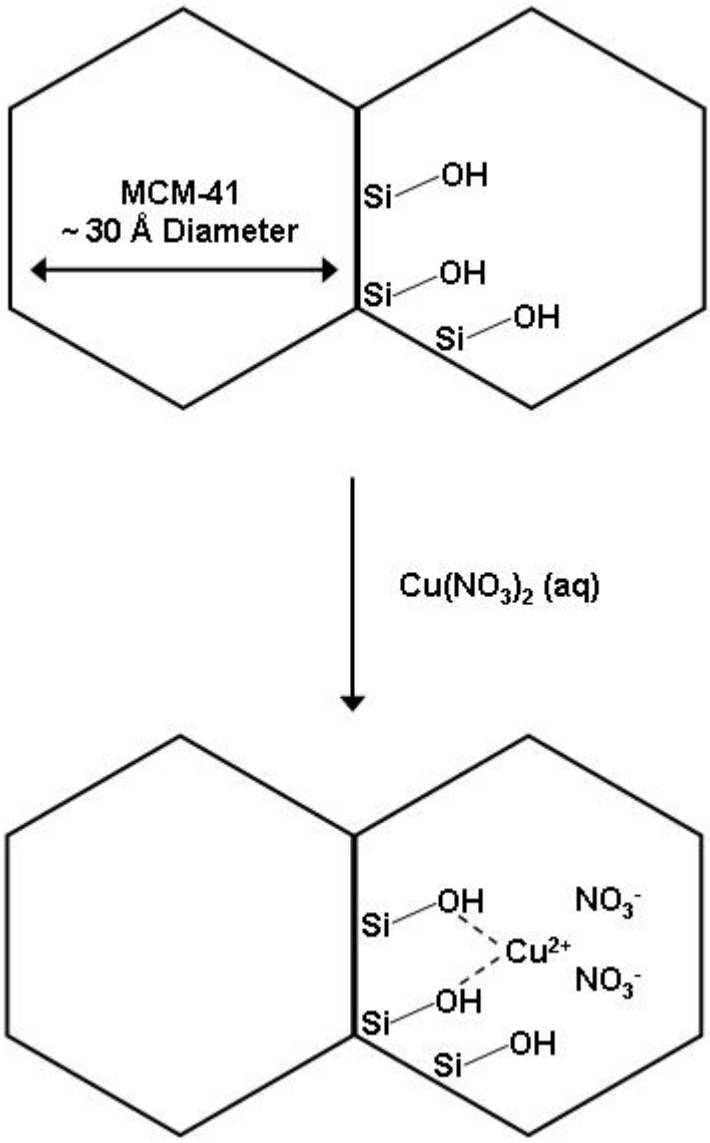

Figure 1-3. Incipient wetness impregnation of $Cu(NO_3)_2$ on the mesoporous silica MCM-41.

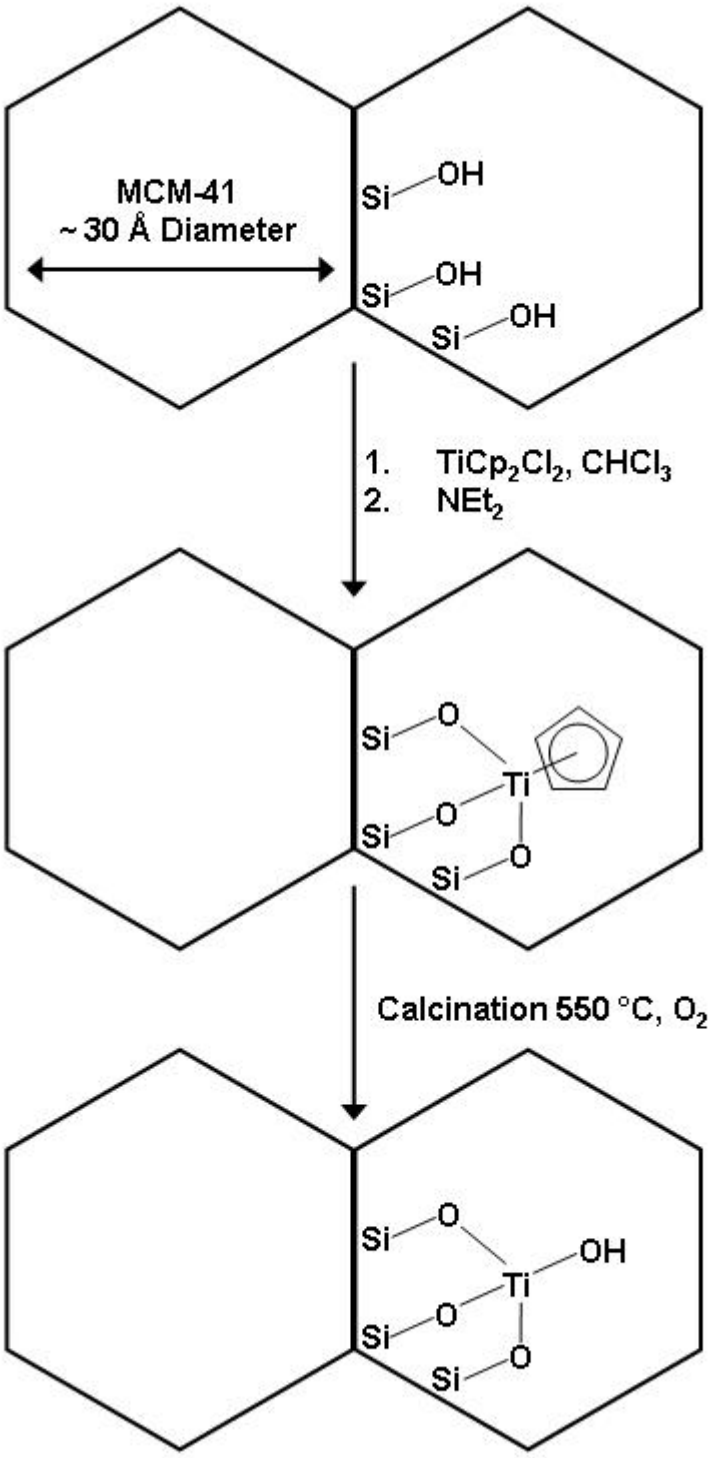

Figure 1-4. Grafting of titanocene dichloride onto the surface of MCM-41.

surface consists of siloxane bridges (≡Si-O-Si≡) and silanol groups (≡Si-OH). The metal becomes anchored to the support when one or more of its ligands is replaced by a hydroxyl group on the surface of the support.

The silanol groups with which the metal complex interact can take three forms: spatially isolated, vicinal, or geminal (Figure 1-5).[29] It is possible that each silanol site could produce a unique metal site when reacted with a metal compound. It has been shown that thermal treatment of silica reduces the number of hydroxyl groups per unit area. While not a guarantee that all of the hydroxyl groups will be spatially isolated, this thermal dehydroxylation of silica has been used to steer syntheses towards the formation of monosiloxy metal sites (≡Si-O-ML_n).[29]

Many studies of the reaction of metal compounds with silica surfaces have depended upon gravimetric analysis to establish the number of bonds between the metal and the support. However, gravimetric analysis is inherently an averaging technique that will provide a precise description of the structure only when it is known that all of the metal compound has reacted with the silica and either: 1) uniformly one bond has formed between the metal compound and the support or; 2) the maximum number, n, bonds has formed between the metal compound MX_n and the support where X = a halide or alkoxide. Likewise, EXAFS, another widely used structural technique suffers as it also is an averaging technique.[30,31]

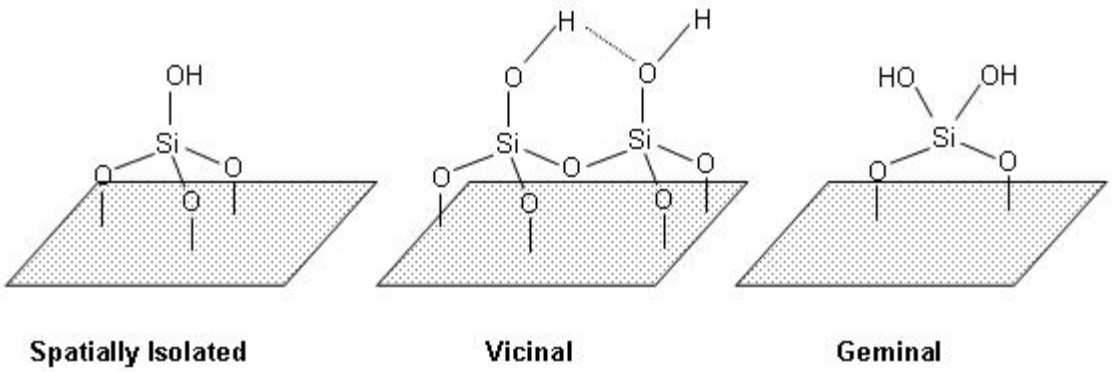

Figure 1-5. The three types of silanol groups on a silica surface.

Perhaps some of the most elegant work in the field of grafting metals onto silica surfaces has been done by Susannah Scott's group. Vanadyl reagents were selected for one study so that ^{51}V magic angle spinning (MAS) NMR could be used to characterize the resulting solids. Unlike EXAFS and gravimetric analyses, NMR can in theory show all species present that are within the detection limit of the technique. Although three different vanadyl species are possible (Figure 1-6), gravimetric analyses showed that regardless of the pretreatment temperature (from 25 to 500 °C) $O{=}VX_3$ (X = O^iPr or Cl) reacted with silica to yield only the ≡Si-O-V(O)X_2 species. In the case of vanadyl chloride this was confirmed by ^{51}V MAS NMR, in which a single resonance attributed to the ≡Si-O-V(O)Cl_2 species was observed at -295 ppm. However, the presence of intense spinning side bands could mask up to a five percent contribution from the theoretically possible (≡Si-O-)$_2$V(O)Cl species.[32] A later EXAFS experiment corroborated the single presence of the ≡Si-O-V(O)Cl_2 species.[33]

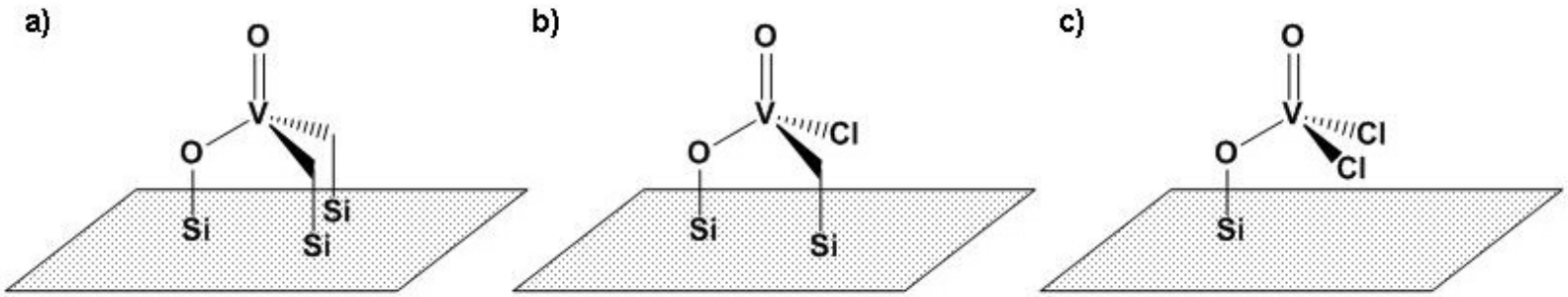

Figure 1-6. Schematic of the three sites possible from the reaction of vanadyl chloride with a silica surface. Of the three only the species depicted in c) is formed.

Scott's work in reacting silica with titanium isopropoxide shows that not all grafting reactions are as straightforward as the vanadyl reactions.[34] Scott found that treating silica samples pretreated at either 200 or 500 °C with identical amounts of titanium isopropoxide, $Ti(O^iPr)_4$, yielded two solids with the same amount of titanium incorporated. This was an unexpected result as silica treated at 500 °C has roughly half the amount of hydroxyl groups available for reaction as silica treated at 200 °C (0.40 mmol OH/g and 0.86 mmol OH/g respectively). Analysis of the by-products showed that propene was evolving in addition to the expected isopropanol. Gravimetric, FT-IR, and ^{13}C MAS NMR analyses led Scott to conclude that dimeric titanium species were being generated, and that the structure of these species was dependent on the temperature at which the silica was treated prior to reaction as shown in the equations and Figure 1-7 below.

Silica-200: $2 \equiv SiOH + 2\ Ti(O^iPr)_4 \rightarrow [(\equiv SiO)Ti(O^iPr)_2]_2(O) + 3\ ^iPrOH + C_3H_6$

Silica-500: $\equiv SiOH + 2\ Ti(O^iPr)_4 \rightarrow (\equiv SiO)Ti_2(O^iPr)_5(O) + 2\ ^iPrOH + C_3H_6$

Scott has shown that the possibility of chemical reactions between precursor molecules cannot be ignored, and that the pretreatment temperature of the silica does not always affect the type of metal site formed in the reaction between a metal alkoxide or chloride and silica.[25,34] Furthermore, the incipient wetness and grafting techniques are incapable of producing fully embedded or "framework" species— that is metal species that have exchanged all their ligands for bonds to the silica surface. The amount of metal incorporated into the catalyst is also limited by the number of hydroxyl groups available on the silica

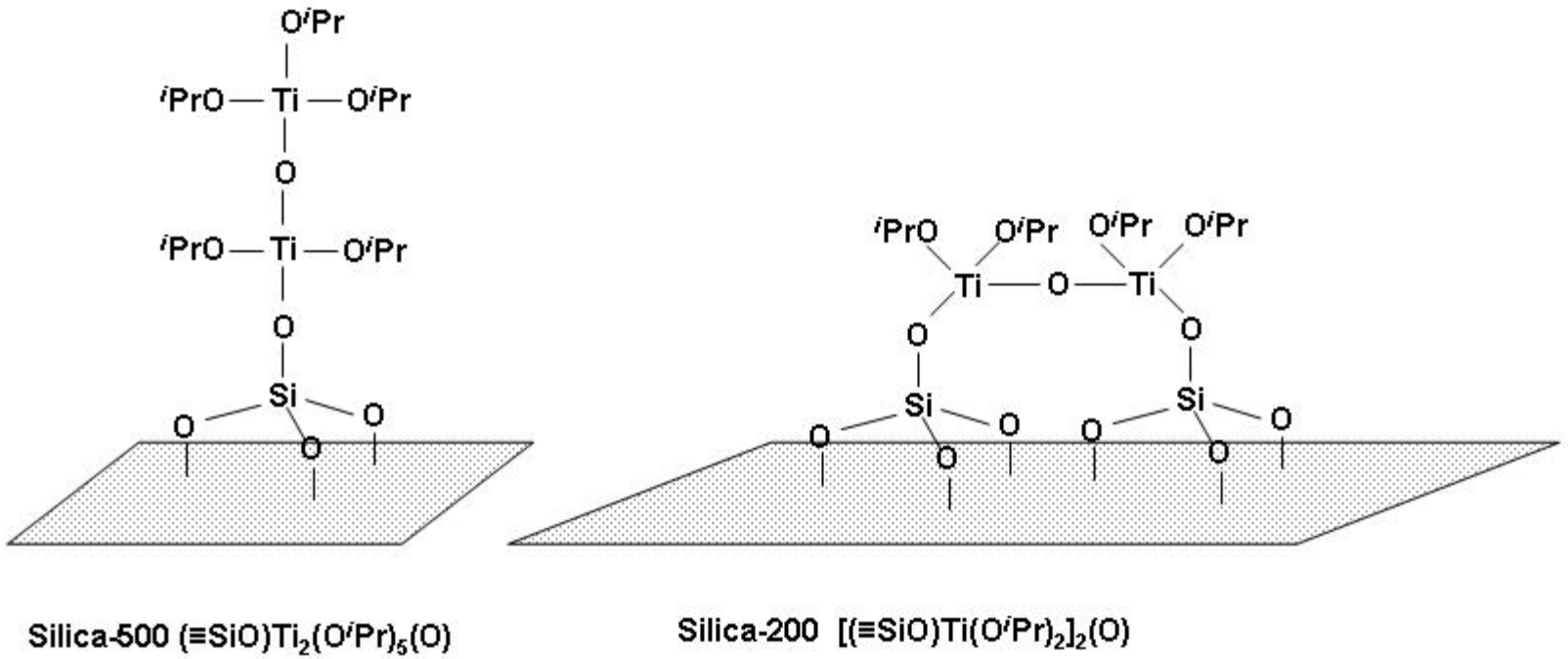

Silica-500 (≡SiO)$Ti_2(O^iPr)_5(O)$

Silica-200 $[(\equiv SiO)Ti(O^iPr)_2]_2(O)$

Figure 1-7. Structures of the titanium dimers on silica proposed by Scott's group.

surface. It is clear that at this point in time the incipient wetness and grafting methods are not generally applicable methods that can produce a single "tailored" site uniformly throughout a heterogeneous catalyst.

Hydrothermally Synthesized Materials

Zeolites are a large family of naturally occurring and synthetic crystalline aluminosilicates that exhibit the important structural characteristics of long range order and microporous (pore diameter ≤ 2nm) pore networks.[35] They are tectoaluminosilicates (each oxygen atom joins together two tetrahedral atoms) comprised of $[SiO_4]^{4-}$ and $[AlO_4]^{5-}$ tetrahedra.[36] A network of interconnected $[SiO_4]^{4-}$ tetrahedra such as quartz, SiO_2, is electrically neutral. The substitution of Al^{3+} for Si^{4+} in the zeolite framework necessitates the inclusion of cations to provide charge balance.[35] Properly only aluminosilicates can be called zeolites,[36] but, purely siliceous[37] materials with zeolitic structures have been prepared extending their application to areas where Lewis or Brønsted acid properties are not desirable. In this section the term zeolite refers both to aluminosilicates and silicates having a crystalline structure with a microporous pore network.

Zeolites are excellent catalysts which are used extensively in the refining of petroleum and the production of fine and specialty chemicals.[38] Their commercial success is in large part due to the continual synthesis or discovery of new zeolites with chemical properties that allow the development of new technologies or improvements in existing synthetic processes.[36] Zeolitic

materials are especially interesting from the standpoint of heterogeneous catalysis as their high surface area and porosity allow a large number of catalytic sites to be incorporated while maintaining site dispersion. This class of materials is an extremely versatile family of catalysts because of their: 1) uniform pore size, high surface area, and high adsorption capacity, 2) thermal, hydrothermal, and chemical stability, 3) adsorption properties which can be varied from hydrophobic to hydrophilic, 4) the intricate pore structure that allows for different types of shape selectivity, and 5) the many chemically interesting main group elements and transition metals that can be incorporated into the structure.[36-38] For example, P, Ge, B, and Zn can be included as major components of the structure, while Ti, Fe, Co, Cr, V, Mg, and Mn can be added at low weight percentages.[36,37]

A typical zeolite synthesis begins with the mixture of silicon and aluminum sources with a cation in a basic solution. The cation may also function as a structure directing agent (SDA) which is often a quaternary amine. Then the aqueous mixture is heated in an autoclave at temperatures between 100 and 250 °C. At first the solids formed in the reactor are amorphous, but as time passes the solids begin to crystallize into zeolites. In accordance with Lowenstein's rule no Al-O-Al linkages should be observed in zeolites.[36] Quaternary amines having C:N ratios between 11 and 16 have been found to be effective in the production of highly siliceous zeolites (Si:Al ratio > 12).[39] Purely siliceous zeolites have been synthesized by removing aluminum from the reaction mixture.

In general, metals of catalytic interest are inserted into zeolite structures through isomorphous substitution. Isomorphous substitution is defined as the replacement of an element in the crystalline framework (in this case Al or Si) by another element similar in ionic radius and coordination requirements.[40] This approach has clear limitations. First, some elements (notably Mo and W) will not isomorphously substitute into zeolite lattice because their charge, ionic radius, or coordination requirements are not similar enough to Al or Si. Second, "excessive" substitution of an element into the framework can disrupt the crystalline lattice. For example the inclusion of more than three weight percent of Ti in TS-1, a zeolite having the MFI structure, leads to the formation of TiO_2 domains and lower catalytic activity in olefin epoxidation.[41] Such limitations can be problematic when it is desirable to have as many actives sites as possible while maintaining site isolation in order to maximize the productivity of the catalyst.

The microporous pore structure of zeolites impedes their general application in catalysis. Although the ordered pore structures have been used to impart shape selectivity in some reactions,[42] their application is limited to reactions using reagents with a kinetic diameter smaller than 10 Å.[38,43] Furthermore, mass transport to and from the catalyst sites in the pore structure is slow which limits the rate of reaction that can be attained using these materials.[42] For these reasons a substantial amount of effort has been directed at the synthesis of zeolites with mesoporous (pore diameters from 2 to 50 nm) pores.

MCM-41, SBA-15, and HMS are three common silica materials with ordered mesoporous structures.[44] Of those three MCM-41 and SBA-15 are synthesized through hydrothermal processes.

While the pore structures of these mesoporous materials are ordered, their framework structures are not crystalline. This is unfortunate as the ability to isomorphously substitute elements of interest into specific sites in the crystalline lattice is lost. When incorporated during the hydrothermal synthesis catalytically active metals can be distributed piecemeal throughout the framework structure or aggregate together to form metal oxide domains. The amorphous nature of the pore walls also makes the hydrothermal stability of these mesoporous materials lower than that of related zeolites.[44]

Sol-gel Syntheses

The sol-gel method is a low temperature means of metal oxide synthesis based upon the formation of a solid oxide from the hydrolysis and condensation of a solution of metal salts or alkoxides.[45] This method is amenable to the preparation of materials used for a variety of purposes from refractory materials, ceramics, and superconductors to silica glass and heterogeneous catalysts.[46] The ability to employ easily purified precursors, lack of stoichiometric constraints, and mild reaction conditions that allow the synthesis of hybrid organic-inorganic materials make the sol-gel procedure an attractive synthetic method.[47]

There are two major types of reagents used in the sol-gel process: metal salts and metal alkoxides. Despite the differences in these reagents sol-gel

procedures go through the five basic steps of hydrolysis, condensation, gelation, ageing, and drying. While all the steps are important, the initial steps of hydrolysis and condensation have the most effect on the structure of a silica supported heterogeneous catalyst.

Hydrolysis is an extremely important step because the M(OH) species formed through hydrolysis are almost exclusively responsible for the formation of the M-O-M bonds necessary for gel formation. Metal salts are used in aqueous solution and an equilibrium exists between the aquo-, hydroxo-, and oxo- species of the metal as shown in the equation below. The point of equilibrium for a

$$[M(H_2O)^{z+}] \leftrightarrow [M(OH)]^{z-1} + H^+ \leftrightarrow [MO]^{z-2} + 2\ H^+$$

system depends upon the pH and the charge, coordination number, and electronegativity of the metal.

Hydrolysis of metal alkoxides occurs through the addition of water to the metal center followed by transfer of a proton to the alkoxide ligand and elimination of alcohol as shown in the equation below. There are differences

$$Si(OR)_4 + n\ H_2O \rightarrow Si(OR)_{4-n}(OH)_n + n\ ROH$$

silicon alkoxides and metal oxides that are important with regard to the synthesis of silica supported heterogeneous catalysts. Many metal alkoxides self-associate in solution. For example, $Ti(OMe)_4$ is tetrameric in a benzene solution.[46] While the degree of self-association decreases with the increasing steric bulk of the alkyl group (down to an average of 1.4 for $Ti(O^iPr)_4$ in benzene), self-assocation holds these metals in close proximity and promotes the formation

of oxide domains upon hydrolysis.[46,47] Further complicating the situation is the greater Lewis acidity of the transition metal alkoxides relative to silicon alkoxides as shown by the table of estimated partial positive charges, ∂(M), for a series of metal ethoxides below (Table 1-1).[48] The rate of hydrolysis increases with the partial positive charge on the metal. For example, the relative rate of hydrolysis for any $Ti(OR)_4$ species is estimated to be 10^5 times faster than that of the corresponding $Si(OR)_4$ species.[48]

Condensation is the formation of M-O-M bonds from metal hydroxo species. Condensation can occur between two hydroxo units, hydroxo and aquo units, or hydroxo and alkoxide units as shown in the equations below. As the rate of condensation depends upon the concentration of hydroxo species, the

$$(RO)_3SiOH + HOSi(OR)_3 \rightarrow (RO)_3SiOSi(OR)_3 + H_2O$$

$$Si(OR)_4 + HOSi(OR)_3 \rightarrow (RO)_3SiOSi(OR)_3 + ROH$$

rate of hydrolysis can have a significant influence on the products formed during condensation. Furthermore, the dispersion of a metal in the final product is influenced by the relative rates of homocondensation (formation of M-O-M or M'-O-M') the rates of heterocondensation (formation of M-O-M') for the reagents involved.[49] It is during condensation that metal oxide domains may begin to form.

Gelation occurs when condensation has occurred to such a degree that a gelatin like solid forms across the expanse of the reaction medium. At this point solvent is entrapped in the pore structure of the material. Ageing is the further

Table 1-1. Estimated partial positive charge on the metal center of a series of metal ethoxides.

Ethoxide	$Zr(OEt)_4$	$Ti(OEt)_4$	$Nb(OEt)_5$	$Ta(OEt)_5$	$V(O)(OEt)_3$	$W(OEt)_6$	$Si(OEt)_4$
∂(M)	0.65	0.63	0.53	0.49	0.46	0.43	0.32

cross-linking of un-reacted sites after gelation occurs. Drying is the process by which occluded solvent is removed from the sol-gel product. The method of drying chosen can have a significant impact upon the final properties of the material. Drying by heating the material can lead to the collapse of the pore structure and densification of the material. Materials produced through drying are called xerogels. Supercritical extraction of the solvent can leave the pore structure of such materials intact, and the resulting products are called aerogels.

The mild conditions of the sol-gel process also make it amenable to modification. As with the hydrothermal methods, structure directing agents can be used to produce materials with ordered pore structures.

Non-hydrolytic sol-gel process

A non-hydrolytic sol-gel process has been developed to overcome the formation of metal oxide domains during conventional sol-gel syntheses.[50] In the non-hydrolytic method metal halides are reacted directly with metal alkoxides.

$$MCl_x + M'OR_y \rightarrow Cl_{x-1}MOM'OR_{y-1} + RCl$$

While rapid ligand exchange reactions between metal alkoxides and metal halides are known, a high degree of homogeneity in the product can be obtained if the resulting products have condensation rates of the same order.[49] It has been reported that if the rate of heterocondensation between metals is high under non-aqueous sol-gel conditions that well dispersed titanium on silica can be made.[48,51]

Four Key Principles of Non-aqueous Building Block Approaches to Nano-structured Solids

An important drawback of the incipient wetness, grafting, hydrothermal, and sol-gel synthetic methods is that they allow the formation of multiple active site precursors that can contribute to catalytic activity, limit the type of active site that can be produced, or allow the aggregation of catalyst precursors into oxide domains. An approach that attempts to address these challenges and provide a general approach to the synthesis of single site catalysts is the non-aqueous building block (NABB) method. Four aspects of the NABB method that make its use advantageous over traditional methods for heterogeneous catalysts are: 1) the use of non-aqueous conditions, 2) the site dispersal offered by rigid building blocks, 3) the larger size metric of the structural building blocks compared to single molecules, 4) the opportunity to choose functional groups optimal for the reaction conditions. First, the use of strictly non-aqueous conditions is designed to prevent the condensation of metal- chloride, alkoxide, or hydroxide reagents into metal oxide domains. Second, the rigid structure of the building block should keep sites well-dispersed after the building blocks have been condensed together to form a solid material. The use of polyfunctional building blocks should allow high catalyst loadings to be achieved. Third, the larger size metric provided by building blocks can increase the surface area of a solid as compared to one made of similar simple molecules. Klemperer and co-workers showed this when the sol-gel product of an $Si_8O_{12}(OCH_3)_8$ had a specific surface area of 900 m^2/g which was 400 m^2/g greater than a gel produced from $Si(OCH_3)_4$ under the

same conditions.[52] Finally, the use of appropriately functionalized building blocks and reagents can improve control over the active sites produced in the finished material when compared to traditional synthetic methods.

The Building Block

There are many building blocks available to the synthetic chemist. The question then is what building blocks are best suited for the construction of a material that will be used as a catalyst. A key requirement is that the building block be chemically and thermally robust. This is important for two reasons. First, the building block must be able to come through the synthesis of the material intact. Otherwise, the advantages given by using a building block will be lost. Second, the building block must be able to withstand the conditions the catalyst material will encounter during use. Another requirement for a building block is that it be easy to synthesize, preferably in high yield. Finally, a building block should be appropriately functionalized for its intended use.

We selected the Si_8O_{12} building block (Figure 1-8) for several reasons. First, silica is thermally and chemically robust which is one of the most important requirements for a building block as described above. Secondly, the dimensions of the Si_8O_{12} unit promote site isolation. The length along the edge of the cube from one silicon corner to another is approximately 3.1 Å. A third reason we selected the Si_8O_{12} building block is that it is the most easily synthesized and purified member of the $Si_{2n}O_{3n}R_{2n}$ (n = 3-7; R = H, halide, alkyl, alkoxy) silsesquioxane family. Finally, we selected the Si_8O_{12} building block because it

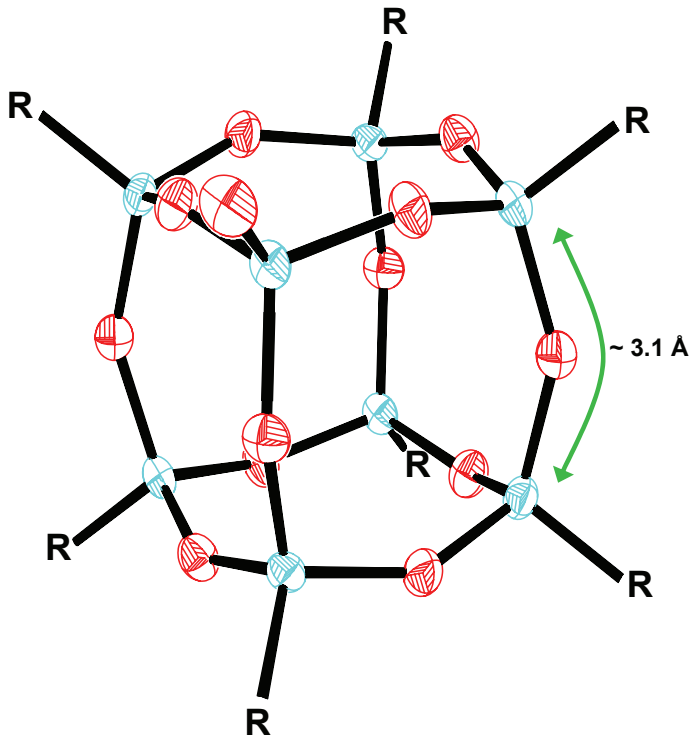

Figure 1-8. ORTEP drawing of $Si_8O_{12}R_8$.

can be functionalized in a manner that supports another fundamental tenet of our synthetic methodology.

"A" plus "B" Functionality

As mentioned earlier in this chapter, one of the problems associated with sol-gel chemistry is the lack of control over the reaction when condensing two different metal alkoxides—say tetraethyl orthosilicate and tetraethyl othrotitanate for example. Little can be done to prevent the orthotitanate from condensing with itself under sol-gel conditions even if the goal was to disperse titanium uniformly within the resulting gel. Vioux and co-workers offered a solution to this problem in what they call a non-hydrolytic sol-gel reaction.[53] The solution is elegant in its simplicity. Molecules with "A" and "B" functionalities are used. "A" and "B" both represent functionalities that will react with one another, but will not react with themselves. This is shown schematically in the equations below. Vioux and co-

$$A + B = AB$$

$$A + A \neq AA$$

$$B + B \neq BB$$

workers chose to react metal halides with metal alkoxides as shown in the equation that follows. One problem with the reaction of metal halides with metal

$$M(OR)_n + M'X_y \rightarrow {}_{n-1}(RO)M\text{-}O\text{-}M'X_{y-1} + RX$$

alkoxides is the possibility of "scrambling" reactions. In the case of "scrambling" rapid ligand exchange occurs when a metal halide is mixed with a metal alkoxide resulting in the formation of an equilibrium mixture of halogenoalkoxides.[53]

$$M(OR)_n + MX_n \leftrightarrow 2\ MX_{n-y}(OR)_y$$

We chose not to use the metal alkoxide functionality for two reasons. First, we felt that we could minimize the possibility of "scrambling" reactions by using a functional scheme which is described in the next section. Second, we wished to avoid the possibility of damaging the Si_8O_{12} core under reaction conditions as described by Klemperer and co-workers when using the alkoxy functionalized Si_8O_{12} building block, $Si_8O_{12}(OCH_3)_8$.[52]

The $Si_8O_{12}(OSnR_3)_8$ Building Block Fulfills the Four Principles

In 1991 Feher and Weller reported that $Si_8O_{12}(OSnMe_3)_8$, octakis(trimethyltin) spherosilicate, could be synthesized in high yield from the reaction of octahydridosilsesquioxane, $Si_8O_{12}H_8$, and bis(trimethyltin) oxide, $O(SnMe_3)_2$ as shown below.[54] They noted in that work and demonstrated in

$$Si_8O_{12}H_8 + 8\ O(SnMe_3)_2 \rightarrow Si_8O_{12}(OSnMe_3)_8 + 8\ HSnMe_3$$

following work that the reaction of $Si_8O_{12}(OSnMe_3)_8$, a.k.a. methyltin cube, with a molecule containing a metal halide bond caused the bond between the corner oxygen and the tin heteroatom to be cleaved.[54,55] This effectively changes the Si_8O_{12} building block into a Si_8O_{20} building block with a distance of about 4.9 Å between the corner oxygen atoms (Figure 1-9). Furthermore, methyltin cube has eight identical ≡Si-O-$SnMe_3$ reactive sites that could potentially allow the synthesis of materials with very high loadings of metals.

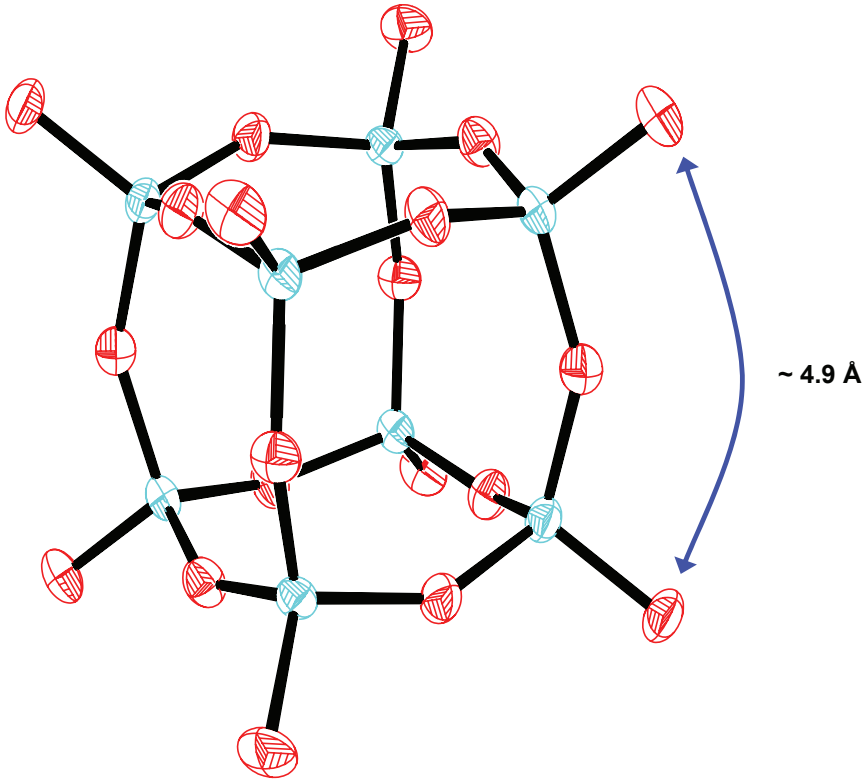

Figure 1-9. ORTEP drawing of Si_8O_{20} building block.

The work of Feher and Weller effectively brought the four advantages of the non-aqueous building block method together in one package. Reaction conditions were rigorously anhydrous. The building block was proven to yield materials with higher surface areas than materials synthesized using single molecules as shown by Klemperer and co-workers.[52] The reaction scheme of metathesis between the tri-alkyltin functionalized building blocks and metal halides coupled with the 4.9 Å separation between reactive sites should favor the production of atomically disperse metal sites. What remained was to take the principles of the NABB method and demonstrate that the method could be used to construct well-defined single site catalysts, and that the method would be applicable to a wide variety of metals accessible through their respective halides.

The Non-aqueous Building Block Synthetic Method

The NABB method is also unique in that it allows an unprecedented control of the structure of the active site through a variety of means. In order to examine the various means of control available, it helps to examine some specific reactions involving $Si_8O_{20}(SnMe_3)_8$ and silicon tetrachloride. If we represent a molecule of methyltin cube as ≡Si-O-$SnMe_3$ and react that molecule with a single molecule of silicon tetrachloride, $SiCl_4$, the reaction would proceed as shown below. Two things are apparent from this simple reaction. The first is

$$\equiv Si\text{-}O\text{-}SnMe_3 + SiCl_4 \rightarrow \equiv Si\text{-}O\text{-}SiCl_3 + ClSnMe_3$$

that two distinct silicon species detectable by ^{29}Si NMR are present in the product. The silicon at the corner of the methyltin cube becomes a Q^4 site with a

chemical shift expected near -110 ppm. The silicon atom in the -$OSiCl_3$ segment of the product is a pseudo Q^1 site with a chemical shift expected near -45 ppm. The second thing that is apparent is that three potentially reactive chlorine sites remain in the -$OSiCl_3$ segment of the product.

Let us continue this thought experiment, assuming that we have three molecules of methyltin cube to react with the product from above. One should

$$\equiv Si\text{-}O\text{-}SiCl_3 + 3\ \equiv Si\text{-}O\text{-}SnMe_3 \rightarrow Si(O\text{-}Si\equiv)_4 + 3\ ClSnMe_3$$

note that the silicon atom that originated from the $SiCl_4$ molecule is now itself a Q^4 site and therefore indistinguishable using ^{29}Si NMR from the Q^4 sites formed at the corners of the methyltin cube. It is also apparent from this thought experiment that the structure of the final product depends upon the stoichiometry of the reaction. As we saw, the addition of a limiting amount of $SiCl_4$ to a solution of methyltin cube can produce $Si(O\text{-}Si\equiv)_4$ sites. However, the use of higher stoichiometries could produce $Cl_2Si(O\text{-}Si\equiv)_2$ or $ClSi(O\text{-}Si\equiv)_3$ species.

Indeed studies of the reaction between silicon tetrachloride and the methyltin cube have shown that the structure of the product is dependent upon the stoichiometry of the reaction.[56] Stoichiometric ratios of less than one $SiCl_4$ per methyltin cube show that all four chlorides react producing fully-embedded $Si(O\text{-}Si\equiv)_4$ in the resultant solid as observed by ^{29}Si magic angle spinning (MAS) NMR. When stoichiometric ratios of greater than one $SiCl_4$ per methyltin cube are used a mixture of capping $Cl_3Si(O\text{-}Si\equiv)$, bridging $Cl_2Si(O\text{-}Si\equiv)_2$, and possibly some fully-embedded $Si(O\text{-}Si\equiv)_4$ sites are formed. We refer to this process

where the halide containing the metal of interest is added first to a solution of methyltin cube and simple stoichiometric adjustments are made to affect the structure of the metal center in the product as the process of *normal addition* in order to differentiate it from the process described next. A representation of *normal addition* is shown in Figure 1-10.

What if capping sites, sites where only one bond from metal halide to methyl tin cube is formed, are the only species desired? Simply reversing the order the reagents are added to the reaction vessel can produce the capping species preferentially. We refer to this as the *inverse addition* process and it is shown in the equation below and in Figure 1-10. The molecular all-capping

$$\text{excess } MX_n + \equiv Si\text{-}O\text{-}SnMe_3 \rightarrow \equiv Si\text{-}O\text{-}MX_{n-1} + XSnMe_3$$

species $Si_8O_{20}(SiCl_3)_8$ has been successfully produced by adding a solution of methyltin cube to a solution containing a large excess of $SiCl_4$.[57] Similarly, the inverse addition reaction between vanadyl chloride, $V(O)Cl_3$, and methyltin cube yields a solid where $\equiv Si\text{-}O\text{-}V(O)Cl_2$ capping groups are the preferred product.[58]

If we return to our thought experiment, you may notice that we have only considered the reaction of methyltin cube with pure metal halides. However, a variety of metal compounds that contain both halide and hydride, alkyl, or aryl groups are known. One can easily picture, as shown below, that the reaction between methyltin cube and methyltrichlorosilane, $MeSiCl_3$, could only produce a material with a maximum of three bonds from cubes to the methylsilyl unit. We

$$MeSiCl_3 + \text{excess } \equiv Si\text{-}O\text{-}SnMe_3 \rightarrow MeSi(O\text{-}Si\equiv)_3 + 3\ ClSnMe_3$$

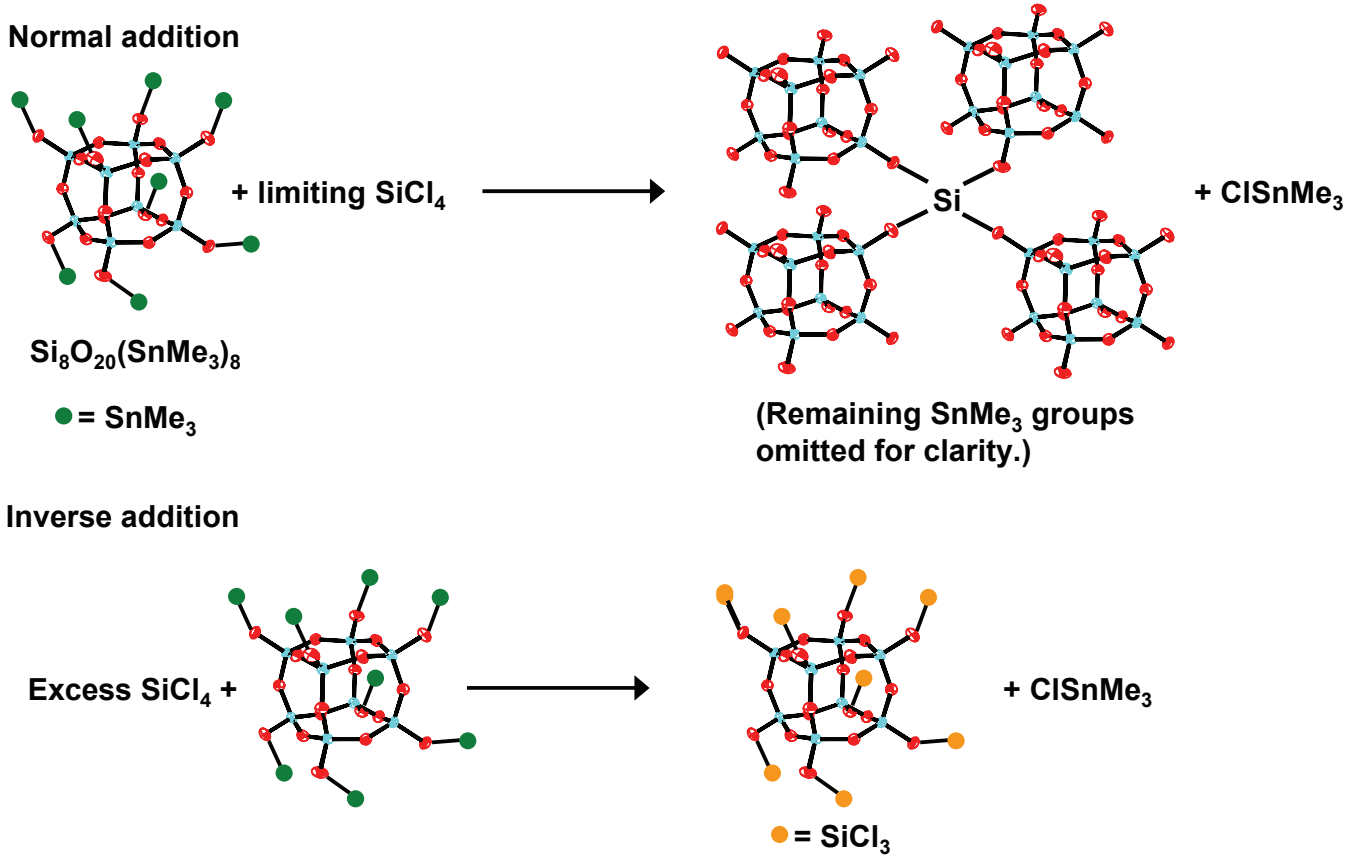

Figure 1-10. Representations of *normal addition* (top) and *inverse addition* (bottom).

refer to selecting reagents with nonreactive groups to control the structure of the product as the use of *blocking groups.* A model study using trichlorosilane,$HSiCl_3$, shows that blocking groups can be used to limit the number of bonds formed between a metal halide and the cube.[56,59] If necessary the blocking groups can be removed post-synthesis via calcination to yield M-OH groups typical of those found on the surfaces of metal oxides.

From a consideration of the above we have been able to formulate a general process for the preparation of atomically dispersed, site isolated, single site catalysts. We call this the process of *sequential additions* and it uses the principles of *normal addition, inverse addition,* and *blocking groups* in combination with the fact that we wish to disperse a metal in a silica matrix. If we wish to form a metal site with a connectivity of two without the use of blocking groups, we can react methyltin cube with a limiting amount of a silicon halide and leave tin sites available at unreacted corners of the cube. (Connectivity refers to the number of bonds formed between the metal halide and cubes. For example, a $Cl_2Ti(O\text{-}Si\equiv)_2$ site would have a connectivity of two.) We can then add a different metal halide, zirconium tetrachloride for example. If the proper amount of tin sites remain the product will contain $Cl_2Zr(O\text{-}Si\equiv)_2$ sites exclusively as shown in Figure 1-11. Remaining tin sites can then either be removed from the system by reaction with trimethylsilyl chloride, or reacted with other reagents as the researcher deems appropriate.

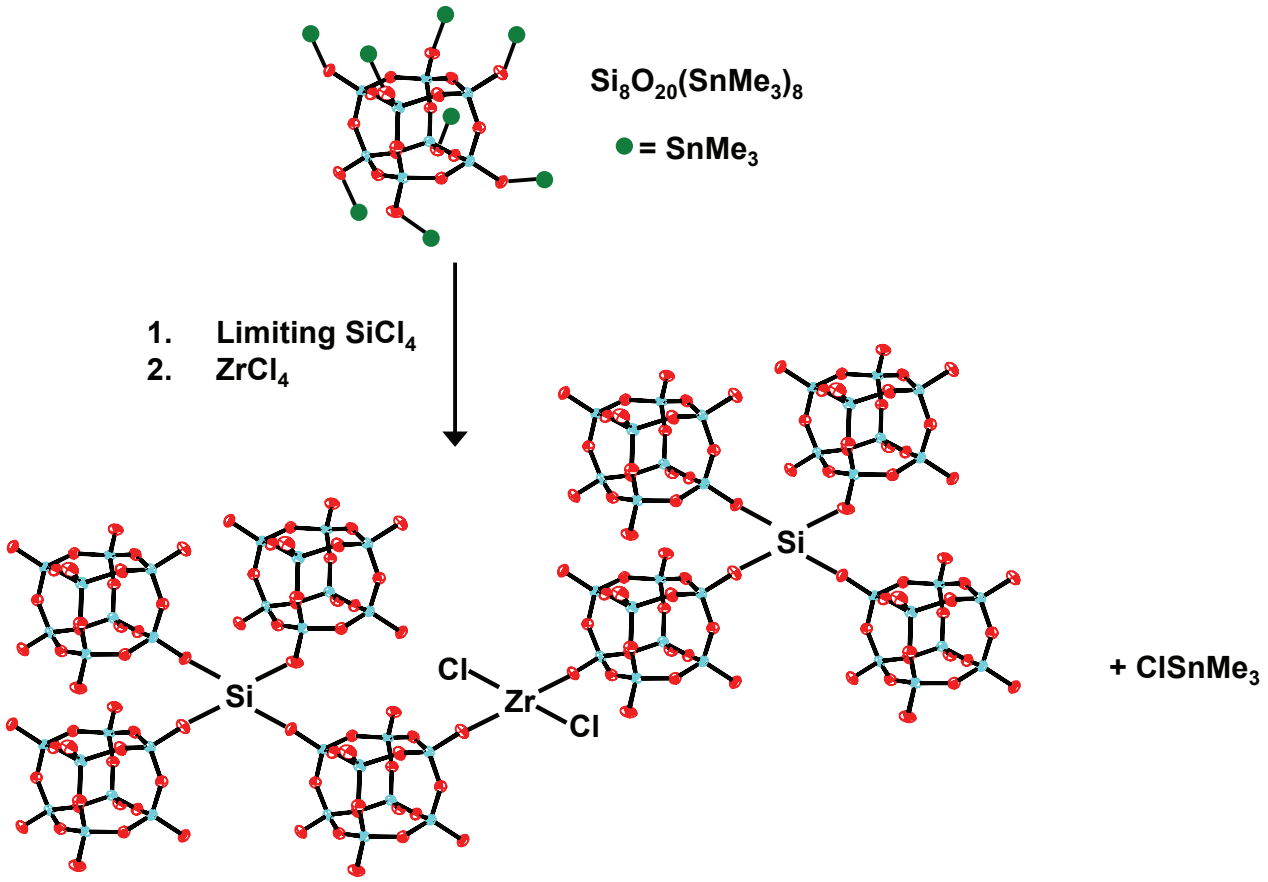

Figure 1-11. Representation of the non-aqueous building block method of *sequential additions*.

Now let us consider two processes designed to control the structure of the NABB method product specifically through influencing the rate of reaction. These means of control are among the least explored in the non-aqueuous building block method. Temperature is an obvious means of influencing the rate of a reaction. It has been shown that in the case of the addition of $SiCl_4$ to methyltin cube that an increase in temperature from 50 to 80 °C favors the formation of silicon centers with higher connectivity.[56,59]

The use of coordination compounds of metal halides can also influence the rate of reaction. For example, I found that the addition of titanium tetrachloride to a solution of butyltin cube (analogous to methyltin cube and described in Chapter 2) produced a visible solid product within minutes. However, the reaction of bis(pyridine)titanium tetrachloride (a solid), $TiCl_4 \cdot py_2$, with butyltin cube proceeds more slowly and does not produce a solid product after 24 hours. Unlike the case of titanium, the reaction of $SiCl_4$ with butyltin cube was found to proceed slowly, and a solid product was not produced after 48 hours. Presumably, the absence of a solid product means that no reaction occurred or that a preponderance of capping species were produced. However, the reaction of bis(pyridine)silicon tetrachloride, $SiCl_4 \cdot py_2$, was found to produce a solid product that was recognizable after 18 hours.

It is clear from these examples that reaction temperature and the use of coordination compounds of metal halides are two more means of influencing the structure of the product available in the NABB method. While these means are

directed at influencing the rate of reaction, their impact on the structure of the product is powerful. As studies of the non-aqueous building block method continue control of reaction temperature and the use of coordination compounds must be considered in attempts to synthesize specific active site precursors.

The non-aqueous building block method shows great potential for the synthesis of nano-structured heterogeneous catalysts. As we have seen, this method offers many means to control the structure of the active site in the product including: the use of blocking groups, the use of coordination compounds, temperature selection, and the multi-faceted process of sequential additions. The NABB method overcomes many of the shortcomings of traditional methods of heterogeneous catalyst synthesis while being generally applicable to a variety of high valent transition metal and main group halides including: P, Al, Si, B, Ti, Zr, and V.[55-61] The major limits of the non-aqueous building block method may be those imposed by the reactivity and coordination constraints of the metal being inserted into the building block matrix.

Dissertation Overview

Catalysts touch nearly every aspect of modern life. As we have seen in this chapter, there is an industrial demand for highly active and selective catalysts that can easily be separated from the reaction mixture. However, traditional methods appear to be inadequate for the synthesis of these next generation catalysts. While the catalysts synthesized through these means are effective, their propensity to form materials with multiple sites that could be

responsible for the observed activity have made it very challenging in most cases to identify the active sites in heterogeneous catalysts. Given the lack of methods available for the synthesis of single-site catalysts, it is clear that new methodologies need to be developed so that structure-activity relationships can be determined for heterogeneous catalysts. Ideally, these methods will be generally applicable to a wide variety of transition metals and give rise to truly nano-structured catalysts. One such method that holds promise in elucidating structure-activity relationships and synthesizing nano-structured catalysts is the non-aqueous building block method.

Chapter 2 describes the synthesis of the butyltin cube, $Si_8O_{20}(Sn^nBu_3)_8$. As discussed in that chapter, this building block is crucial to the scope of the non-aqueous building block method. This material addresses issues associated with the cost and toxicity involved with the synthesis of the methyltin cube, $Si_8O_{20}(SnMe_3)_8$, making the application of the non-aqueous building block method possible on an industrial scale.

Chapter 3 describes the reactivity of $Si_8O_{20}(Sn^nBu_3)_8$ with $SiCl_4$, $SiCl_4 \cdot py_2$, and $TiCl_4$. Methods for the structural characterization of non-aqueous building block methods including a quantitative ^1H NMR method for determining the amount of $ClSn^nBu_3$ by-product formed during non-aqueous building block reactions. The chapter also includes information on the stoichiometry necessary to form titanium non-aqueous building block materials with specific titanium connectivity values.

Chapter 4 examines epoxidation reactions catalyzed by titanium-on-silica. The oxidants made available by titanium-on-silica catalysts are discussed, and the activity and structural characterization of several titanium-on-silica catalysts from the literature are described. The results of experiments measuring the activity and selectivity of titanium non-aqueous building block catalysts in the epoxidation of cyclohexene are discussed, and comparisons with literature catalysts are made.

Chapter 2. Significance, Synthesis, and Characterization of Octakis(tri-*n*-butyltin)spherosilicate

Rationale

Previous research about the Si_8O_{20} building block conducted by the groups of Feher and Barnes used octakis(trimethyltin)spherosilicate, $Si_8O_{20}(SnMe_3)_8$, as the source of the building block.[55,58-60] While facile, the reaction in the equation below reported by Feher for the synthesis of $Si_8O_{20}(SnMe_3)_8$, uses bis(trimethyltin)oxide, $O(SnMe_3)_2$, which is not commercially available and is synthesized in two steps from highly toxic trimethyltin chloride.[54] However, the tri-*n*-butyltin analogue,

$$Si_8O_{12}H_8 + O(SnMe_3)_2 \rightarrow Si_8O_{20}(SnMe_3)_8 + 8\ HSnMe_3$$

bis(tri-*n*-butyltin)oxide, $O(Sn^nBu_3)$ or *n*-butyltin ether, is commercially available and relatively inexpensive due to its widespread use as a fungicide and anti-fouling agent in marine paints.[62] Thus, concerns about the toxicity of trimethyltin compounds and their high cost motivated attempts to synthesize octakis(tri-*n*-butyltin)spherosilicate, $Si_8O_{20}(Sn^nBu_3)_8$.

Cost Comparison

In contrast to the *n*-butyltin ether, the methyl analogue must be synthesized from trimethyltin chloride, $ClSnMe_3$. The synthesis is a two-step process in which the chloride is first converted to the hydroxide with water, which

is then dehydrated using calcium hydride to yield $O(SnMe_3)_2$ as shown in the following equations. Neglecting yield considerations and other costs associated

$$Me_3SnCl + NaOH\ (aq.) \rightarrow Me_3SnOH + NaCl\ (aq.)$$

$$2\ Me_3SnOH + CaH_2 \rightarrow Me_3SnOSnMe_3 + 2\ H_2 + CaO$$

with the synthesis, the amount of $ClSnMe_3$ needed to produce one mole of bis(trimethyltin) oxide is over 25 times more expensive than a mole of *n*-butyltin ether purchased directly from a commercial supplier.[62]

Safety considerations

While cost was a driving force behind the exploration of the synthesis of the tri-n-butyltin analogue of $Si_8O_{20}(SnMe_3)_8$, toxicity was also a major factor. All trialkyltin compounds exhibit some level of toxicity. $ClSnMe_3$ is particularly toxic and known to cause cerebral edema.[62] A direct comparison of the LD50 (12.6 mg/kg for $ClSnMe_3$ versus 148-234 mg/kg for $O(Sn^nBu_3)_2$) shows that trimethyltin chloride is substantially more toxic than *n*-butyltin ether.

Normally the toxic effects of chemicals are avoided by avoiding exposure to the toxins. The great danger of trimethyltin compounds is their high vapor pressure which increases the risk of exposure to this potent class of compounds. In contrast to $ClSnMe_3$ which readily sublimes at atmospheric pressure, $O(Sn^nBu_3)_2$ has a boiling point of 180 °C at a pressure of 2 torr.[62] While the use of standard Schlenk techniques can mitigate the exposure risks associated with trimethyltin compounds, the lower relative vapor pressure and toxicity of the *n*-

butyltin ether make its use in large scale syntheses preferable from a safety standpoint.

Synthesis

The substitution of the *n*-butyltin ether for the methyltin analogue in the reaction with the octahydrido siloxane, $H_8Si_8O_{12}$, results in the synthesis of pure $Si_8O_{20}(Sn^nBu_3)_8$, butyltin cube, in high yield. Because commercially available *n*-butyltin ether is provided at 96% purity, the $O(Sn^nBu_3)_2$ was vacuum distilled prior to use. In a typical synthesis, 4 g (9.4 mmol) of $H_8Si_8O_{12}$ was added to a magnetically stirred round-bottomed flask containing 47 g (79.1 mmol, 5% molar excess) of neat *n*-butyltin ether at 0 °C. The reaction was allowed to proceed for one hour. Removal of the tri-*n*-butyltinhydride, HSn^nBu_3, by-product is easily facilitated by short-path distillation under reduced pressure. However the butyltin cube product is extremely soluble in the remaining *n*-butyltin ether, and a rubbery solid results following removal of the HSn^nBu_3. Two methods proved successful in separating the product from the excess *n*-butyltin ether.

First, continued short-path distillation under reduced pressure utilizing high temperature yields a pure product in essentially quantitative yield. This method requires the use of an oil bath with temperatures from 200 to 230 °C, and careful heating of the distillation head to prevent condensation of the *n*-butyltin ether before it reaches the condenser. Sufficient time, at least 18 hours, must also be allowed for the residual $O(Sn^nBu_3)_2$ to diffuse out of the rubbery solid.

Second trituration of the rubbery solid with cold (-20 °C) methanol, and collection of the product via vacuum filtration also yields a pure product. The trituration method results in recovered yields of 70 to 80%.

Characterization

$Si_8O_{20}(Sn^nBu_3)_8$ was characterized using multinuclear NMR, infrared (IR) spectroscopy, Raman spectroscopy, and elemental analysis. The results of elemental analysis are as follows: found 40.40% C and 7.57% H, calculated for $Si_8Sn_8O_{20}C_{96}H_{216}$: 40.24% C and 7.60% H.

The results of the multinuclear NMR studies are as follows: ^{1}H NMR: δ 1.09 (t, 72H); δ 1.38 (t, 48H); δ 1.54 (m, 48H); δ 1.84 (m, 48H); ^{13}C NMR: δ 14.2 (s); δ 16.4 (s) ^{1}J(SnC) = 356, 373 Hz; δ 27.7 (s) ^{3}J(SnC) = 60.3, 63.1 Hz; δ 28.4 (s) ^{2}J(SnC) = 17.8 Hz; ^{119}Sn: (149.18 MHz, C_6D_6) δ 85.9 (s); and ^{29}Si: δ -101.0 (s). The resonances at 1.09 and 1.38 ppm in the ^{1}H NMR spectrum were assigned to the terminal methyl group and the methylene group closest to tin on the *n*-butyl chain of the trialkyltin groups respectively. Those assignments were made upon the basis of the splitting patterns of the resonances and their relative integration values. The resonances at 1.54 and 1.84 are assigned to the interior methylene groups of the *n*-butyl chain, but have not been assigned to specific positions on the chain. ^{13}C NMR resonances were assigned upon the basis of the ^{n}J(C-^{117}Sn,^{119}Sn) coupling constants.[63-66] Figure 2-1 shows the ^{1}H and ^{13}C NMR spectra along with assignments.

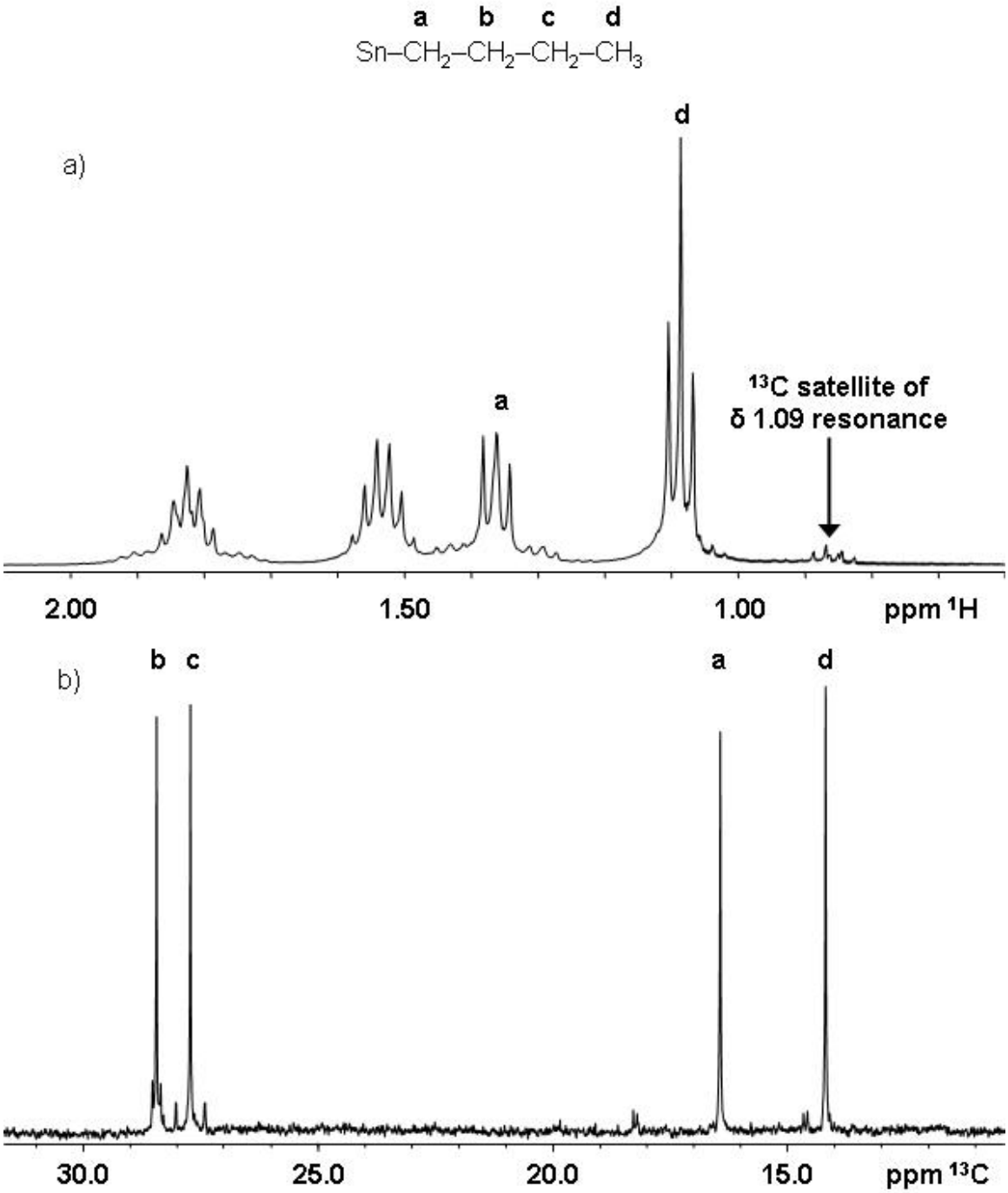

Figure 2-1. a) Alkyl region of ^{1}H NMR spectrum for $Si_8O_{20}(Sn^nBu_3)_8$.

b) Alkyl region of ^{13}C NMR spectrum for $Si_8O_{20}(Sn^nBu_3)_8$.

The infrared and Raman spectra (Figures 2-2 and 2-3 respectively) were assigned according to bands reported in the literature for $O(Sn^{n}Bu_3)_2$[67] and $H_8Si_8O_{12}$[68-71]. Assignments for major bands are given in Table 2-1.

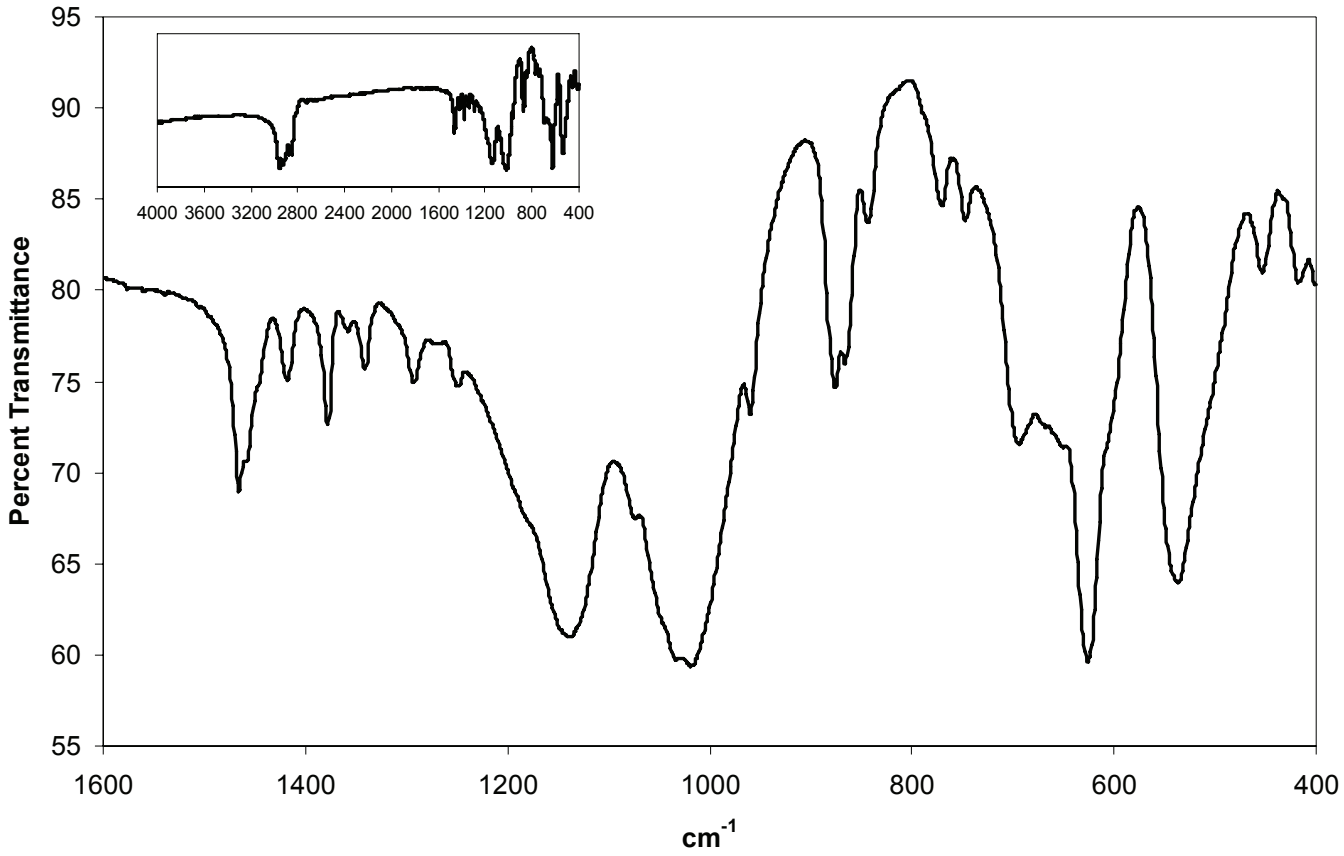

Figure 2-2. Expansion of the fingerprint region of the FT-IR spectrum of $Si_8O_{20}(Sn^nBu_3)_8$ with full spectrum inset.

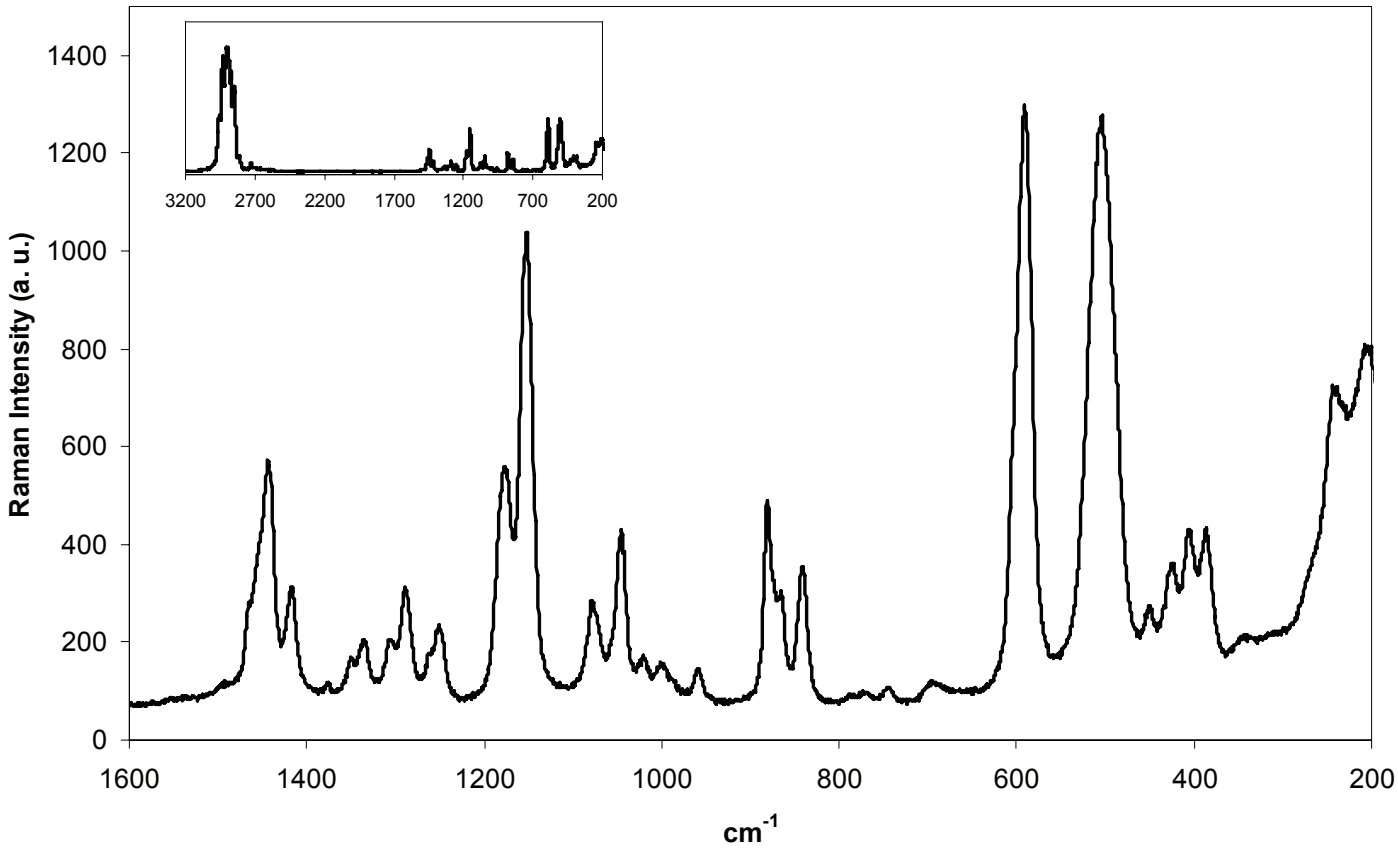

Figure 2-3. Expansion of the fingerprint region of the Raman spectrum of $Si_8O_{20}(Sn^nBu_3)_8$ with full spectrum inset.

Table 2-1. Assignments of major Raman and IR bands in the vibrational spectra of $Si_8O_{20}(Sn^nBu_3)_8$.

Raman (cm^{-1})	IR (cm^{-1})	Assignment
1442	1466	∂_{as} CH_3
1415	1419	∂_{as} CH_2
—	1378	∂_s CH_3
1174	—	∂_s CH_2
1151	—	∂ CH
—	1143	v_{as} (Si-O-Si)
1075	1075 (shoulder)	v C-C
—	1036-1022	v (Si-O-Si)
1045	—	v C-C
880	877	ρ CH
—	867	ρ CH
840	842	ρ CH
—	696	v_s (Si-O-Si)
—	628	v_s (Si-O-Si)
589	—	v_{as} SnC_3
—	540	v_s (O-Si-O)
503	—	v_s SnC_3

Chapter 3. Synthesis and Characterization of Titanium Non-aqueous Building Block Materials

Introduction

Heterogeneous catalysts are notoriously difficult to characterize. Most of the heterogeneous catalysts generated using traditional synthetic methods are structurally complex for one or more of the following reasons: 1) they frequently lack long range order (are amorphous), 2) the active sites are located on the surface of supports that are not structurally uniform and, 3) they consist of multiple species that involve the active metal (multiple sites). (Traditional methods for the synthesis of heterogeneous catalysts are discussed in the first chapter of this dissertation.) Even zeolites which are well-ordered materials with crystalline structures and ordered networks or micropores can present problems with regard to determining the structure of catalytic sites. While diffraction methods are available to probe the bulk structure of crystalline materials, they are not generally sensitive to structural correlations involving dilute atomic components.[72] Thus, diffraction methods are not well-suited for the characterization of catalytic sites which are typically incorporated at a low weight percent or in defect sites that could be responsible for catalytic activity. The question then is, “What methods can be used to characterize heterogeneous catalysts?”.

Perhaps the simplest method to begin the structural characterization of a material, albeit indirectly, is the gravimetric method or variations thereon. If one

understands the chemical reactions that occur and the mass of the product and the mass(es) and identity(ies) of the by-product(s) of the reaction then one can make reasonable conclusions about the identity and structure of the reaction product using stoichiometry. Simple gravimetric measurements were used to help characterize the structure of materials previously prepared using the non-aqueous building block method.[57] Scott and Basset have used gas chromatography and quantitative FT-IR spectroscopy to identify and measure the amount of by-products formed during syntheses of catalytic materials to aid in structural determinations, yet the principle is the same as gravimetry.[29,32,34]

Solid state NMR (SSNMR) has been used to characterize heterogeneous catalysts. Solid acid catalysts have been extensively characterized using SSNMR both by directly probing the local structure around NMR active nuclei such as ^{29}Si, ^{27}Al, and ^{1}H and monitoring their interaction with probe molecules, such as NH_3.[73] ^{29}Si and ^{51}V NMR have been used to aid the structural characterization of non-aqueous building block (NABB) materials.[56-59]

Vibrational spectroscopy has been used to characterize a variety of catalysts supported on metal oxides.[74] FT-IR spectroscopy has been used to investigate the surface functionality of metal oxides and the structure of those oxides after reaction with various catalyst precursors.[29] Raman spectroscopy has been used to look for vibrations specific to metals with catalytic potential bound to metal oxide supports.[75]

X-ray absorption spectroscopy has also been used to probe the structure of heterogeneous catalysts.[30] X-ray absorption near edge spectroscopy (XANES) studies can provide information about the oxidation state and symmetry of metal sites in a material. Fits of extended X-ray absorption fine structure (EXAFS) data can be used to determine the number, atom type, and distances of atoms neighboring the metal center.

While the above is not an exhaustive list of the methods used to characterize heterogeneous catalysts, it includes many of the methods most commonly used for their characterization. In the study of the structure of titanium centers in materials produced from the non-aqueous building block method, a variation on gravimetric analysis was used to gain the first information about the structure of the titanium centers. Then structural information gathered using FT-IR, Raman, SSNMR, XANES, and EXAFS was used to form a more complete understanding of the structure of the titanium sites in those materials. The procedure for synthesizing these Ti non-aqueous building block materials, the data collected using various techniques, and conclusions about the effect of reaction stoichiometry on the structure of the titanium center in these materials are presented below.

Experimental

The metal halides used in the non-aqueous building block method are sensitive to water and hydroxide species on the surface of glass. As such, special care was taken to exclude those species during synthesis. All the

glassware used in the syntheses was treated with chlorotrimethylsilane (Sigma-Aldrich, 97%) followed by triethylamine (Sigma-Aldrich, 99.5%) to remove hydroxyl groups from the surface of the glass. Hexanes and toluene (Fisher Scientific) were dried using an alloy of sodium and potassium and distilled prior to placement in solvent bulbs. Pyridine (Fisher Scientific) was distilled and dried using calcium hydride. Hexanes, toluene, and pyridine were kept in solvent bulbs equipped with high vacuum Teflon® stopcocks (J. Young Scientific Glassware, Ltd.) with their appropriate drying agent. They were degassed using three freeze-pump-thaw cycles and stored under vacuum prior to use. $Si_8O_{20}(Sn^nBu_3)_8$ was synthesized according to the method described in the second chapter of this dissertation.

Silicon(IV) chloride (Acros Organics, 99.8%) and titanium(IV) chloride (various suppliers and grades) were distilled under a nitrogen gas purge. During distillation the fraction collected below the boiling point of the metal halide was discarded. The constant boiling fraction of distillate boiling within 2 °C of the boiling point was collected in a solvent bulb equipped with a high vacuum Teflon® stopcock. The metal halides were degassed using three freeze-pump-thaw cycles and stored under vacuum prior to use.

A conventional nitrogen gas/vacuum manifold was used to facilitate the transfer of solvents and metal halide vapors to the reaction vessel. Solvents were transferred to the reaction vessel directly through the manifold. However, metal halides were transferred to the reaction vessel using glass “T”s to prevent

contamination of the manifold.[59] Metal halides were transferred from solvent bulbs to glass capillary tubes (3 or 5 mm diameter) equipped with Teflon® stopcocks. Metal halides were then subsequently transferred from capillary tubes to the reaction vessel.

Change in the volume of the liquid in the vessels was used to initially estimate the amount of material transferred from the solvent bulbs and capillary tubes to the reaction vessels. As the internal diameter of the capillary vessels was known, the change in height of the liquid column in the vessel was used to monitor the volume change. The small diameter of the capillary tubes allowed the addition of precise amounts of metal halides to the reaction vessel. Final determination of the amount added to the reaction was based upon gravimetric measurements of the capillary tube.

General Procedure for the Synthesis of Building-Block Materials

In a typical reaction to make cross-linked solids based upon the cubic Si_8O_{20} spherosilicate building block, 4.00 g of $Si_8O_{20}(Sn^nBu_3)_8$ (butyltin cube) was placed in a beaker and dissolved in hexanes. The butyltin cube/hexanes solution was then quantitatively transferred to a Schlenk type reaction vessel. A Teflon® coated magnetic stir bar was placed inside the vessel, and a glass transfer "T" was placed on the ground glass joint of the vessel. The hexanes were removed *in vacuo* through the stopcock of the reaction vessel. The vessel was then placed in an oil bath and heated *in vacuo* at 80 °C from 12 to 18 hours in order to remove any coordinated water molecules from $Si_8O_{20}(Sn^nBu_3)_8$.

Approximately 50 mL of solvent was vapor transferred from a solvent bulb through the vacuum manifold into the reaction vessel at -78 °C. The reaction vessel was then allowed to warm until the butyltin cube completely dissolved. The reaction vessel was then again cooled to -78 °C, and stirring was begun. An appropriate amount of metal halide was added to the reaction vessel via vapor transfer through the glass "T". As mentioned above, the amount of metal halide added was estimated by the change of the liquid column height inside the glass capillary and later quantified by the change in mass of the capillary Schlenk vessel.

Quantitative ^{1}H NMR Sample Preparation

Samples for quantitative ^{1}H NMR (QNMR) spectroscopy were prepared according to the following procedure. Perdeuterobenzene (Cambridge Isotopes, 99.6%) was dried over sodium-potassium alloy, degassed using three freeze-pump-thaw cycles, and taken into a N_2 (g) glove box. Separate perdeuterobenzene solutions of metal halide, butyltin cube, and mesitylene (internal standard) were prepared inside the glove box and stored in silylated glass vials equipped with Teflon®-backed silicone septa. NMR tubes were silylated, taken into the glove box to be filled with dry N_2 (g), and capped with a latex septum prior to removal. Subsequent manipulations were conducted in the atmosphere using syringes and standard Schlenk techniques. A rubber stopper with an appropriate sized hole was used to facilitate measuring accurate masses of the NMR tube through the process by allowing the tube to be held vertically

during measurement. Solutions were transferred from the vials to the NMR tube via syringe. The mass of the solution added to the NMR tube was determined to the nearest tenth of a milligram by difference.

Butyltin cube solution was added to the NMR tubes first. Metal halide solution was then added to the tube, and it was vigorously shaken. Mesitylene solution was added to the tubes after the reaction had proceeded for 30 minutes in order to prevent interference with the reaction.

Preparation of Samples for Structural Characterization

A typical reaction began with 8.00 g of butyltin cube. Following heating of the butyltin cube *in vacuo* to remove any physisorbed water, 100 mL of hexanes was vapor transferred into the reaction vessel containing the butyl tin cube. Then the desired amount of $TiCl_4$ was added to the reaction vessel via vapor transfer. The reaction was then allowed to warm to room temperature and proceed for two hours.

After two hours had passed, a weighed amount of the solid bis(pyridine) complex of silicon tetrachloride, $SiCl_4 \cdot py_2$, was added to the reaction vessel under a $N_2(g)$ purge. An excess was added for each sample. The number of moles added to the reaction was equal to the initial number of moles of tri-*n*-butyltin in the starting material less the number of moles of $TiCl_4$ added. The stoichiometry for each sample is shown in Table 3-1 below. The reaction was allowed to proceed for 18 hours.

Table 3-1. Stoichiometry used to prepared titanium non-aqueous building block catalysts.

Sample	$TiCl_4$:butyltin cube	$SiCl_4 \cdot py_2$:butyltin cube
Ti-4	0.25	7.75
Ti-3	1.0	7.0
Ti-2	2.0	6.0

Volatile liquids were then removed *in vacuo*. Excess $SiCl_4 \cdot py_2$ was removed using vacuum sublimation at 80 °C. Samples were then taken into a N_2(g) filled glove box. Sample preparation for the various methods of characterization was performed in the glove box.

Instrumentation

Silicon-29 magic angle spinning (MAS) NMR spectra were recorded on a Varian Inova spectrometer at a frequency of 79.43 MHz and a spinning rate of 3.5 kHz. Moisture sensitive samples were packed into 5 mm pencil rotors in a N_2 (g) glove box, and sealed with paraffin wax.

Infrared spectra were obtained using a N_2 (g) purged Bio-Rad FTS-60A spectrometer operating at a resolution of 2 cm^{-1}. Samples were mixed with an appropriate amount of potassium bromide and pressed into pellets.

Raman spectra were acquired in the backscattering mode on the "microstage" of a Dilor XY Raman spectrometer. Samples were placed in an NMR tube while in a N_2(g) glove box. The tube was capped, and then the cap

was wrapped with Parafilm® immediately following removal from the box. The 514.5-nm line of a Coherent Innova 200 argon ion laser was used for excitation.

X-ray absorption spectroscopy (XAS) spectra were collected in fluorescence mode at the X-19A (focused beam, 12 channel solid state Ge detector) and X-18B (broad beam, PIPS detector) beamlines on the X-ray storage ring of the National Synchrotron Light Source (NSLS) in Upton, New York operating at 2.8 MeV with a typical beam current of 200-300 mA. Data were collected at the titanium K-edge (4966 eV) and analyzed using IFEFFIT[76] and the Athena and Artemis programs.[77]

Quantitative ^{1}H NMR spectra were recorded in a method similar to that of Maniara, et. al.[78] The spectra were recorded on a Varian NMR with a ^{1}H frequency of 300 MHz. A 30° pulse was used with a recycle delay of 20 seconds. The recycle delay was slightly greater than four times T_1 for the longest resonance of interest– the methyl protons of tri-n-butyltin chloride at δ 0.86 ppm. T_1 values were measured on the same instrument using a standard population inversion experiment.

Experiments at each stoichiometric ratio were performed in triplicate. The data collected was processed and analyzed using MestReC version 4.9.9.6. A detailed procedure for processing the data is presented later in this chapter.

Solid-state NMR Study of Titanium Non-aqueous Building Block Materials

Since the structure of the titanium site in the non-aqueous building block materials (NABB) is of principle interest, titanium NMR would be a desirable

means of characterizing these materials. However few solid-state titanium NMR studies have been published to date.[79] One reason for this is the large quadrupole moments of ^{47}Ti and ^{49}Ti (the two NMR active isotopes) which broaden the signals observed in the spectra of titanium compounds.[79] Another experimental difficulty associated with titanium NMR is the similarity in resonance frequency of the two isotopes. Even at magnetic field strengths of 14.1 Tesla (^{1}H resonance frequency = 600 MHz) the resonance frequencies of the ^{47}Ti and ^{49}Ti isotopes differ only by about 9 kHz and, "most spectra will consist of completely overlapped resonances from the two isotopes because of the width of the lines."[79]

Silicon NMR spectra, on the other hand, are relatively easily obtained. An experiment was performed to determine if the ^{29}Si chemical shift of an atom in a NABB material is sensitive to the structure of titanium atoms in close proximity. Figure 3-1 shows a schematic of the possible structures of the titanium sites in the NABB materials. The silicon atoms whose chemical shift might be affected by the structure of titanium atoms are bound to them through an oxide linkage.

A NABB material was made from the addition of $TiCl_4$ to a solution of butyltin cube in a molar ratio of eight to one. This ratio is equal to one mole of $TiCl_4$ for every equivalent of tin present in the reaction. One should note that while there is a stoichiometric balance between titanium and tin there is actually a four-fold excess of chloride relative to tin in the reaction. This sample is referred to as Ti-XS to reflect the stoichiometric excess of chloride versus the

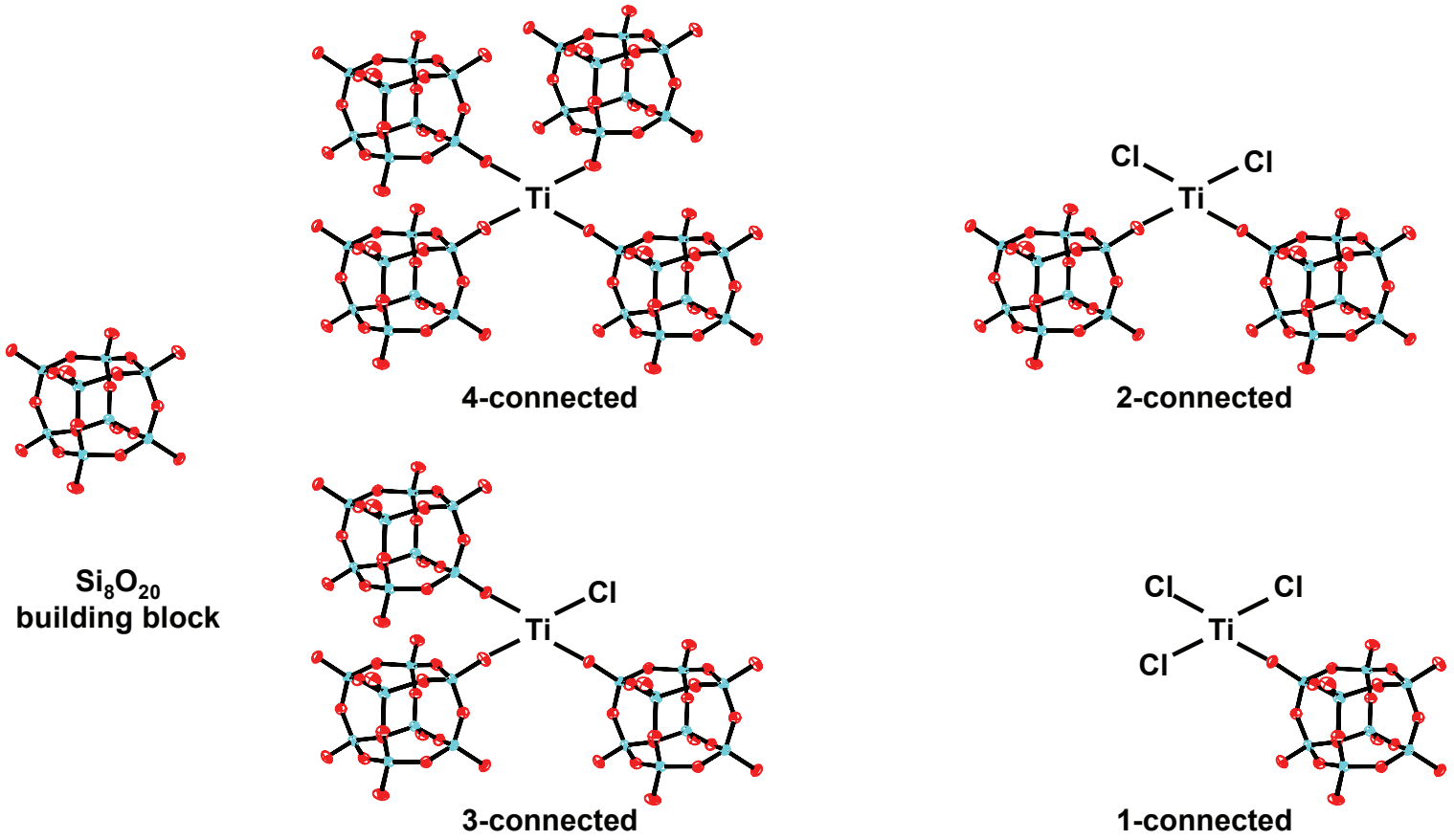

Figure 3-1. The various titanium centers that could be produced by the non-aqeuous building block method.

amount of tin sites available for reaction. Because a solid formed quickly following the addition of $TiCl_4$ to the butyltin cube solution it is unlikely that the product of the reaction is the molecular $Si_8O_{20}(TiCl_3)_8$ species which would remain soluble. The stoichiometry of the Ti-XS sample makes it likely that many titanium sites are present in the material.

Let us perform a thought experiment to test the assertion that many titanium sites are likely to be present in the Ti-XS sample. If one assumes that 4-connected sites are formed exclusively, the reaction will progress up to a point where the material is so extensively cross-linked that four tin sites will no longer be within the reach of a single $TiCl_4$ molecule. At that point the reaction will either cease, or other titanium species will form according to the number of tin sites within "reach". At a minimum, 4-connected and 1-connected species would be expected in the sample if the reaction consumes all the reaction sites available.

The ^{29}Si MAS NMR spectrum of the Ti-XS sample is shown in Figure 3-2. The spectrum shows only one resonance at -114 ppm. A resonance signal at approximately -101 ppm is expected if tin sites remain in the sample. The single resonance in the spectrum of the Ti-XS material, where the only linking center is titanium but where a distribution of 4-, 3-, 2-, and 1- connected titanium centers are expected is evidence that the chemical shift of ^{29}Si bound to titanium through oxygen is insensitive to the titanium chemical environment. Because of this evidence, I elected not to use ^{29}Si MAS NMR to attempt to obtain structural

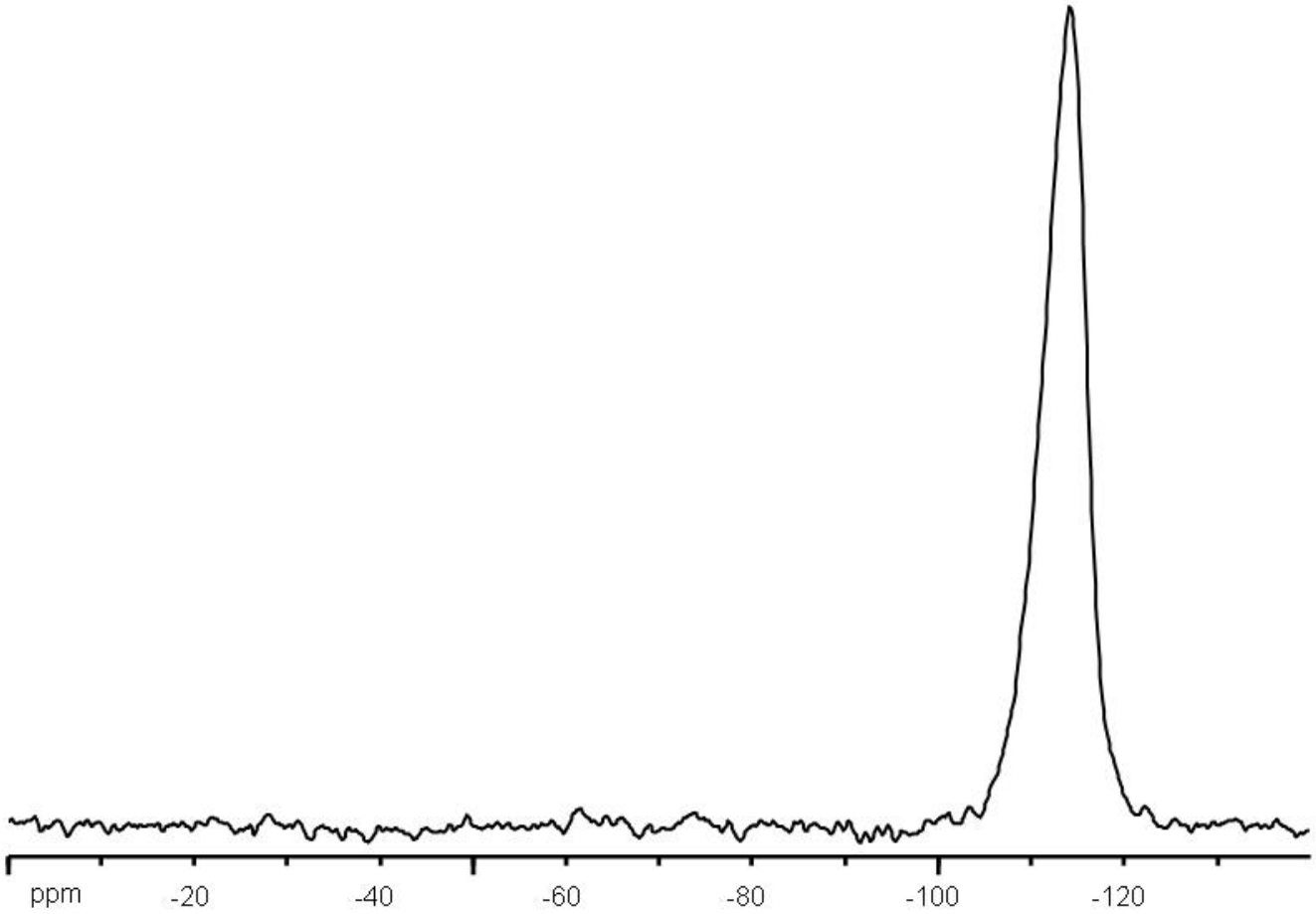

Figure 3-2. ^{29}Si MAS NMR spectrum of Ti-XS sample showing the insensitivity of the ^{29}Si chemical shift to the connectivity of the Ti center.

information about the nature of the titanium site(s) in non-aqueous building block materials.

Reaction Analysis via Quantitative NMR

One of the major differences between the reaction of the methyltin cube, $Si_8O_{20}(SnMe_3)_8$, and the butyltin cube, $Si_8O_{20}(Sn^nBu_3)_8$, is the properties of the tin chloride by-product in their reaction with metal chlorides. Trimethyltin chloride is the reaction by-product from the methyltin cube and is highly volatile (as noted in the second chapter of this work).[62] It is easily and quantitatively removed from the reaction mixture, and gravimetric analysis of the reaction is relatively easy.[57,59] However, the tri-butyltin chloride by-product from the reaction of the tributyltin cube is only slightly volatile, and is not easily removed from the Schlenk reaction vessels.

This is significant because gravimetric analysis has proven to be a useful tool in determining the average number of metathesis reactions per metal halide used in the synthesis.[57] This number is often referred to as the average "connectivity" of the linking metal halide, and provides information about the number of M-(O-Si) links in the system. The connectivity is limited by the fact that in general it only provides average connectivity values except in cases when either all of the halide groups or only one of the halide groups undergo reaction. In other cases a mixture of linking sites with different connectivities could be present that could yield the same numerical average as a sample containing only 2-connected titanium, $Ti(OSi\equiv)_2Cl_2$, linking groups for example.

For this reason, an experimental protocol to perform quantitative ^{1}H NMR spectroscopy (QNMR) was developed as an alternative to gravimetric analysis. The details regarding the collection of the spectra are given in the experimental section of this chapter. The accuracy of quantitative analysis of the spectra was found to be highly dependent upon the phasing and background corrections performed on the spectra. A reproducible procedure for phasing and background correction of the spectra using the Mestre-C program was developed. This procedure is explained below.

After importing the FID into Mestre-C, a Fourier transform with a line broadening factor of 0.1 Hz was applied. Figure 3-3 shows a typical spectrum immediately after the Fourier transform is applied. Figure 3-4 shows an expansion of the initial spectrum from 6.3 to 7.8 ppm. The resonance at 6.7 ppm is from the aromatic protons on mesitylene, and the resonance at 7.15 ppm is from residual protons in the dueterobenzene solvent. This expansion clearly shows that the spectrum is not well phased.

Manual phasing was applied using 7.15 ppm as the pivot point. Zero order phasing was applied first using the 7.15 and 6.7 ppm resonances as a guide. Those resonances are now symmetrical as shown in Figure 3-5. Figure 3-6 shows the effect of the zero order phasing on the whole spectrum. A blow up of the area from 0.4 to 2.4 ppm that contains the resonances used to quantify the amount of tri-n-butyltin chloride is shown in Figure 3-7. The resonance at 2.15 ppm is due to the methyl protons on mesitylene and the resonance at 0.85 ppm

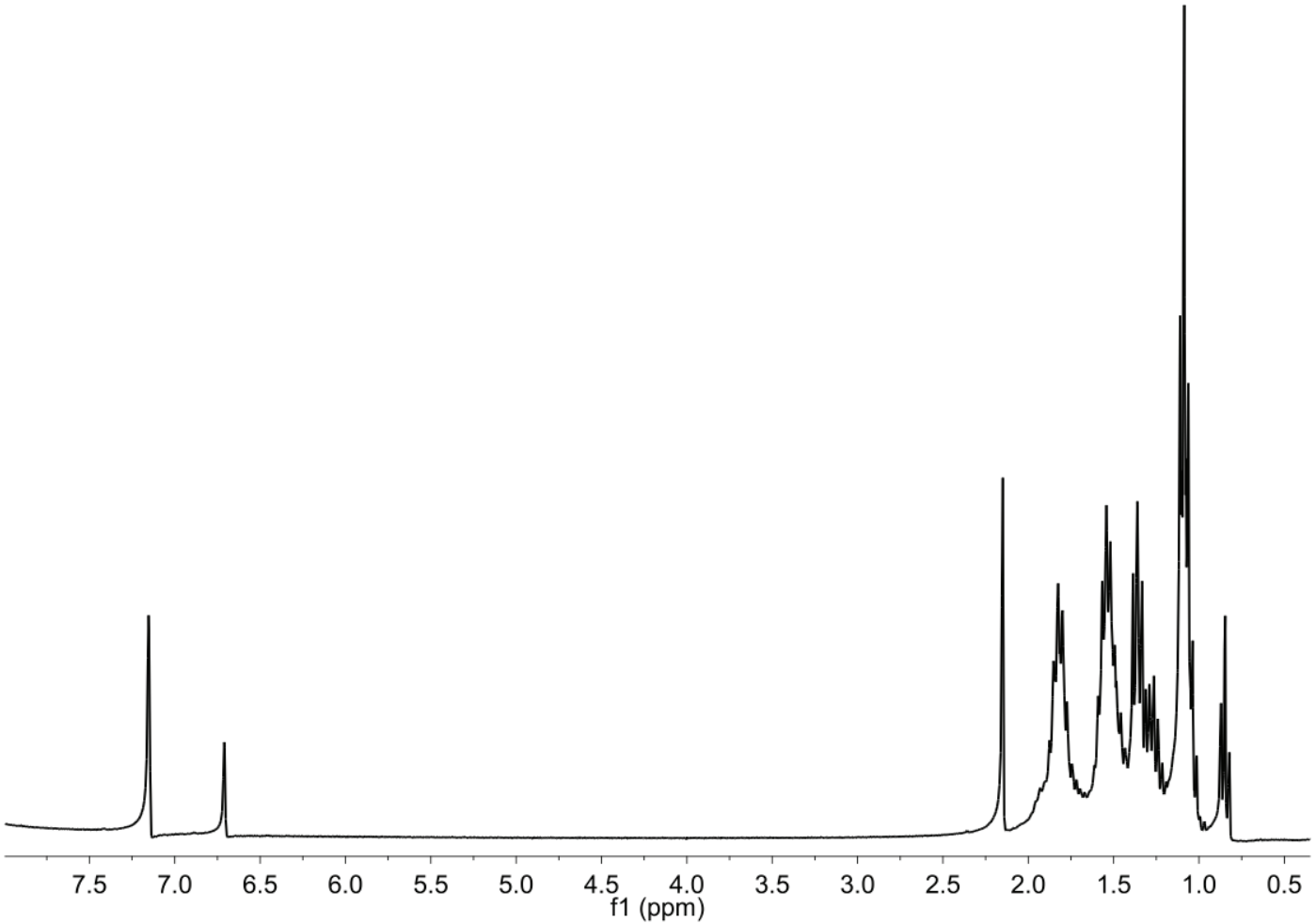

Figure 3-3. Typical ^{1}H QNMR spectrum before phasing is applied.

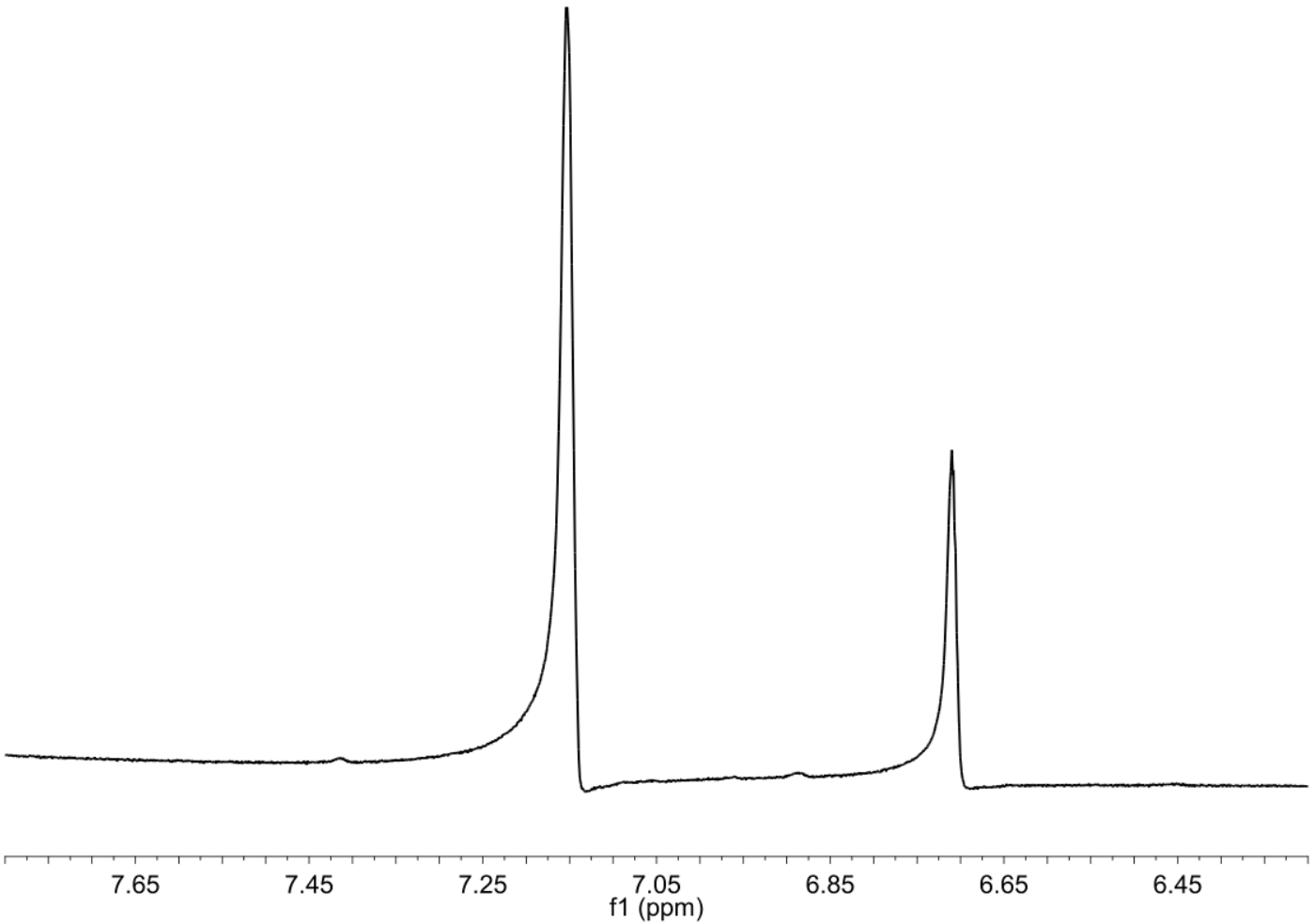

Figure 3-4. Expansion of aromatic region showing need for phasing.

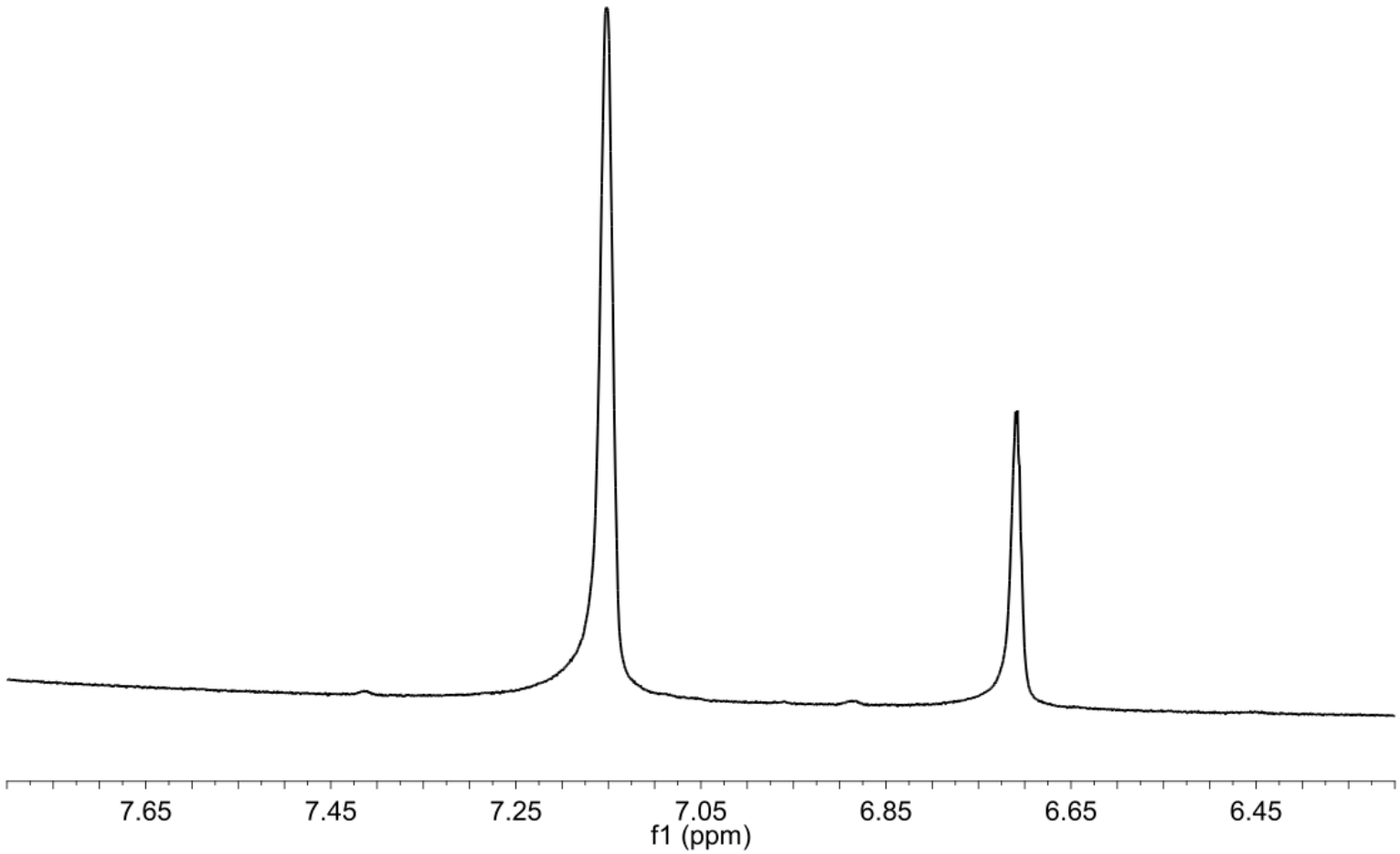

Figure 3-5. Aromatic region after the application of zero order phasing.

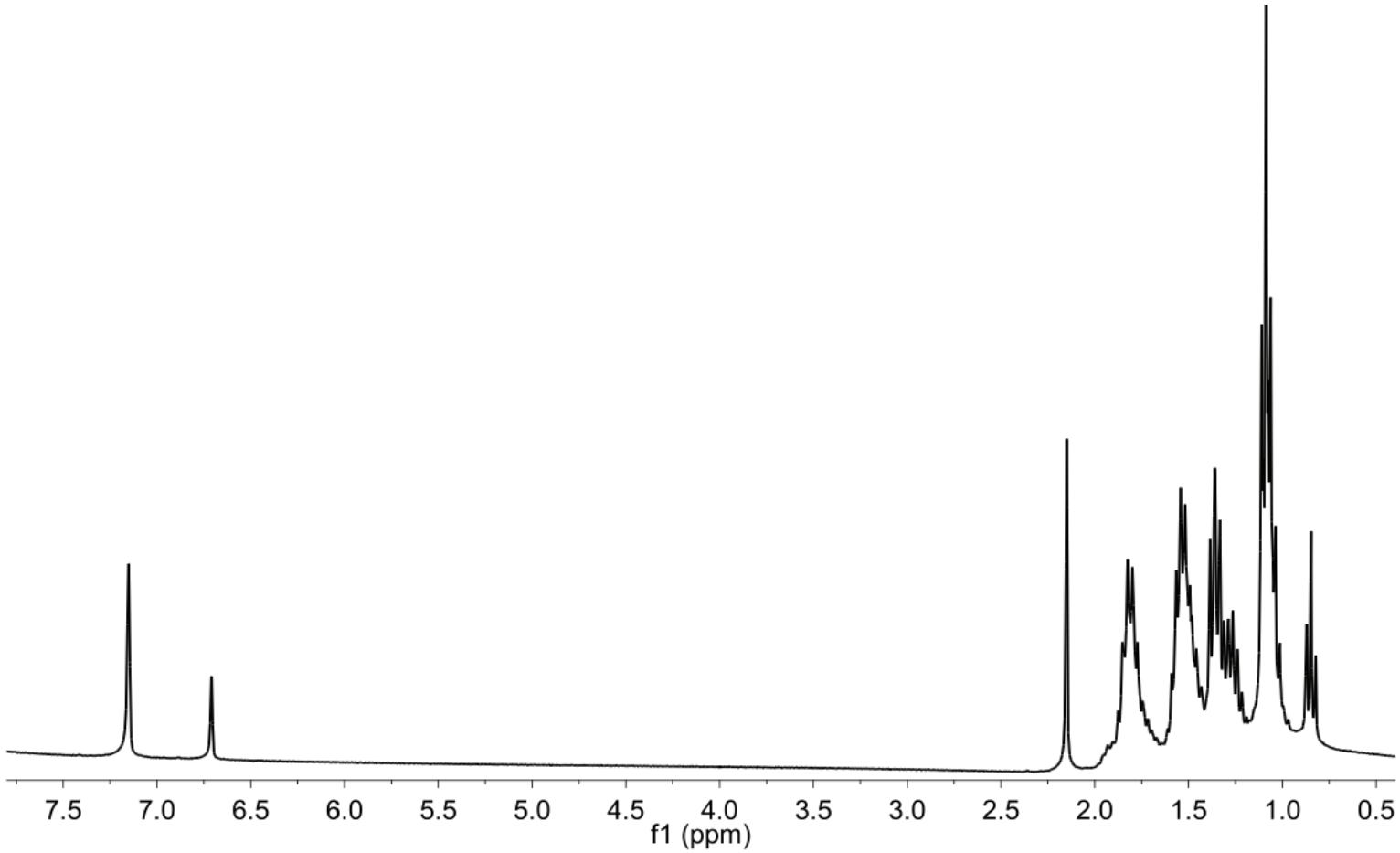

Figure 3-6. Effect of zero order phasing on the entire spectrum.

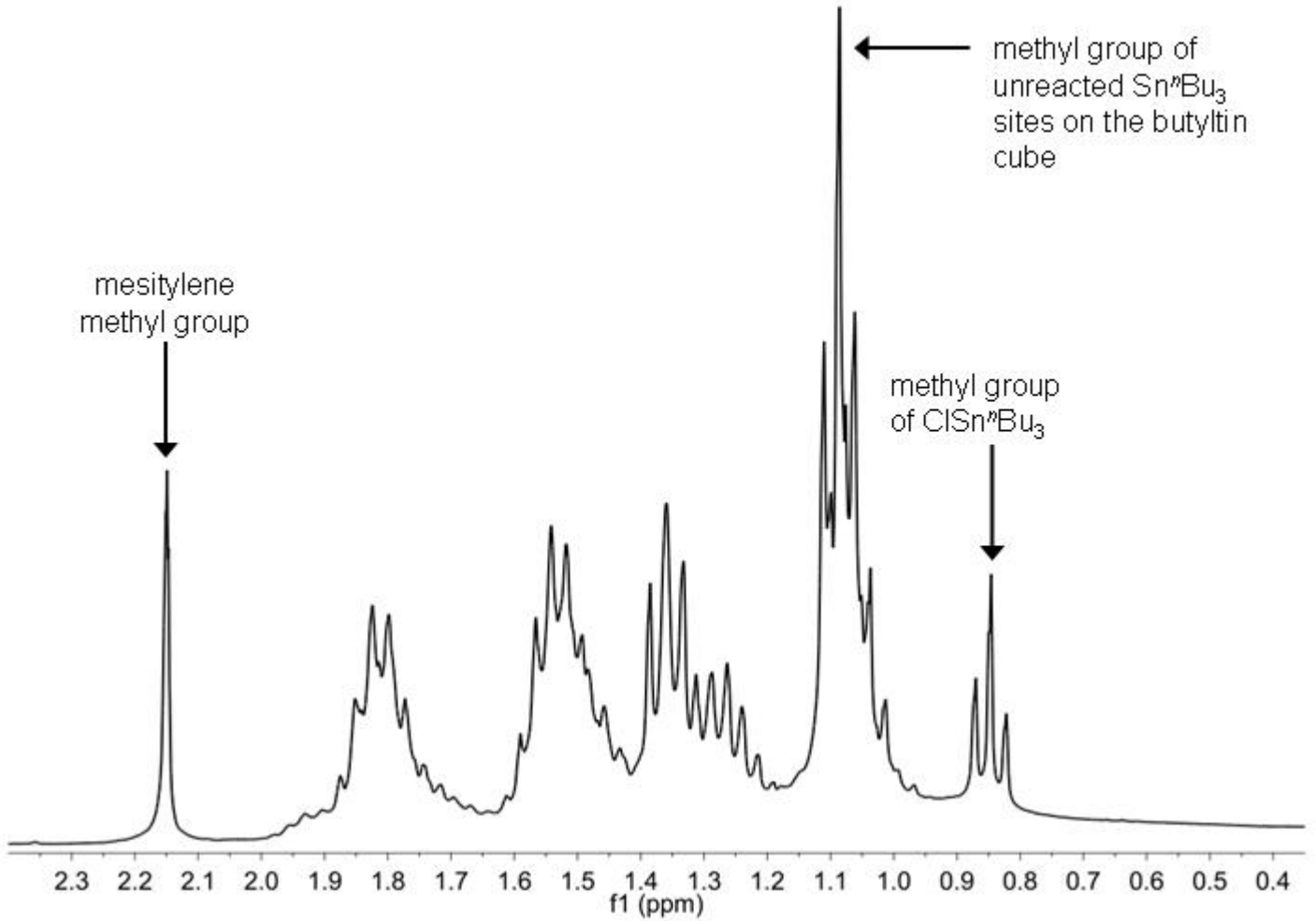

Figure 3-7. Expansion of 0.4 to 2.4 ppm region. Only zero order phasing has been applied.

is due to the methyl protons in $ClSn^nBu_3$. First order phasing was applied to bring the baseline on each side of the group of resonances between 2.15 and 0.85 ppm to the same level. That is to say a straight horizontal line drawn from the baseline immediately below the 2.15 ppm resonance would intersect the baseline immediately above the 0.85 ppm resonance.

Figure 3-8 shows the expansion after proper application of first order phasing. A third order polynomial baseline correction was then applied.

The properly phased spectrum with corrected baseline is shown in Figure 3-9. An expansion of the area with the resonances of interest is shown in Figure 3-10. Integration for the quantitative analysis was done strictly from 2.20 to 2.10 and 0.90 to 0.80 ppm for the methyl resonances of mesitylene and tri-n-butyltin chloride, respectively, in every spectrum.

The area of the resonance due to the aromatic mesitylene protons was also measured for purposes of estimating the error involved in processing the spectrum. The integral for that resonance was measured between 6.80 and 6.60 ppm. The typical error associated in the measurement of the two different types of protons was about 1.3%. The greatest error seen in that measurement was 3.5%.

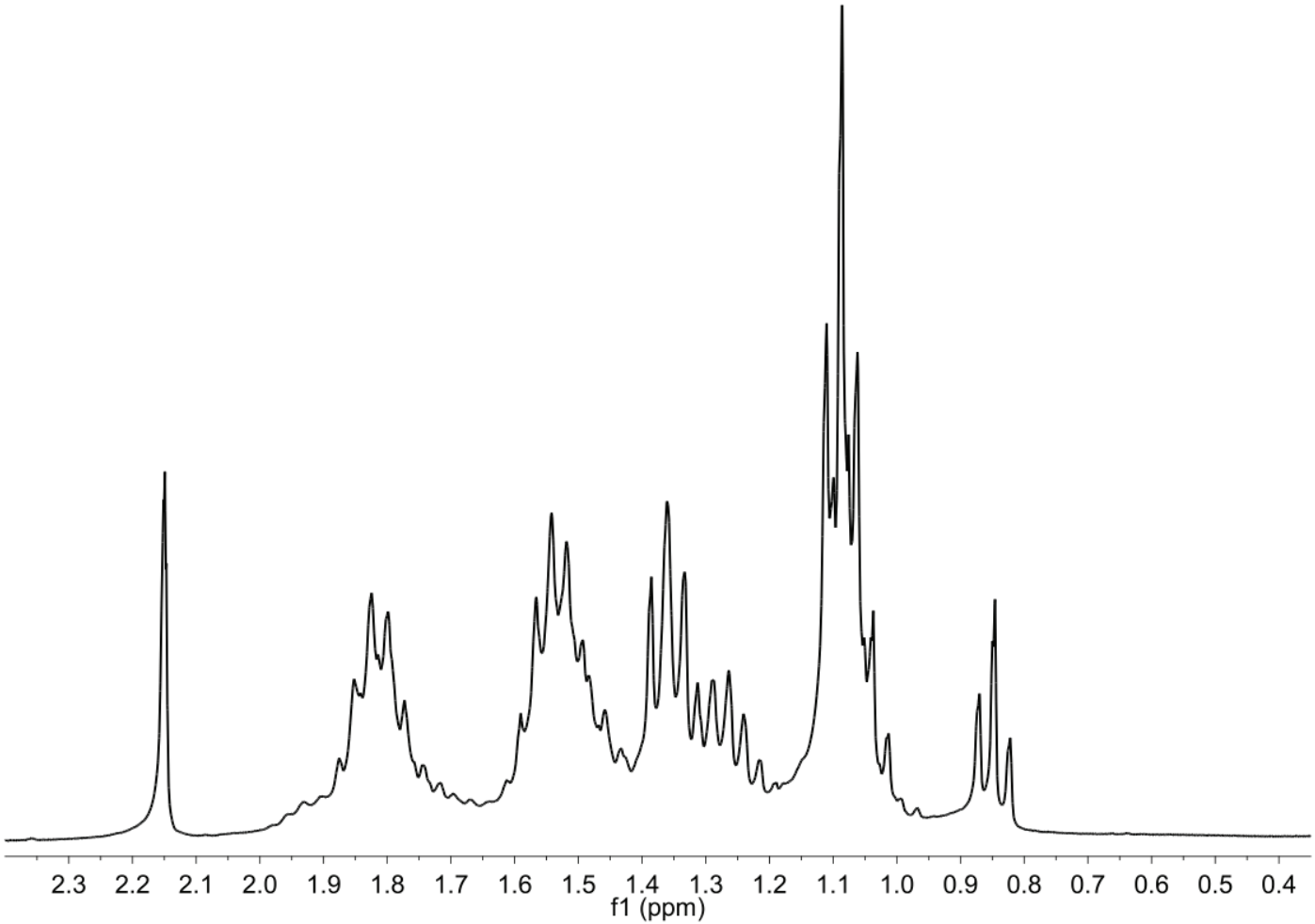

Figure 3-8. Expansion of 0.4 to 2.4 ppm region with zero and first order phasing applied.

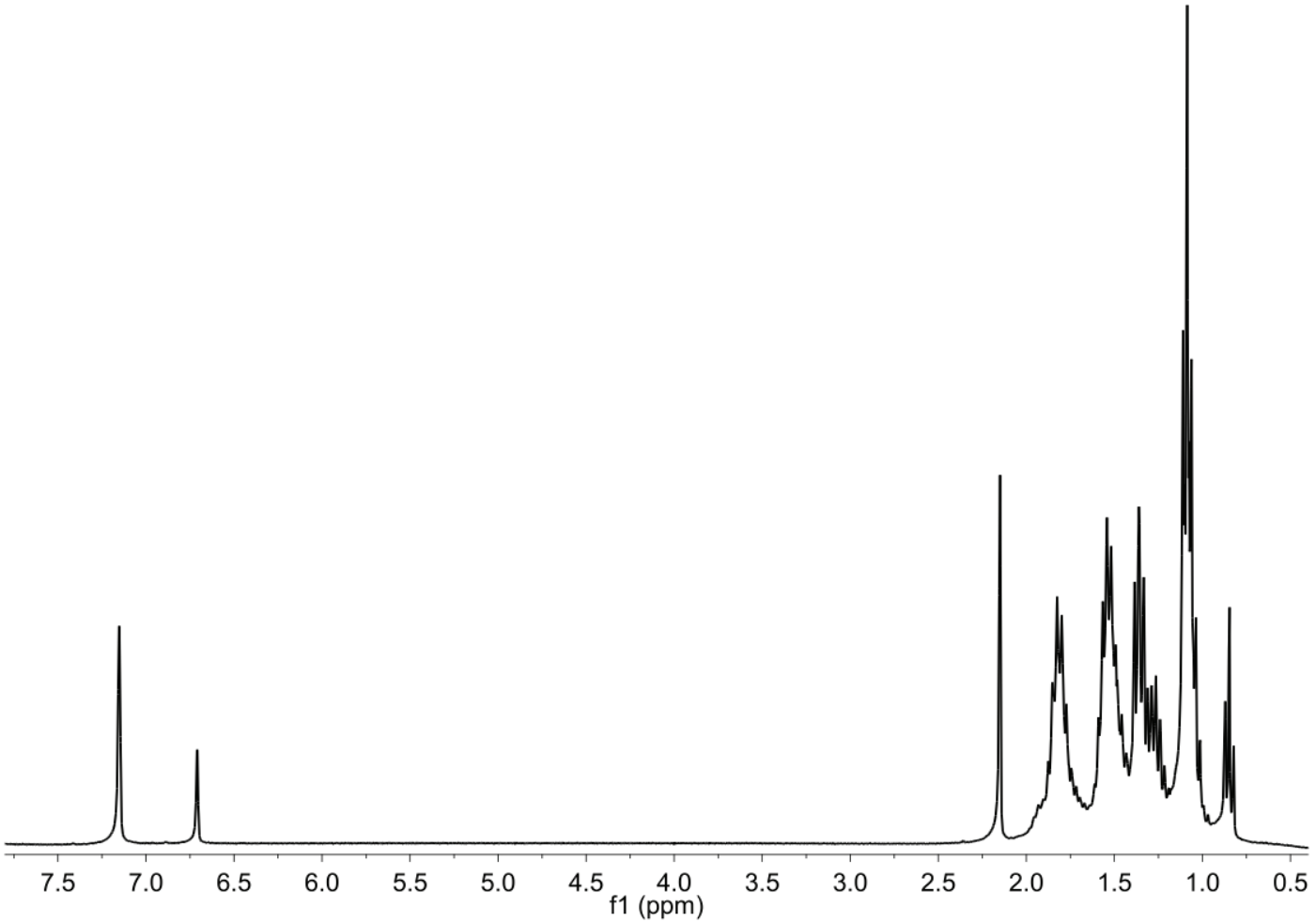

Figure 3-9. Entire spectrum after phasing and background correction.

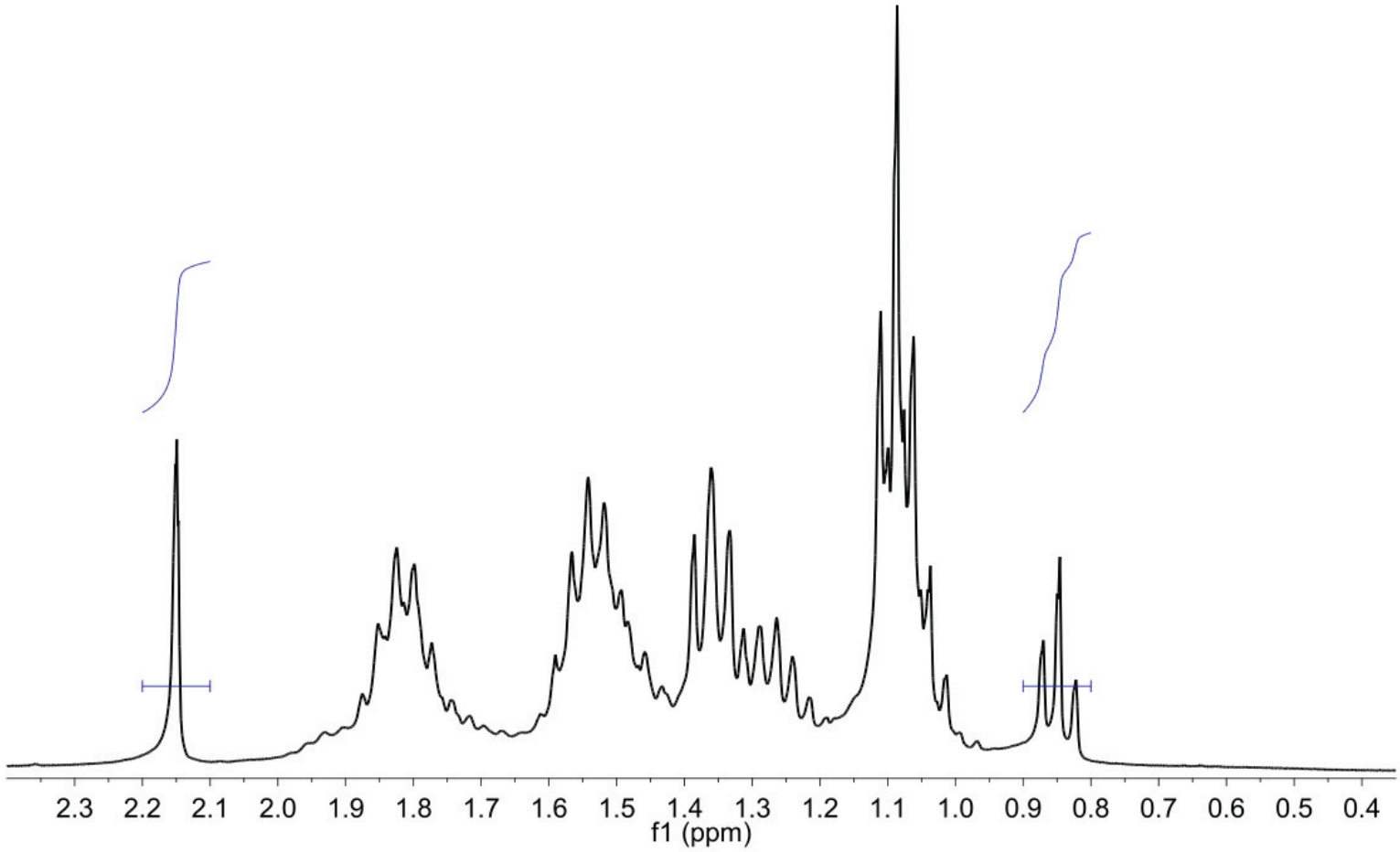

Figure 3-10. Expanded spectrum showing the areas integrated for quantitative analysis.

Quantitative ^{1}H NMR Results

Reaction of Tributyltin Cube with Silicon Tetrachloride

Two systems were analyzed using quantitative NMR. First, the reaction of a limiting amount of $SiCl_4$ with tributyltin cube was examined. This was done because the formation of a cross-linked solid during the reaction was not observed although it is expected based upon the work of Clark.[56,59] ^{29}Si MAS NMR spectra from Clark's work show that even at ratios as high as 2 $SiCl_4$ per methyltin cube 4-connected linking sites, $Si(OSi\equiv)_4$ (commonly known as Q^4 sites), were almost exclusively formed in the resultant solid products. However, this was not found to be the case for the tributyltin cube.

The reaction of 0.5 equivalents of $SiCl_4$ per tributyltin cube was monitored over 42 hours using QNMR. The first two-thirds of an hour of the experiment were conducted at room temperature. Afterwards, the temperature was raised to 80 °C and the reaction was monitored at various times. The complete results are presented in Table 3-2 below. The times quoted in that table are referenced from the start of the reaction.

The relationship between the areas their methyl group peaks and the amounts of mesitylene $ClSn^nBu_3$ are given in Equation 1 below. That relationship simplifies to the one shown in Equation 2. When measured at 0.67 h

$$\frac{\text{moles } ClSn^nBu_3}{\text{area of } ClSn^nBu_3 \text{ methyl}} = \frac{\text{moles mesitylene}}{\text{area of mesitylene methyl}} \qquad (1)$$

$$\text{moles } ClSn^{n}Bu_3 = \frac{\text{area of } ClSn^{n}Bu_3 \times \text{moles mesitylene}}{\text{area of mesitylene methyl}} \quad (2)$$

the integral values for the mesitylene and $ClSn^{n}Bu_3$ methyl groups were measured as 363,722 and 108,932 respectively. 2.82×10^{-5} moles of mesitylene and 1.06×10^{-5} moles of $SiCl_4$ were in the reaction mixture. Inserting the values given into Equation 2 gives the expression shown in Equation 3. The value of Equation 3 is given in Equation 4. Finally, the number of moles of $ClSn^{n}Bu_3$ present must be normalized to the amount of metal halide used in the reaction to determine the amount of links formed between butyltin cube building blocks and the metal center. This relationship is shown in Equation 5. Numerical values are inserted, and the expression is solved in Equation 6. Equation 6 provides the value given for the elapse time of 0.67 h in Table 3.2.

$$\text{moles } ClSn^{n}Bu_3 = \frac{108{,}932 \times 2.82 \times 10^{-5}}{363{,}722} \quad (3)$$

$$\text{moles } ClSn^{n}Bu_3 = 8.45 \times 10^{-6} \quad (4)$$

$$\frac{\text{moles } ClSn^{n}Bu_3}{\text{moles } SiCl_4} \quad (5)$$

$$\frac{8.45 \times 10^{-6}}{1.06 \times 10^{-5}} = 0.8 \quad (6)$$

The results clearly show that the reaction does not proceed in the same manner as that of the reaction of $SiCl_4$ with methyltin cube. After two-thirds of an hour, less than one equivalent of chloride reacted per equivalent of $SiCl_4$ on average. After 41.5 hours or reaction time at 80 °C, mimicking Clark's reaction

Table 3-2. QNMR results for the reaction of butyltin cube with $SiCl_4$.

Elapsed Time (h)	Temperature (°C)	Equiavlents $ClSn^nBu_3$ Produced per $SiCl_4$ (±0.1)
0.67	23	0.8
1.5	80	1.2
19.5	80	1.6
41.5	80	1.9

conditions, an average of nearly two equivalents of chloride reacted per equivalent of $SiCl_4$. This is much less than the average of four equivalents of chloride reacted per equivalent of $SiCl_4$ determined by Clark under similar reaction conditions.

In order to achieve typical heterogeneous catalyst compositions of one to two weight percent of a metal dispersed in a material, it is important to be able to cross-link the butyl tin cube building blocks with a linker that contains a "catalytically inert" element such as silicon. This led me to examine the reaction of butyltin cube with the bis(pyridine) complex of $SiCl_4$, $SiCl_4 \cdot py_2$. $SiCl_4 \cdot py_2$ is a solid which readily sublimes and is easily prepared from the reaction of $SiCl_4$ with pyridine.[80] Hexanes and toluene were found to suitable solvents for the synthesis in lieu of the carbon tetrachloride used in the literature.

In a test reaction eight moles of $SiCl_4 \cdot py_2$ per mole of butyltin cube were added to a Schlenk vessel containing butyltin cube dissolved in toluene. The $SiCl_4 \cdot py_2$ is not soluble in the reaction mixture, and the compound is visible as large, dense particles. As the reaction progresses over a period of 18 hours a

flocculant solid becomes visible which is an indication that a reaction between $SiCl_4 \cdot py_2$ and the butyltin cube has taken place. Volatiles were removed *in vacuo*, and unreacted $SiCl_4 \cdot py_2$ was removed via sublimation.

The ^{29}Si MAS SSNMR of the product (Figure 3-11) shows that the product is a cross-linked solid material consisting of Si_8O_{20} cores linked by silicon species of several connectivities. The resonance centered at -43 ppm is a silicon group with a connectivity of one. As the connectivity increases the ^{29}Si chemical shift becomes more negative. The resonances centered at -68 and -89 ppm have connectivities of 2 and 3 respectively. The resonance centered at -112 ppm is from Q^4, $Si(OSi)_4$, species. The resonance centered at -102 ppm is due to unreacted tin sites that remain in the product.

The successful synthesis of cross-linked materials from the reaction of $SiCl_4 \cdot py_2$ and butyltin cube led to the decision to use $SiCl_4 \cdot py_2$ as the "catalytically inert" linker for the studies reported in this dissertation. The results of structural and catalytic studies contained herein demonstrate that the use of $SiCl_4 \cdot py_2$ as a second linking agent does not negatively affect the properties of the final product.

Reaction of Tributyltin Cube with Titanium Tetrachloride

In contrast with $SiCl_4$, $TiCl_4$ reacts quickly with butyltin cube and forms a precipitate within minutes of its addition. QNMR studies of the reaction between titanium tetrachloride and tributyltin cube show that the reaction is complete within one hour. The results shown in Table 3-3 below show that the average

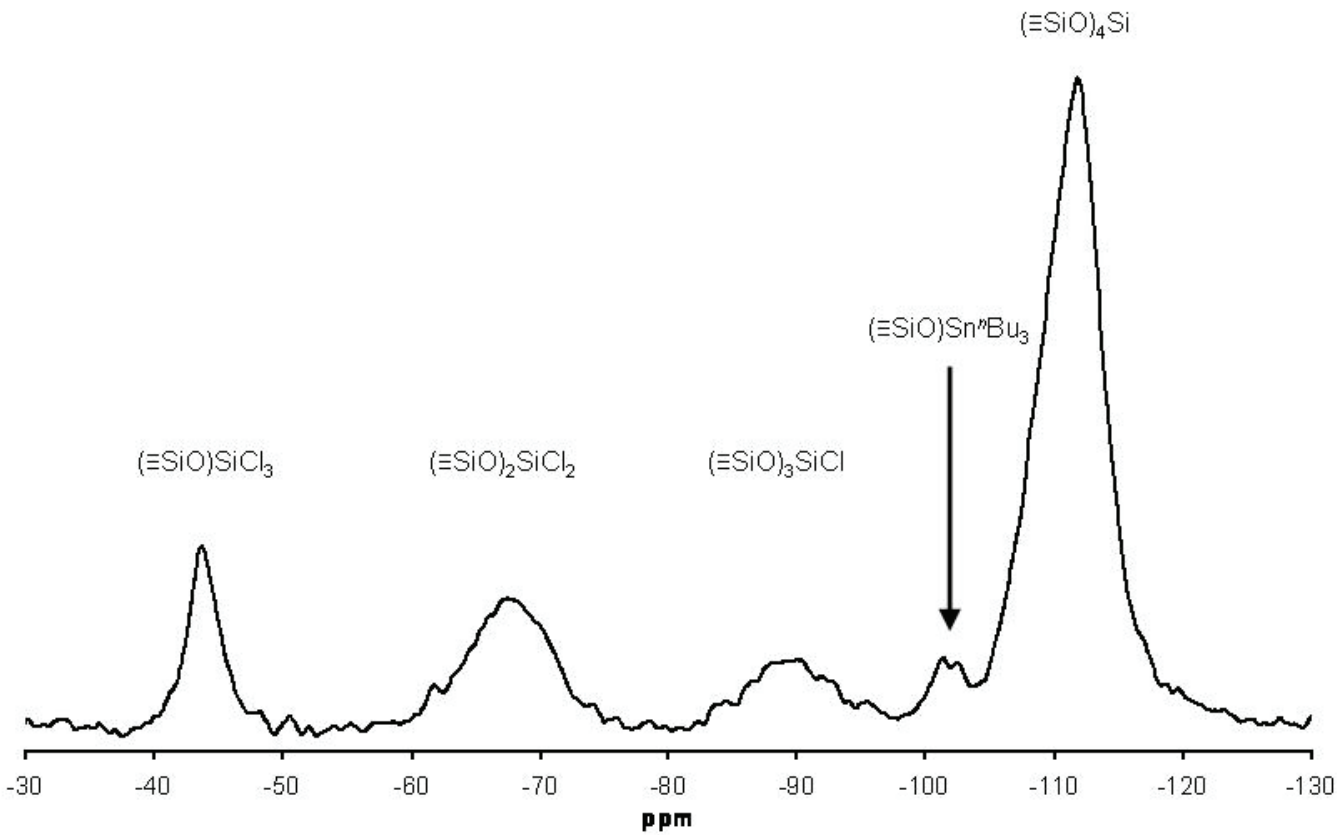

Figure 3-11. ^{29}Si MAS NMR spectrum of the product of the reaction between butyltin cube and $SiCl_4 \cdot py_2$.

Table 3-3. QNMR results for the reaction of butyltin cube with $TiCl_4$.

$TiCl_4$ per butyltin cube	Cl reacted per $TiCl_4$ (±0.1)
0.25	4.0
0.5	3.7
0.75	3.4
1.0	3.1
2.0	2.0

connectivity of the titanium decreases as the stoichiometric ratio of $TiCl_4$ to butyltin cube increases. At a low $TiCl_4$ to tributyltin cube ratio of 0.25 to 1 sites with a connectivity of 4, $Ti(OSi\equiv)_4$ centers, are formed exclusively (Figure 3-12). As the stoichiometric ratio is increased the average connectivity of the titanium sites decreases. When an equimolar ratio of $TiCl_4$ to butyltin cube is used the average connectivity of titanium is very close to three. If the ratio of $TiCl_4$ to butyltin cube is doubled to 2 to 1, the average connectivity of the titanium is 2.

The QNMR results for the reaction of titanium tetrachloride with tributyltin cube are definitive. Stoichiometry clearly affects the average structure of the product. At low $TiCl_4$ to tributyltin cube building block ratios exclusively 4-connected linking Ti groups are obtained. As the stoichiometric ratio is increased the number of Ti-O-Si bonds formed decreases leaving unreacted Ti-Cl groups in the material. QNMR also established that specific stoichiometric ratios can be used to produce materials with titanium sites of integral connectivity values.

Based upon the stoichiometric ratios provided by QNMR spectroscopy samples of titanium non-aqueous building block materials were synthesized for

further structural characterization. These materials will be referred to as the Ti-X series where "X" is a number that gives the average connectivity of the titanium sites in the material as determined by quantitative ^{1}H NMR spectroscopy. The sample designation, QNMR results, and the presumed structure of the titanium sites in the material are shown in Table 3-4 below. A schematic representation of the titanium connectivity with sample name is shown in Figure 3-12.

Infrared Spectroscopy

There are a number of reports in the literature that associate the presence of a relatively strong band at 960 cm^{-1} with the presence of tetrahedrally coordinated framework titanium, $Ti(OSi\equiv)_4$, in titanium on silica materials.[34,41,75,81-83] At the same time, however, Li, et. al. point out that there is evidence that the band may be due to surface hydroxyl groups (≡Si-OH) or defect sites in the silica

Table 3-4. Titanium non-aqueous building block sample designations with proposed structures.

Sample Name	Weight % Ti	TiCl4:butyltin cube	QNMR Results ClSnnBu3:TiCl4	Proposed Structure
Ti-4	0.90	0.25	4.0	Ti(OSi≡)4
Ti-3	3.45	1.0	3.1	Ti(OSi≡)3Cl
Ti-2	6.08	2.0	2.0	Ti(OSi≡)2Cl2
Ti-XS	N/A	8.0	N/A	Many Ti sites

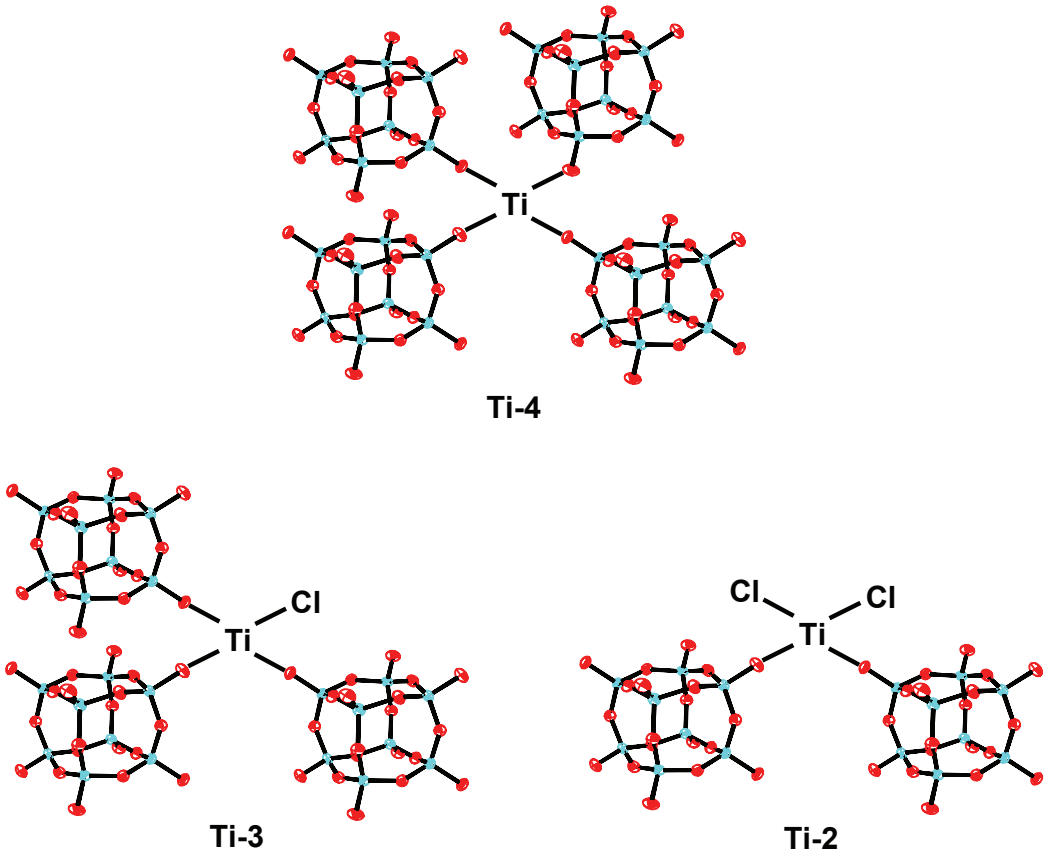

Figure 3-12. Schematic representations of the titanium sites in three titanium non-aqueous building block materials.

matrix.[84] It is also possible, that that a 960 cm^{-1} can be obscured by the strong, broad Si-O-Si bands in silica materials.

Li, et. al. state that the assignment of the 960 cm^{-1} to framework titanium is incorrect based upon the lack of resonance enhancement of this band in UV resonance Raman experiments.[84] Bordiga and co-workers refute this claim based upon several lines of evidence.[75] First, they show a linear correlation between the strength of the 960 cm^{-1} band and the amount of titanium incorporated into the framework of TS-1. Second, they note that an isolated titanium atom in a crystalline silica material can be considered a defect site. Third, they note that in TS-1 the band attributed to silanol groups is at 978 cm^{-1}. Fourth, they assert that resonance enhancement of the 960 cm^{-1} band in UV resonance Raman experiments is prohibited by selection rules for the resonance enhancement process. Finally, they note the work of Soult, et. al.[85] which reports a vibrational structure at 966 ± 24 cm^{-1} that is unambiguously attributed to titanium in the silicalite structure.

Scott and co-workers also make a contribution to the assignment of the band at 960 cm^{-1} observed in samples of titanium on silica.[34] For samples of silica partially dehydroxylated at 500 °C treated with $Ti(O^{i}Pr)_4$ or $Ti(NEt_2)_4$ IR bands are observed at 951 and 957 cm^{-1} respectively. In order to determine if the IR bands were related to the presence of titanium an isotopic labeling study was conducted. The reactions were repeated using silica partially dehydroxylated at 500 °C in which the surface hydroxyl groups had been labeled

with ^{18}O (80% enrichment level), and are shown in Figure 3-13. The IR band for the silica treated with $Ti(O^{i}Pr)_4$ did not shift and was assigned to a skeletal vibration of the isopropyl groups. However, the IR band for the silica treated with $Ti(NEt_2)_4$ shifted from to 936 cm^{-1}. On this basis, the band at 957 cm^{-1} for the silica treated with $Ti(NEt_2)_4$ was assigned to a Si-O-Ti vibration.

As the reader can see, there is some diversity of opinion regarding the assignment of the 960 cm^{-1} IR band. The description of the titanium sites in the literature that associates the 960 cm^{-1} with the presence of titanium is also not exact. However, the overall consensus that emerges from the literature is that the 960 cm^{-1} is a sign of the presence of Ti-O-Si bonds.

Mindful that some care should be used when IR spectroscopy is used to look for evidence of Ti-O-Si bonds in materials, the IR spectra of unreacted butyltin cube and the Ti-XS sample were compared (Figure 3-14). In the spectrum of the butyltin cube a very small, narrow shoulder at 960 cm^{-1} is visible on the broad Si-O-Si band centered at 1030 cm^{-1}. In the Ti-XS spectrum a strong, broad shoulder is visible at 950 cm^{-1}. This 950 cm^{-1} band is more intense than the Si-O-Si band at 1030 cm^{-1}. As Ti-XS has only cube-O-Ti-O-cube linkages in the material, the Ti-O-Si band is expected to be quite intense which is consistent with the 950 cm^{-1} band observed in Figure 3-14.

IR spectra for the Ti-4, Ti-3, and Ti-2 materials are shown in Figure 3-15. The spectrum of pure butyltin cube is included for reference. All the materials show bands near 950 cm^{-1}, although the bands in Ti-4 and Ti-3 are shifted to

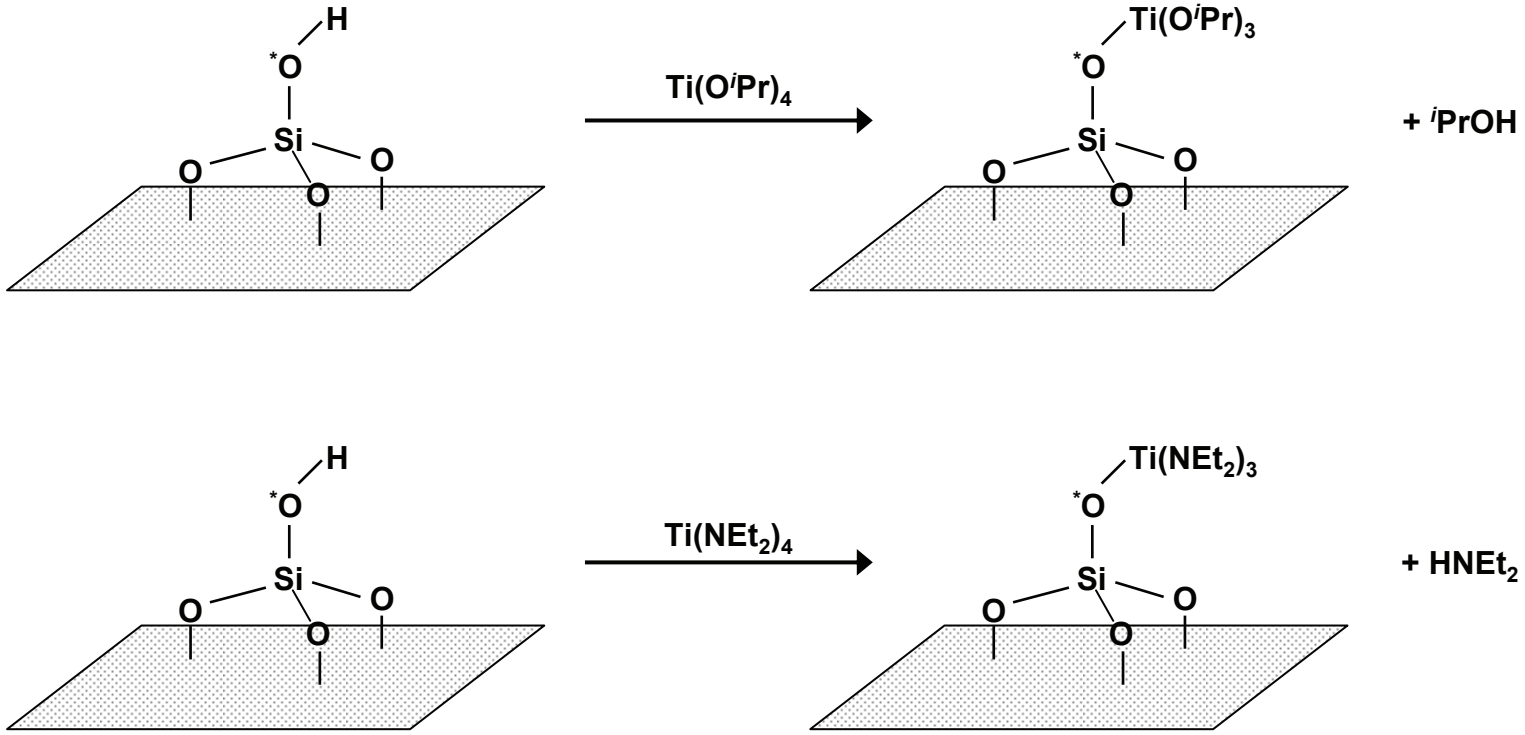

^{18}O enriched silica

Figure 3-13. Reaction of ^{18}O enriched silica with Ti(O^{i}Pr)$_4$ and Ti(NEt$_2$)$_4$. The isotope effect is only observed in the FT-IR spectrum for the Ti(NEt$_2$)$_4$ treated silica.

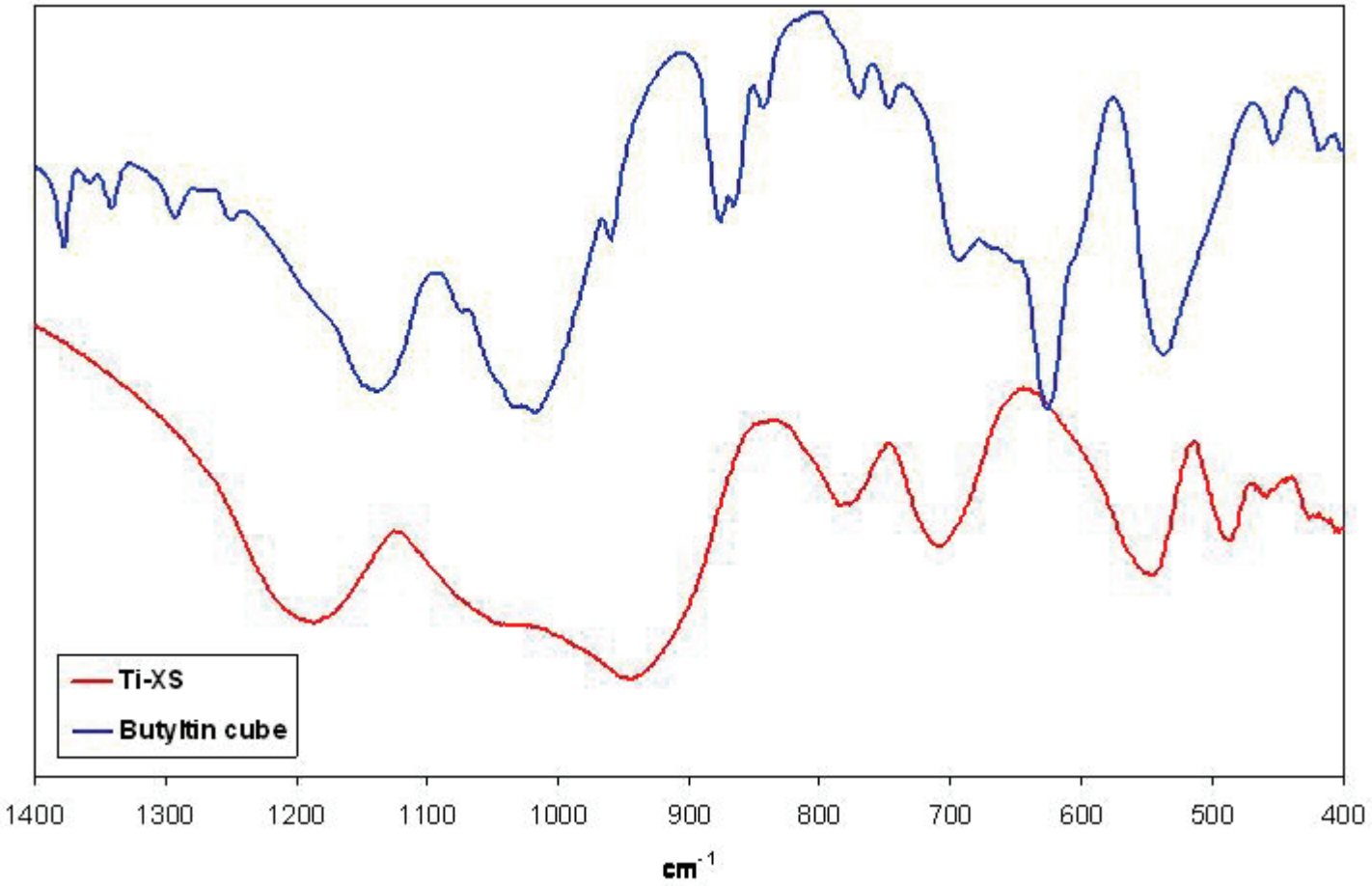

Figure 3-14. Overlay of the IR spectra of Ti-XS and pure butyltin cube.

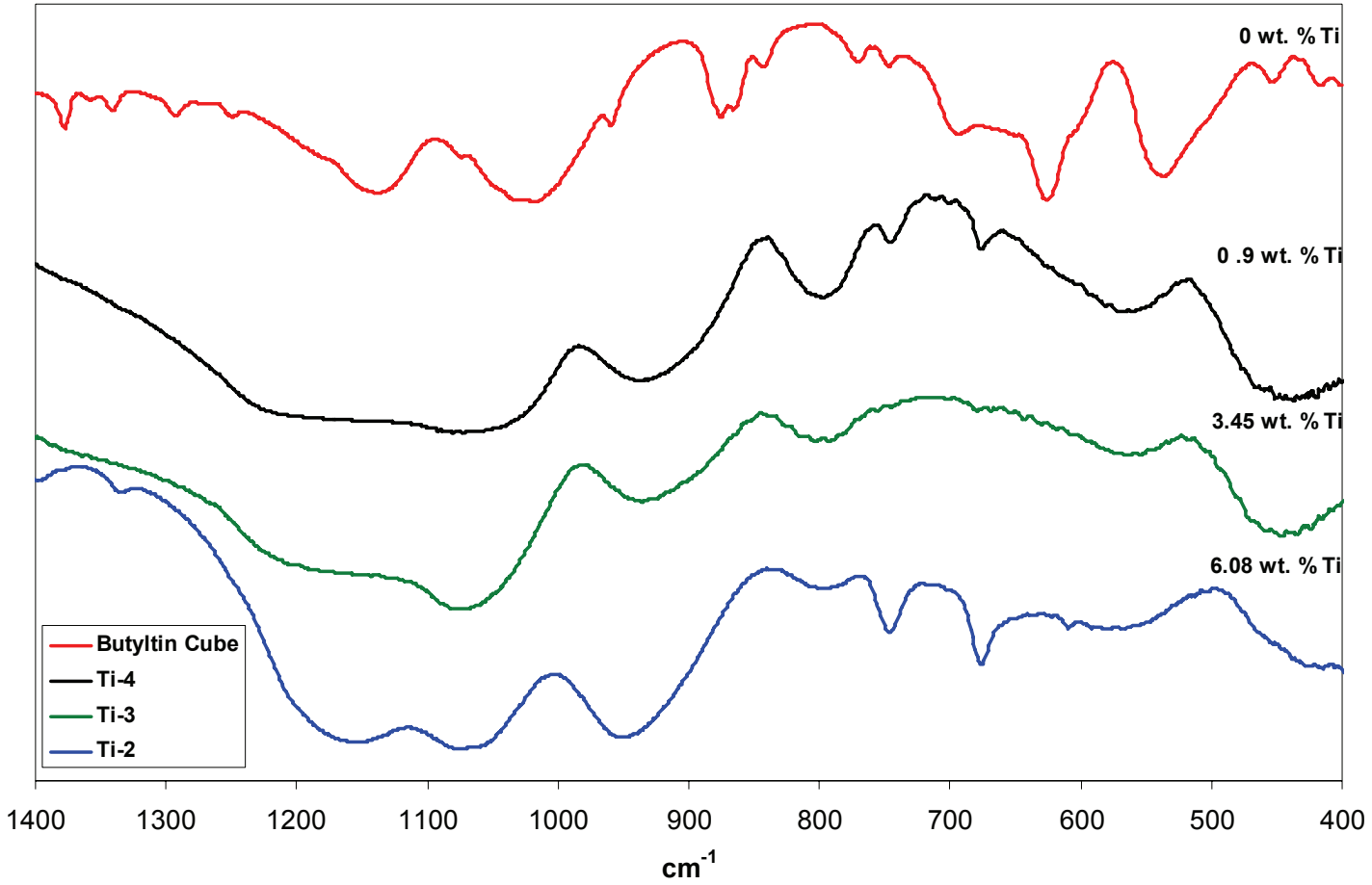

Figure 3-15. Overlay of the IR spectra of butyltin cube and the Ti-X series of NABB materials.

slightly lower wavenumber. While the IR spectra do not allow for quantitative analysis the intensity of the 950 cm^{-1} band increases with titanium loading. The 950 cm^{-1} in all the Ti-X materials is ascribed to the presence Ti-O-Si bonds.

Another important piece of information can be derived from the IR spectrum of Ti-XS. No band from hydroxyl groups is discernible in the 3500 to 3700 cm^{-1} region. This indicates that the syntheses of the Ti-materials were successfully conducted under rigorously anhydrous conditions, and that it is unlikely that hydrolytic condensation of the $TiCl_4$ occurred during the reaction.

Raman Spectoscopy

One article from the literature suggested that Raman spectroscopy could be used to aid in the identification of the titanium species in the sample.[86] Specifically, Raman spectroscopy was used to identify $(\equiv SiO)_2TiCl_2$ and $(\equiv SiO)TiCl_3$ species on the surface of partially dehydroxylated silica gel through bands attributed to Ti-Cl vibrations. A band at 404 cm^{-1} was assigned to the symmetric stretch of a Ti-Cl bond in a $–TiCl_3$ group.[86] A band at 435 cm^{-1} was assigned to the same kind of vibration in a $=TiCl_2$ group.[86]

Ti-XS was analyzed using Raman spectroscopy because it should contain a high density of Ti-Cl species bound to silica. Although the literature results were reproducible, the bands assigned to the $(\equiv SiO)_2TiCl_2$ and $(\equiv SiO)TiCl_3$ groups were not detected in Ti-XS or in any of the other non-aqueous building block samples containing titanium.

Anatase and rutile are the common polymorphs of synthetic titania.[87] Both of those polymorphs are detectable by Raman spectroscopy,[88] with anatase being the most common form of titania detected in samples of titanium on silica.[81,89-92] Furthermore, anatase TiO_2 has strong Raman bands which are discernable at low concentrations.[91] Spectra of samples that contain anatase TiO_2 show Raman bands at 140, 390, 513, and 637 cm^{-1}.[89] Raman bands typical of the rutile phase occur at 143, 235, 447, and 612 cm^{-1}. No Raman bands for anatase or rutile titania were found in samples Ti-4, Ti-3, and Ti-2. Bands from anatase or rutile titania were also not observed in samples of the three materials that had been calcined at 550 °C for 24 hours.

These observations lead us to conclude that the titanium sites in the titanium non-aqueous building block materials are isolated and atomically well-dispersed. Furthermore, the position of the titanium centers in these materials is so well-fixed that phase separation into TiO_2 and SiO_2 could not occur even at relatively high titanium loadings of six weight percent.

X-ray Absorption Spectroscopy

X-ray absorption spectroscopy (XAS) is a direct method for experimentally probing the electronic and physical characteristics of materials.[93] Using data collected around a given X-ray absorption edge (K, L_I, L_{II}, etc.) it is possible to probe the electronic characteristics and structure around a particular element in a material. The dominant form of interaction between X-rays of proper energy and an atom is the photo-ionization of an electron from one of the core shells of the

atom.[93] Ionization is accompanied by an abrupt jump in the absorbance called the absorption edge which is measurable as a drop in the intensity of transmitted light at the ionization energy. The absorption edge is used as a point of reference when speaking about XAS data.

Raw XAS spectra are typically divided into two parts for analysis. X-ray adsorption near edge spectroscopy (XANES) describes the part of a spectrum that is near the absorption edge. XANES was defined by Bare to be data within 50 eV of the ionization edge.[94] However, Bare points out that XANES is widely used (as it will be here) to describe data that includes pre-edge features (features below the ionization edge) as well as the spectrum up to approximately 50 eV above ionization edge. "XANES is strongly sensitive to formal oxidation state" and the symmetry of the absorbing atom.[95] Extended absorption x-ray fine structure (EXAFS) refers to data that is greater than 50eV above the ionization edge. Structural models based upon EXAFS data are used to determine the distances, coordination number, and species of the neighbors of the absorbing atom.[95]

The normalized XAS spectra collected at NSLS for the Ti-4, Ti-3, and Ti-2 non-aqueous building block materials are given in Figures 3-16, 3-17, and 3-18 respectively.

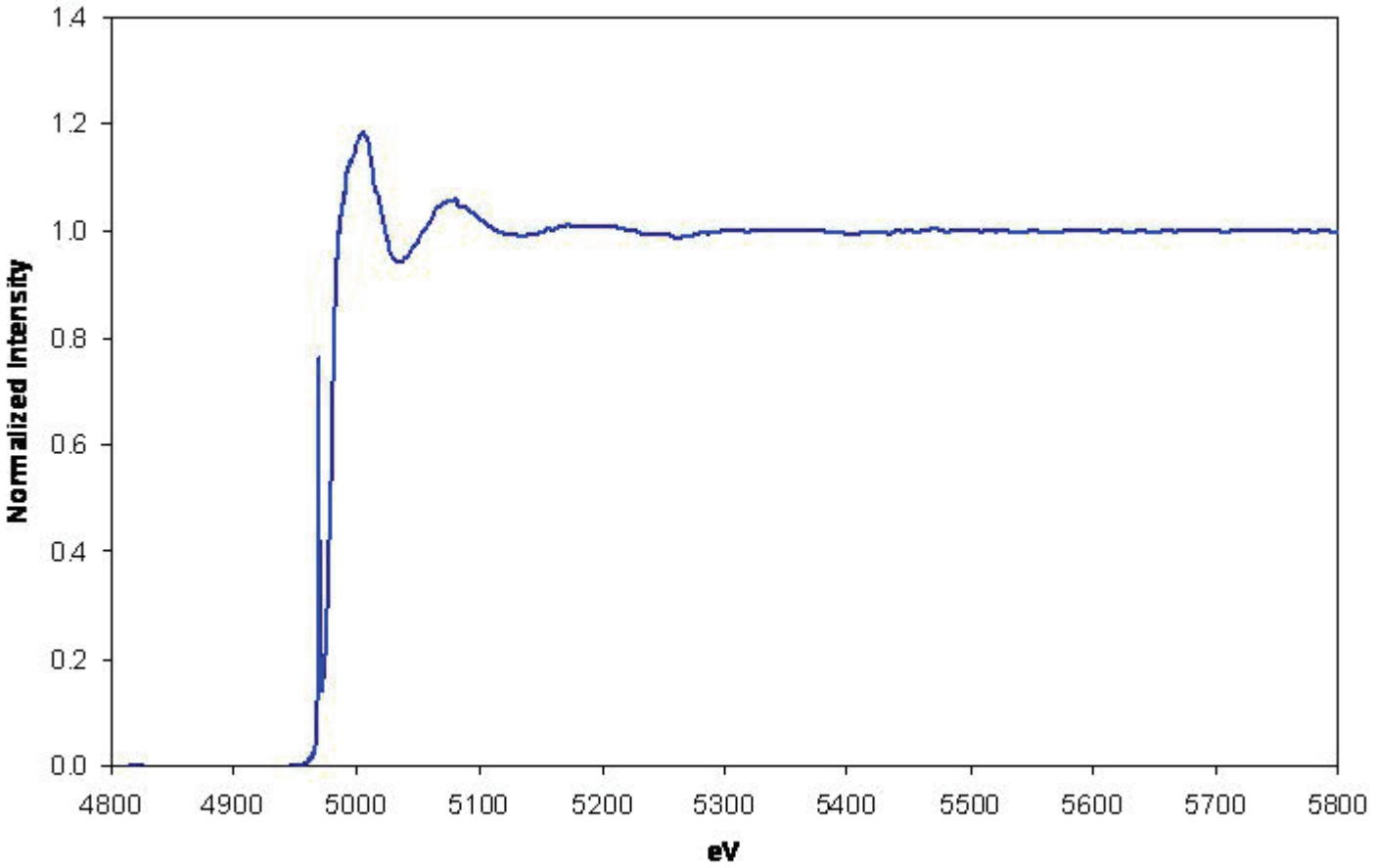

Figure 3-16. Normalized XAS spectrum for Ti-4.

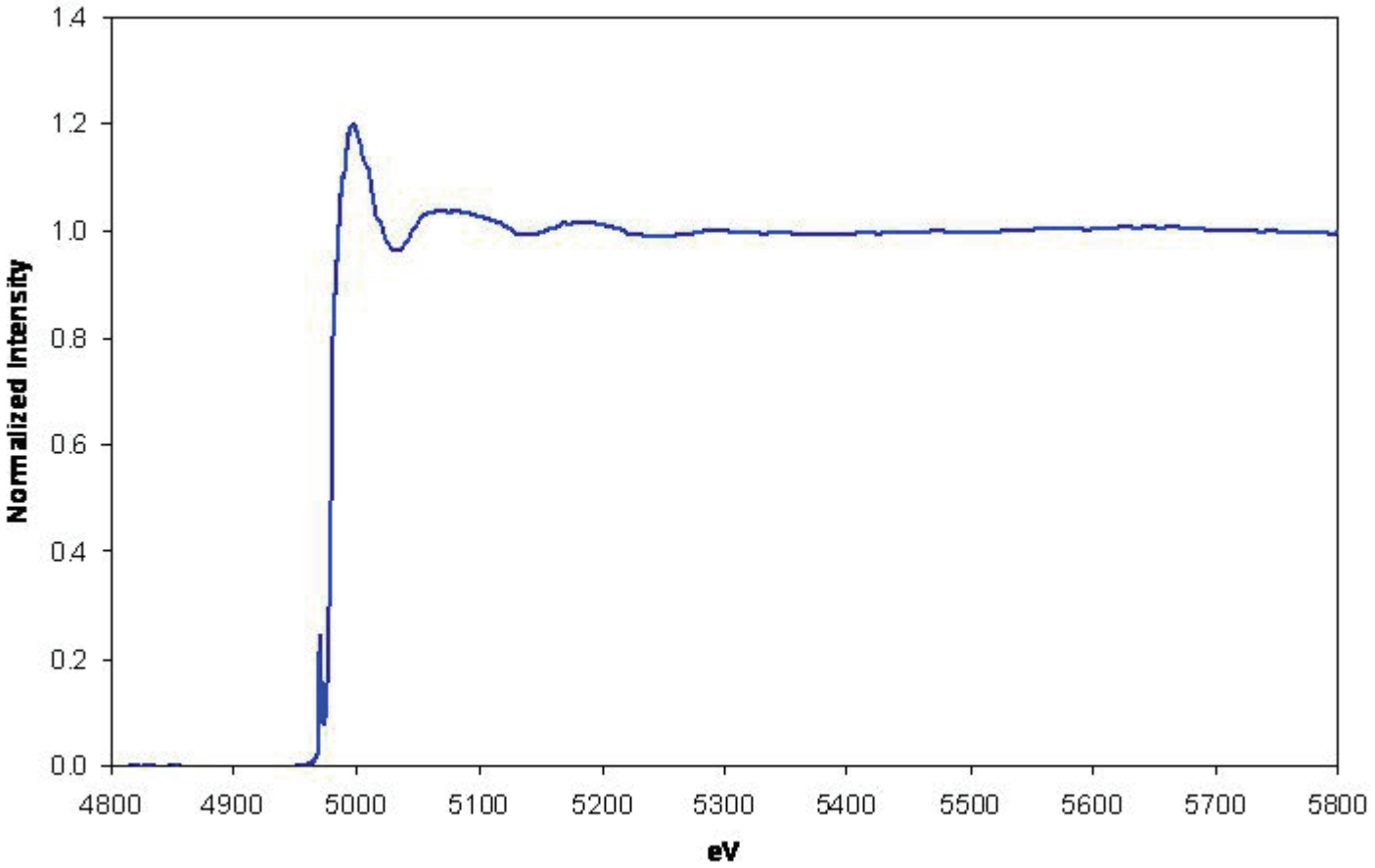

Figure 3-17. Normalized XAS spectrum for Ti-3.

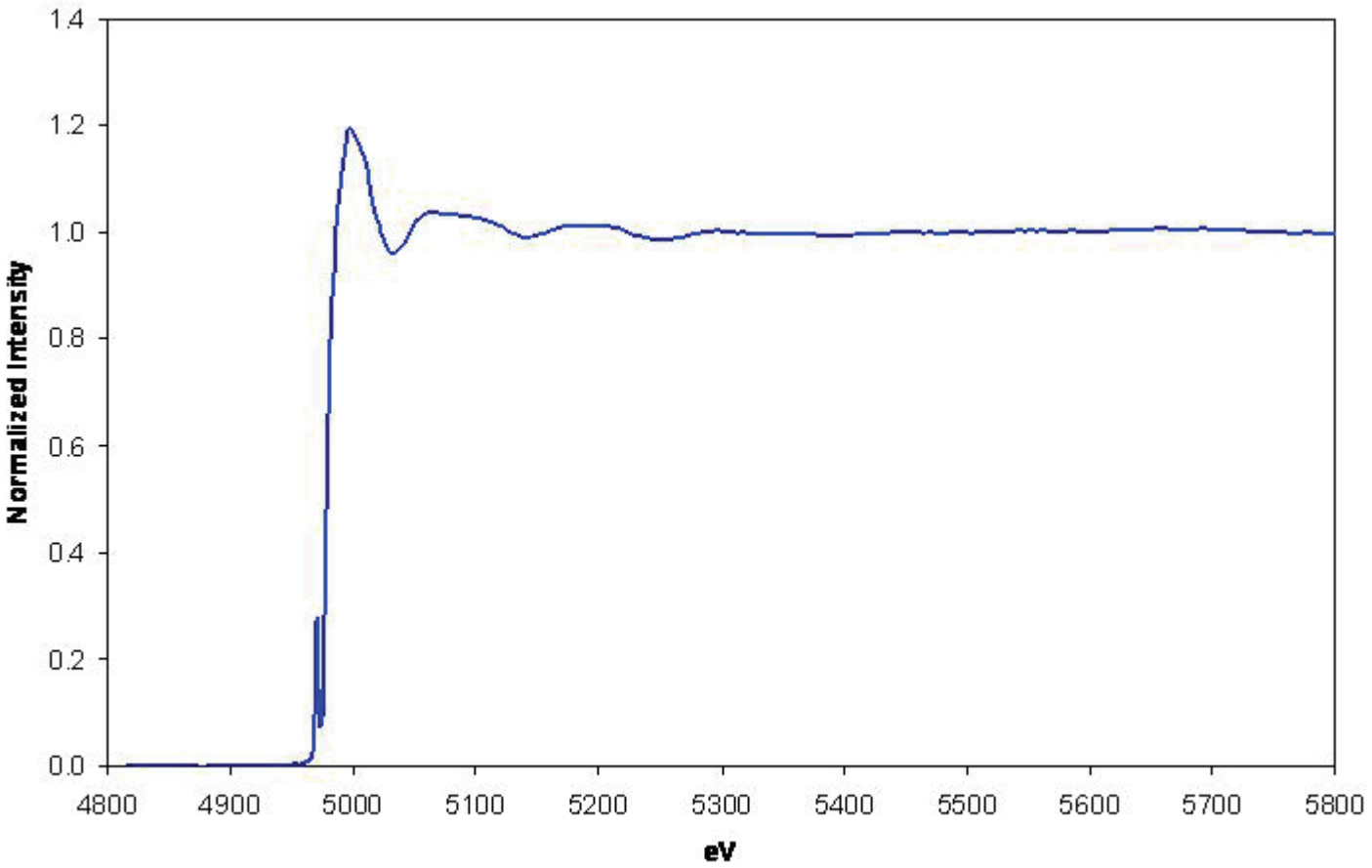

Figure 3-18. Normalized XAS for Ti-2.

XANES

It is well known that a strong pre-ionization edge feature in the XANES region is associated with the presence of titanium in a tetrahedral or pseudo-tetrahedral configuration.[30,31,41,96] The height of the feature is normally 70 to 80% of the normalized edge jump. The feature results from a 1s to 3d transition that is formally allowed only when no center of inversion is present at the absorbing metal center.[97] Practically speaking, this means that a strong, sharp pre-edge feature is observed when titanium is in a tetrahedral state, and that only a weak pre-edge feature is observed for titanium is an octahedral coordination environment. The Ti-4, Ti-3, and Ti-2 samples all show relatively strong pre-edge features consistent with tetrahedral or pseudo-tetrahedral symmetry around the Ti center as seen in the spectra in Figure 3-19. The positions and normalized heights of the pre-edge features for the materials are summarized in Table 3-5.

Farges, Brown, and Rehr have correlated the position of the pre-edge feature and its intensity to identify the oxidation state of titanium atoms in various oxide compounds.[98] According to these researchers, the pre-edge feature of the Ti-4 sample at 4969.3 eV with a normalized height of 0.76 is consistent with pre-edge features observed for titanium compounds containing four coordinate titanium centeres. The positions of the pre-edge features for the Ti-2 and Ti-3 samples at 4970.4 and 4970.5 eV respectively are consistent with those observed for compounds containing five coordinate titanium centers. However, the normalized heights for the pre- edge features of those samples are lower

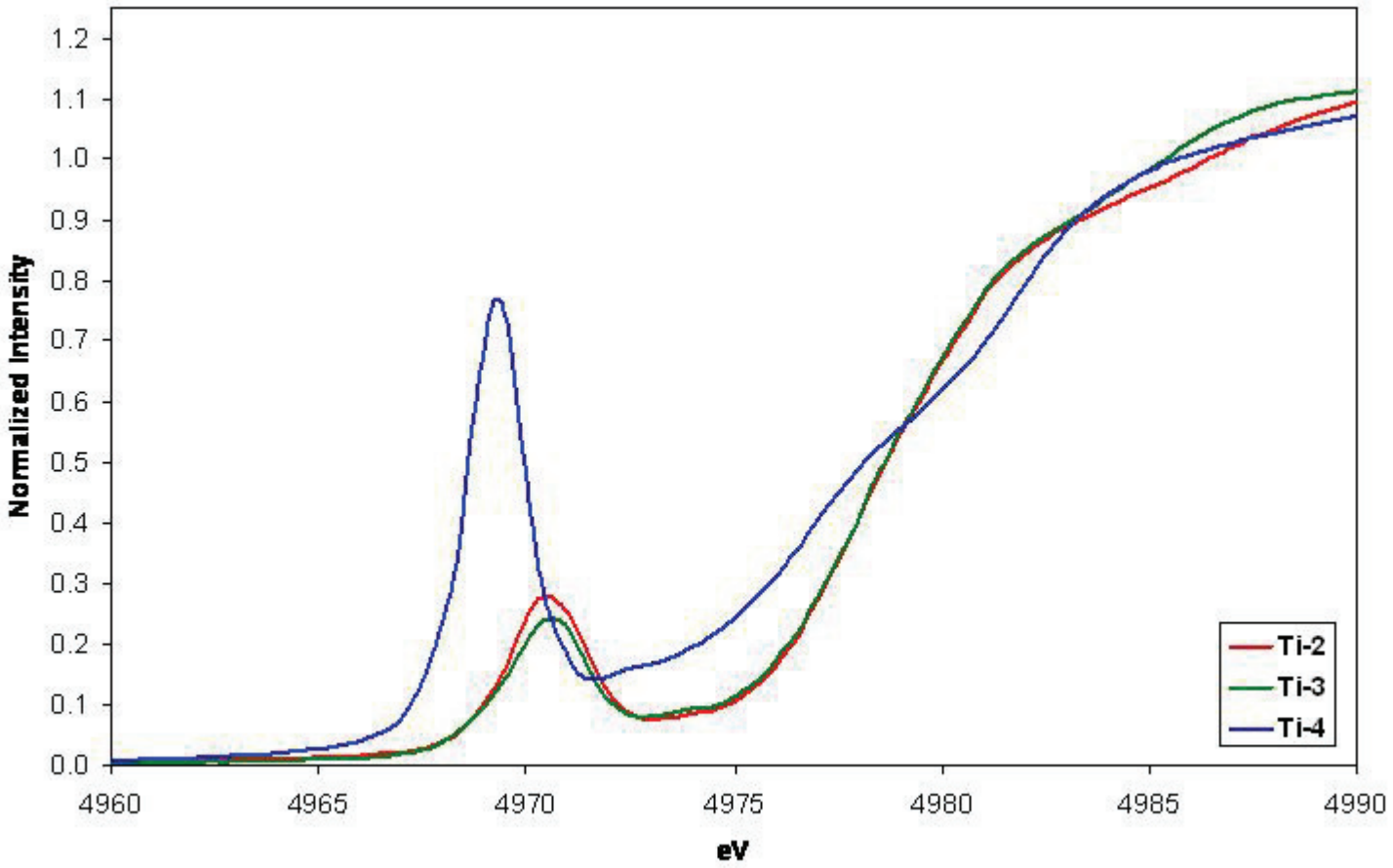

Figure 3-19. XANES spectra of titanium non-aqueous building block materials.

Table 3-5. Summary of XANES pre-edge features.

Sample	Pre-edge Feature Position (eV)	Normalized Height of Pre-edge Feature
Ti-4	4969.3 ± 0.2	0.76
Ti-3	4970.5 ± 0.2	0.28
Ti-2	4970.4 ± 0.2	0.24

than those reported for compounds containing five coordinate titanium centers.

While the work of Farges, Brown, and Rehr has been cited extensively in the literature, (Feb. 8, 2008 SciFinder search shows the article cited 131 times. The number of citations drops to 33 when the results are refined using the research topic "catalyst.") a comparison between the XANES spectra of the oxide compounds containing Ti in their work and the Ti NABB materials studied in our work may not be ideal. The Ti NABB materials contain chlorine directly bound to the titanium centers while the oxides studied by Farges, Brown, and Rehr do not. George, et. al. collected data in the XANES region for a series of titanium compounds containing chlorine.[99] All the compounds had titanium centers with tetrahedral or pseudo-tetrahedral symmetry. They found that the intensity of the pre-edge features of $TiCpCl_3$ and $TiCp_2Cl_2$ were dramatically lower than the intensity of the pre-edge feature observed for $TiCl_4$ as shown in Figure 3-20. The intensity of the pre-edge feature decreased as chlorine content of the compound decreased.

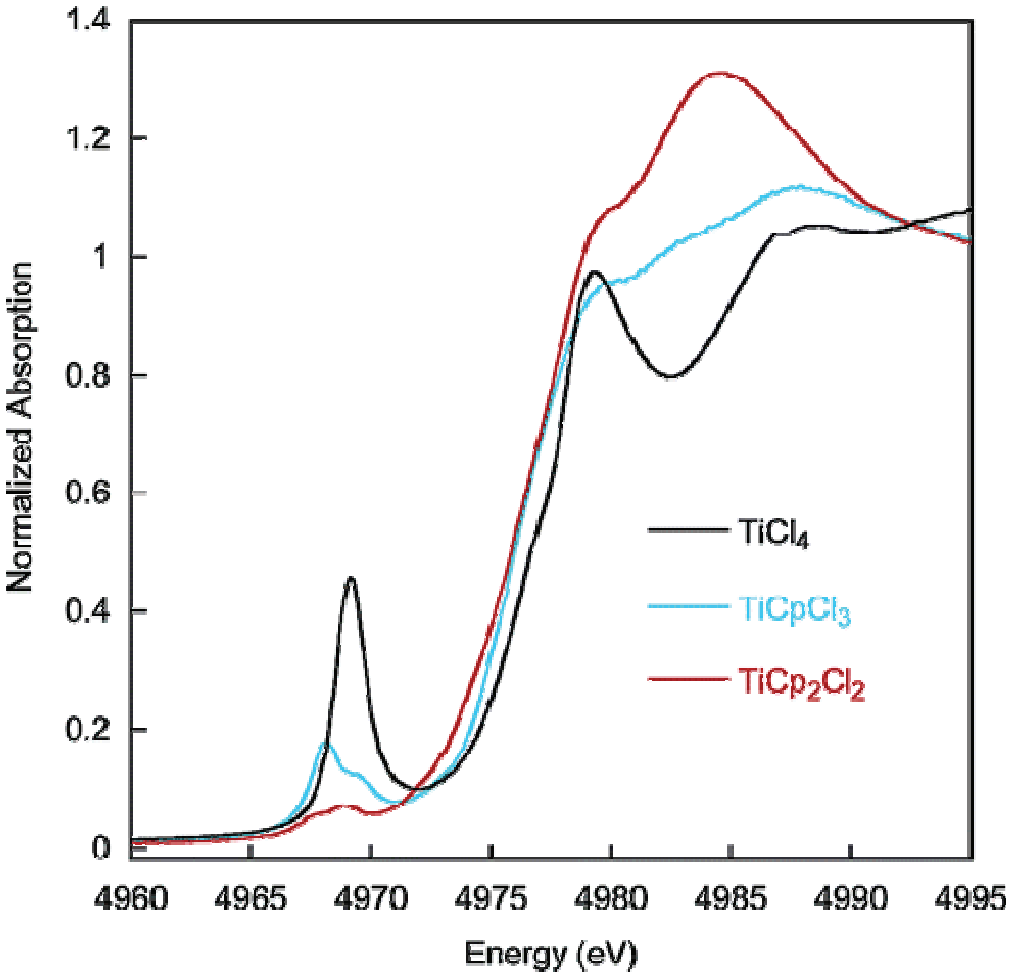

Figure 3-20. XANES spectra showing the effect of change in symmetry from tetrahedral to pseudo-tetrahedral, and 3d-4p mixing.

George, et. al. attribute the intensities of the pre-edge features they observed to differences in metal 3d–4p mixing between the compounds.[100] In a metal center with tetrahedral symmetry, mixing occurs between d orbitals of t_2 symmetry and 4p of t_2 symmetry. The mixing is enhanced by overlap of chloride ligand p orbitals with the metal 3d and 4p orbitals. As the symmetry of the metal center and number of chloride ligands in the molecule decrease the 3d–4p mixing decreases resulting in pre-edge features of lower intensity.

The behavior of the pre-edge features of the Ti-2 and Ti-3 samples is consistent with the effects of metal center symmetry and 3d–4p observed by George, et. al. Both samples have dramatically lower pre-edge intensities than that of the Ti-4 sample which contains tetrahedral titanium. The slightly greater intensity of the pre-edge feature of the Ti-2 material compared to that of Ti-3 may be from an enhancement of the 3d–4p mixing due to the greater number of chloride ligands on the metal center in Ti-2.

Another feature observable in the XANES spectrum of Ti-4 is a shoulder on the ionization edge at 4978.6 ± 0.2 eV. This feature is assigned to a 1s to 4p transition that is simultaneous with ligand-to-metal shakedown.[101-103] A 1s to 4p transition with simultaneous ligand-to-metal shakedown involves the excitation of a metal 1s electron to the vacant metal 4p orbitals. During the lifetime of this excited state, electronic character from a ligand is transferred to the metal 3d orbitals. The 1s to 4p transition with simultaneous ligand-to-metal shakedown is shown schematically in Figure 3-21.

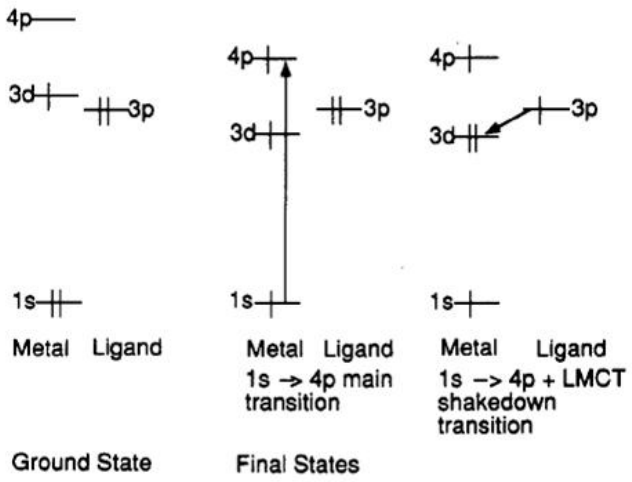

Figure 3-21. Schematic representation of the 1s to 4p ligand-to-metal shakedown transition.

The work of Finnie and co-workers shows that the strength of the 1s to 4p ligand-to-metal shakedown transition grows through the series of titanium ethoxide compounds: $Ti(OEt)_4 < Ti(OEt)_3Cl < Ti(OEt)_2Cl_2 < Ti(OEt)Cl_3$.[104] A similar trend was expected to be observed in the titanium non-aqueous building block material series: Ti-4 < Ti-3 < Ti-2. However, the 1s to 4p ligand-to-metal shakedown transition is not observed for the Ti-2 and Ti-3 samples. A similar series of Ti NABB materials synthesized by Richard Mayes using the methyltin cube building block did display growth of the ligand-to-metal shakedown transition as the number of the chloride ligands on the titanium center increases. At this time it is not understood why the band is not observed in the butyltin cube materials.

Based upon comparison of XANES data reported for titanium compounds in the literature with the XANES data collected for the titanium non-aqueous building block solids with, it is concluded that the titanium centers in all the samples are in the 4+ oxidation state and have tetrahedral or pseudo-tetrahedral symmetry. The weakness of the pre-edge features in the Ti-3 and Ti-2 samples compared to those presented by Farges and co-workers has been explained by comparison to compounds containing chloride ligands directly bound to titanium centers and, the pseudo-tetrahedral symmetry of the titanium centers in the Ti-3 and Ti-2 materials.

EXAFS

Analysis of the EXAFS portion of XAS data for titanium on silica is quite difficult. The first coordination sphere for most of those materials solely consists of oxygen atoms. As the majority of titanium on silica epoxidation catalysts have four oxygen atoms in the first coordination sphere, modeling the number of atoms in the first coordination sphere alone is not helpful in determining the structure of the titanium centers in those materials. The resolution of EXAFS experiments is governed by how far the EXAFS oscillations continue out in k-space as shown in the equation below.[105] Since the EXAFS oscillations for titanium K-edge spectra

$$\Delta R = \pi/2 \cdot k_{max}$$

of titanium on silica materials typically die off at about 12 k, differences in the radii of two scattering shells must be greater than 0.13 Å in order to be resolved under normal circumstances. This severely limits the ability to differentiate between a first coordination sphere oxygen bonded to hydrogen and a first coordination sphere oxygen bonded to silicon. The low Ti content of the samples, the possibility of multiple-scattering contributions at longer distances, and static disorder which enlarges Debeye-Waller factors make determination of the exact coordination environment beyond the first coordination sphere quite challenging and generally lowers confidence in conclusions drawn from such analyses.[104,106]

Despite the difficulties of determining the coordination environment of the second coordination sphere, J. M. Thomas and co-workers reported the structure

of a catalyst made from MCM-41 calcined at 550 °C grafted with titanocene dichloride, $TiCp_2Cl_2$, based upon the coordination number determined for silicon atoms in the second coordination sphere.[27] This material is commonly referred to as Ti↑MCM-41. In a follow up work Gleeson, et. al. detail the method they use to model the second coordination sphere of Ti↑MCM-41.[107]

Gleeson, et. al. present four models of titanium centers, shown in Figure 3-22, that could be present in titanium on silica catalysts. The authors state that, "it is not generally possible to differentiate experimentally between the above models [except (4), since Ti=O is about 0.1 Å shorter than a Ti-O in tetrahedral coordination] using conventional Ti K-edge XAS (both XANES and EXAFS) data analysis procedures." The authors go on to state that the titanyl species can be immediately discarded because it only contains three oxygen atoms in the first coordination sphere. However, their statement about being able to differentiate between titanyl, Ti=O, and Ti-O in a tetrahedral configuration due to the 0.1 Å difference in length between the two bonds reveals a key issue with their analyses and conclusions. Using the resolution equation for EXAFS experiments given above and a k_{max} of 13 (slightly greater than the k_{max} for the best set of data presented in the paper), differences in bond length of 0.12 Å can be resolved. It is *just* possible to differentiate between a Ti=O and a Ti-O bond from the *best* EXAFS data collected by the authors. This is a concern as the authors appear to be pushing and perhaps exceeding the bounds of their data in their analyses.

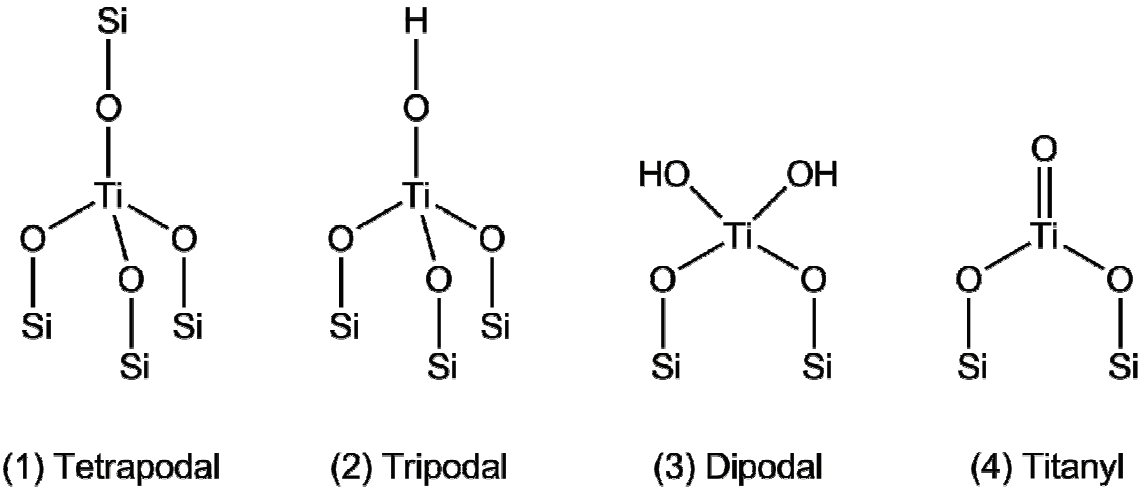

Figure 3-22. Structures of titanium centers possible in titanium-on-silica catalysts.

Furthermore, the authors repeatedly report distinct Ti–Si distances for a model that they cannot differentiate (are within 0.1 Å of each other) based upon the resolution of the data they collected. This decreases my confidence in the validity of the process they have used to determine coordination numbers for the second coordination sphere.

Gleeson, et. al. specifically state that they compared the fits of two different models to their EXAFS data. One model contained three Si atoms in the second coordination sphere. The second model placed four Si atoms in the second coordination sphere. Rather than comparing the statistical parameters normally used to compare fits of EXAFS data[33], the authors present their own statistical parameter called the fit index. The fit index includes a term to account for fit statistics, but what statistical parameters are included and their relative

weighting is not explained. The failure of the authors to present conventional statistical measures such as chi-squared and residuals in addition to their fit index is a concern.

Gleeson, et. al. conclude from their studies that the structure of the titanium centers in TS-1 is $Ti(OSi\equiv)_4$.[107] The explanation of the method used to determine the structure of the second coordination sphere given in that work is also supposed to bolster the conclusion of Thomas and co-workers that the structure of the titanium centers in Ti↑MCM-41 is $Ti(OSi\equiv)_3OH$. The structural parameters of the fits presented not reflecting the limited resolution of the experiment and the failure of the authors to present detailed information about their fit index leave me concerned about the validity of the results presented.

When metal chlorides are used as the linking agents in the non-aqueous building block process, the materials produced are more easily analyzed using EXAFS than materials produced using sol-gel or hydrothermal methods of synthesis. The advantage of the NABB materials is that the first coordination sphere contains both oxygen and chlorine in cases where unreacted sites remain on the metal center. In the case of titanium linking centers, the expected difference in bond lengths between Ti-O (1.8 Å) and Ti-Cl (2.3 Å) makes resolution of the two possible using EXAFS data with normal k-ranges that extend to 12 or 13. The different linking centers expected from the reaction of $TiCl_4$ with butyltin cube are shown in Figure 3-23.

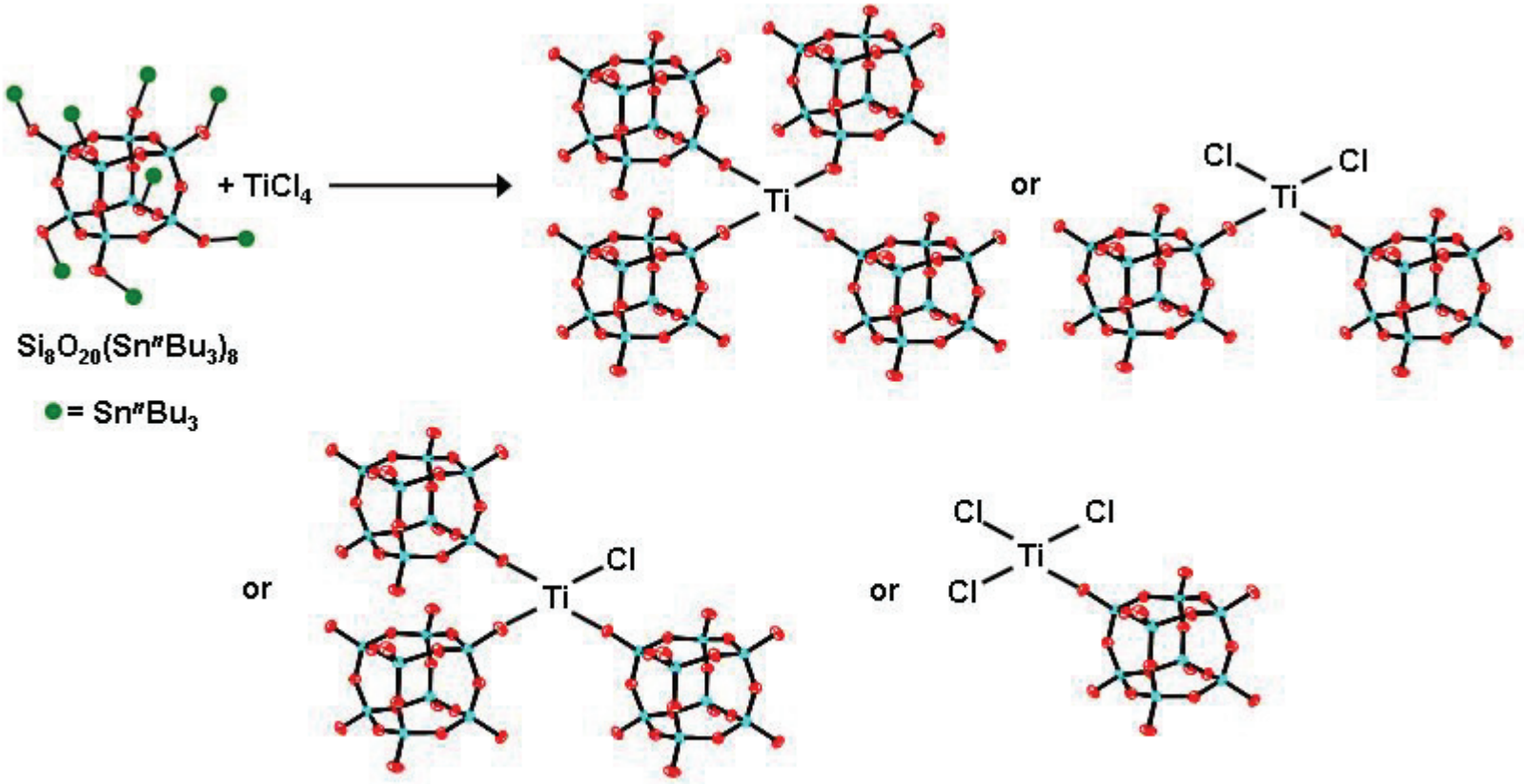

(Remaining $Sn^{n}Bu_3$ groups omitted for clarity.)

Figure 3-23. Oxygen and chlorine atoms are in the first coordination sphere of titanium in materials produced from the non-aqueous building block reaction of butyltin cube and $TiCl_4$.

It is reasonable to assume that the oxygen atoms in the first coordination sphere of these Ti NABB materials are exterior oxygen atoms on the Si_8O_{20} core. In other words, each oxygen atom in the first coordination sphere of titanium in the NABB materials is evidence for a link from the titanium center to a Si_8O_{20} building block. Unreacted Ti-Cl groups in the first coordination sphere are expected to react with water or methanol to form Ti-OH or Ti-OMe groups respectively when the material is treated with one of those reagents prior to the material being used as a catalyst.

Figure 3-24 shows the Fourier transform of the EXAFS data for samples Ti-4, Ti-3, and Ti-2. The plot is not phase corrected. The features from the Ti-O and Ti-Cl bonds are clearly visible, although not completely resolved from one another. The intensity of the Ti-Cl peak in sample Ti-2 is greater than that of Ti-3 as expected. The small feature in the Ti-4 sample in the same region as the Ti-Cl peak is due to a multiple-scattering from Ti-O bonds. Results from fitting the EXAFS data of the individual samples are summarized in Table 3-6.

For sample Ti-4 the amplitude reduction factor, S_0^2, was calculated using FEFF8[108] and held constant during the fitting process. The fit was conducted using data from 4 to 10.5 k with a k^3 weighting. Ti-4 was the only material where the inclusion of the silicon atoms in the second coordination sphere improved the quality of the fit. Therefore, results are given for the first and second coordination spheres. Ti-O-Si-Ti and Ti-O-Si-O-Ti multiple scattering paths at 3.298 and 3.400 Å, respectively, were included in the fit. The results of the fit are summarized in

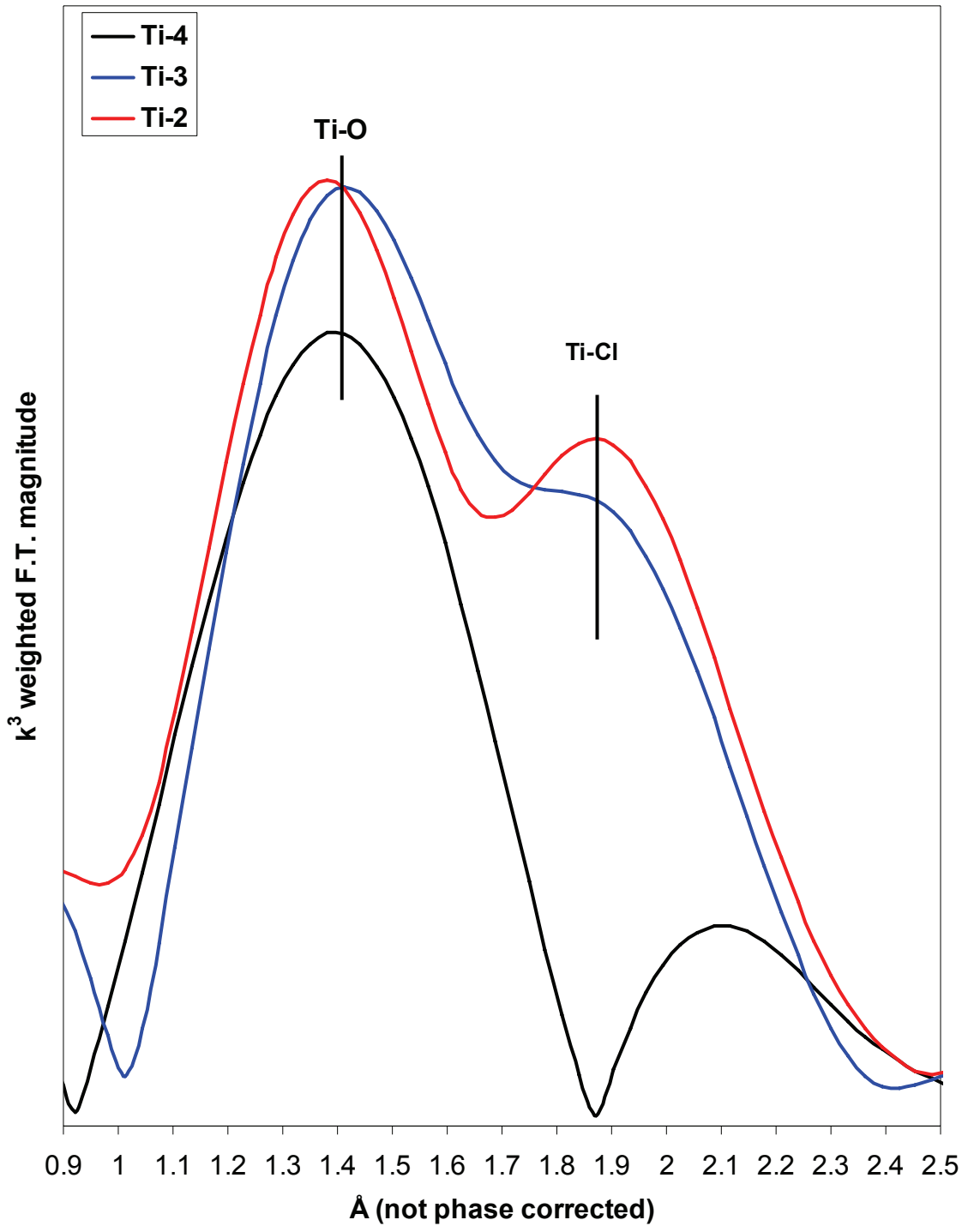

Figure 3-24. Fourier transform of EXAFS data showing Ti-O and Ti-Cl bonds in titanium non-aqueous building block materials.

Table 3-6. Summary of EXAFS fitting results for the Ti non-aqueous building block materials.

Sample	O C.N.	Ti-O Dist. (Å)	Cl C.N.	Ti-Cl Dist. (Å)	σ ($Å^2$)	ΔE_0
Ti-4	3.8 ± 0.2	1.80 ± 0.01	Not modeled	Not modeled	$0.0045 \pm 6 \times 10^{-4}$	-2 ± 2
Ti-3	2.8 ± 0.1	1.81 ± 0.01	1.2 ± 0.1	2.38 ± 0.01	$2 \times 10^{-4} \pm 2 \times 10^{-4}$	-4 ± 2
Ti-2	2.4 ± 0.2	1.80 ± 0.01	1.6 ± 0.2	2.38 ± 0.01	$-2 \times 10^{-4} \pm 1 \times 10^{-3}$	-1 ± 2

Table 3-7. Graphs comparing the fit to experimental data in k-space, r-space, and the real component of the fit in r-space are given in Figures 3-25, 3-26, and 3-27 respectively.

For sample Ti-3 the amplitude reduction factor was calculated using FEFF8[108] and held constant during the fitting process. The fit was conducted using data from 2 to 10.4 k with a k^3 weighting. Attempts to model the second coordination sphere did not improve the quality of the fit. The results of the fit are summarized in Table 3-8. Graphs comparing the fit to experimental data in k-space, r-space, and the real component of the fit in r-space are given in Figures 3-28, 3-29, and 3-30 respectively.

For sample Ti-2 the amplitude reduction factor was calculated using FEFF8.[108] The fit was conducted using data from 2 to 10.5 k with a k^3 weighting. Due to a poor fit of the oxygen and chlorine coordination numbers indicated by a poor match in the amplitude of the peaks in the r-space plot, the amplitude reduction factor was allowed to vary during the fitting process after the bond lengths had been determined. Attempts to model the second coordination sphere did not improve the quality of the fit. The results of the fit are summarized in Table 3-9. Graphs comparing the fit to experimental data in k-space, r-space, and the real component of the fit in r-space are given in Figures 3-31, 3-32, and 3-33 respectively.

Table 3-7. Results of Ti-4 EXAFS fit.

Oxygen Coordination Number	3.8 ± 0.2
Ti-O Distance	1.80 ± 0.1 Å
Δr for Ti-O	0.00(1) ± 0.01
σ^2 for Ti-O	0.004(5) ± 0.0006 Å^2
Silicon Coordination Number	Set equal to oxygen coordination number
Ti-Si Distance	3.14 ± 0.1 Å
Δr for Ti-Si	-0.05 ± 0.01 Å
σ^2 for Ti-Si	0.004 ± 0.001 Å^2
S_0^2	0.965 (set)
ΔE_0	-2 ± 2
Reduced Chi-squared	30.5
R-factor	0.04

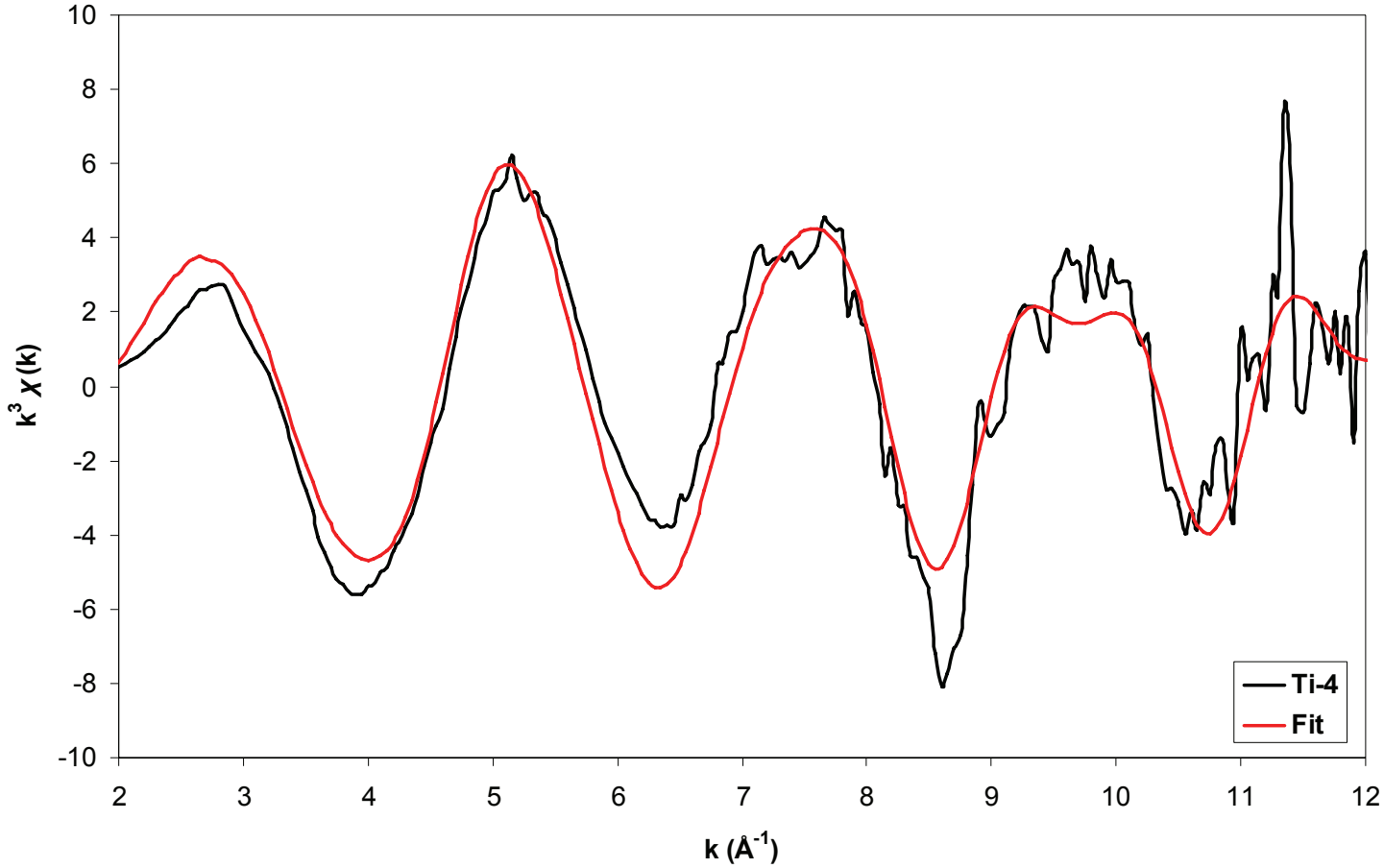

Figure 3-25. K^3 plot comparing the EXAFS data and the $Ti(OSi)_4$ model fit for sample Ti-4.

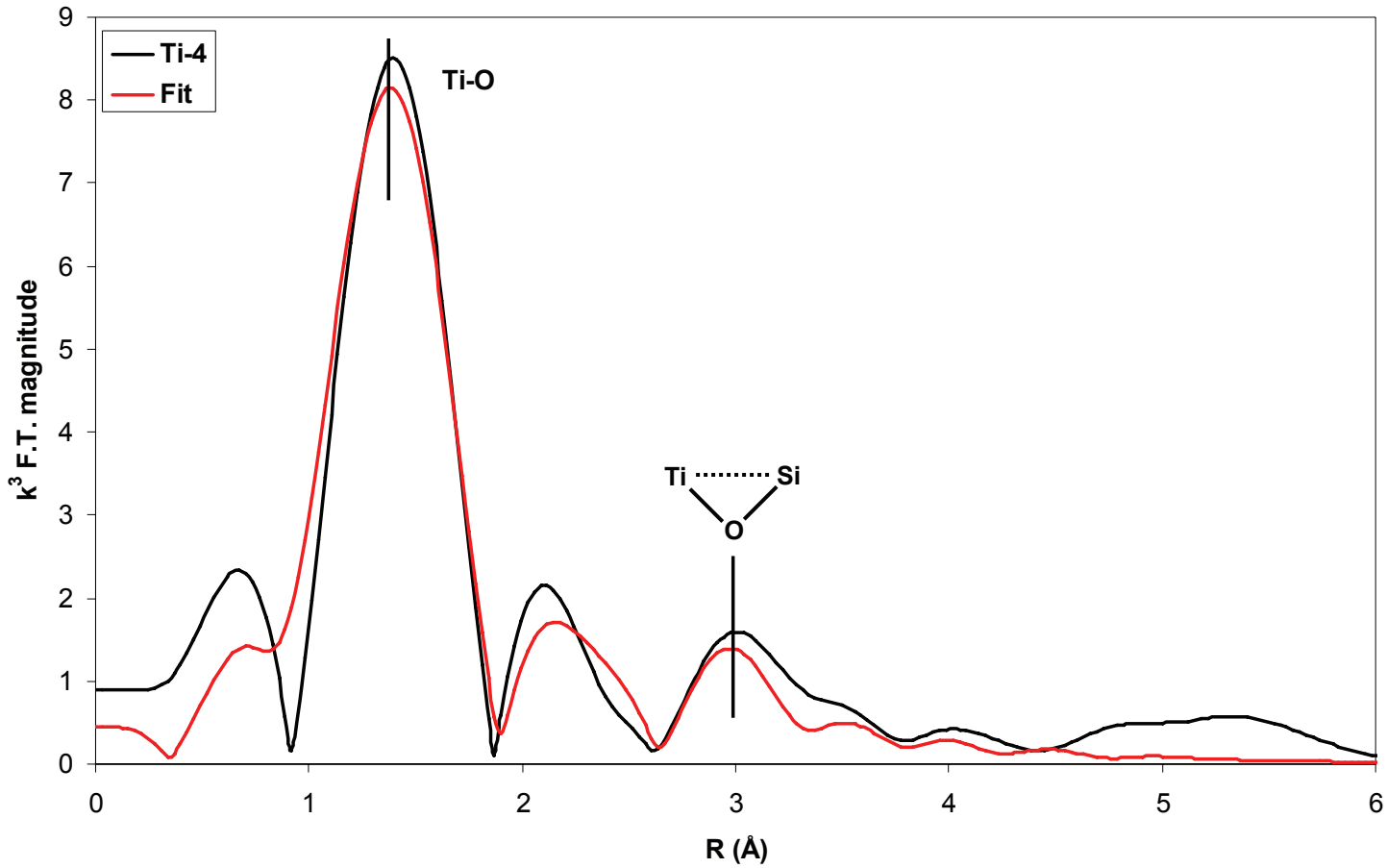

Figure 3-26. R-space plot comparing the EXAFS data and the $Ti(OSi)_4$ model fit for sample Ti-4.

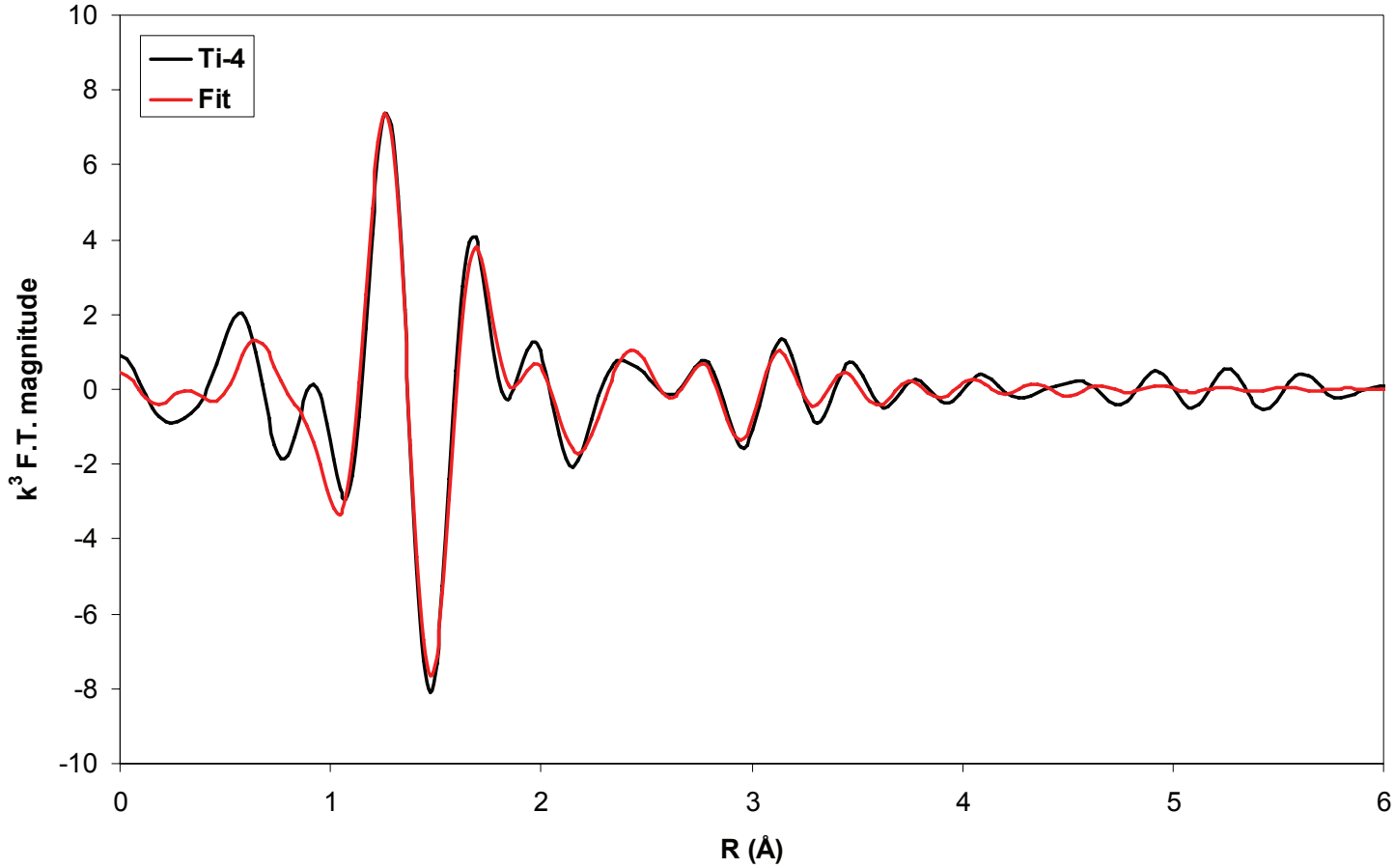

Figure 3-27. Plot of the real portion of the Fourier Transform comparing the EXAFS data and the $Ti(OSi)_4$ model fit for sample Ti-4.

Table 3-8. Results of Ti-3 EXAFS fit.

Oxygen Coordination Number	2.8 ± 0.1
Ti-O Distance	1.81 ± 0.1 Å
Δr for Ti-O	0.033 ± 0.009
σ^2 for Ti-O	0.0002(8) ± 0.0002(5) $Å^2$
Chlorine Coordination Number	1.2 ± 0.1
Ti-Cl Distance	2.38 ± 0.1 Å
Δr for Ti-Cl	-0.02 ± 0.01 Å
σ^2 for Ti-Cl	Set equal to Ti-O σ^2
S_0^2	0.965 (set)
ΔE_0	-4 ± 2
Reduced Chi-squared	23.8
R-factor	0.07

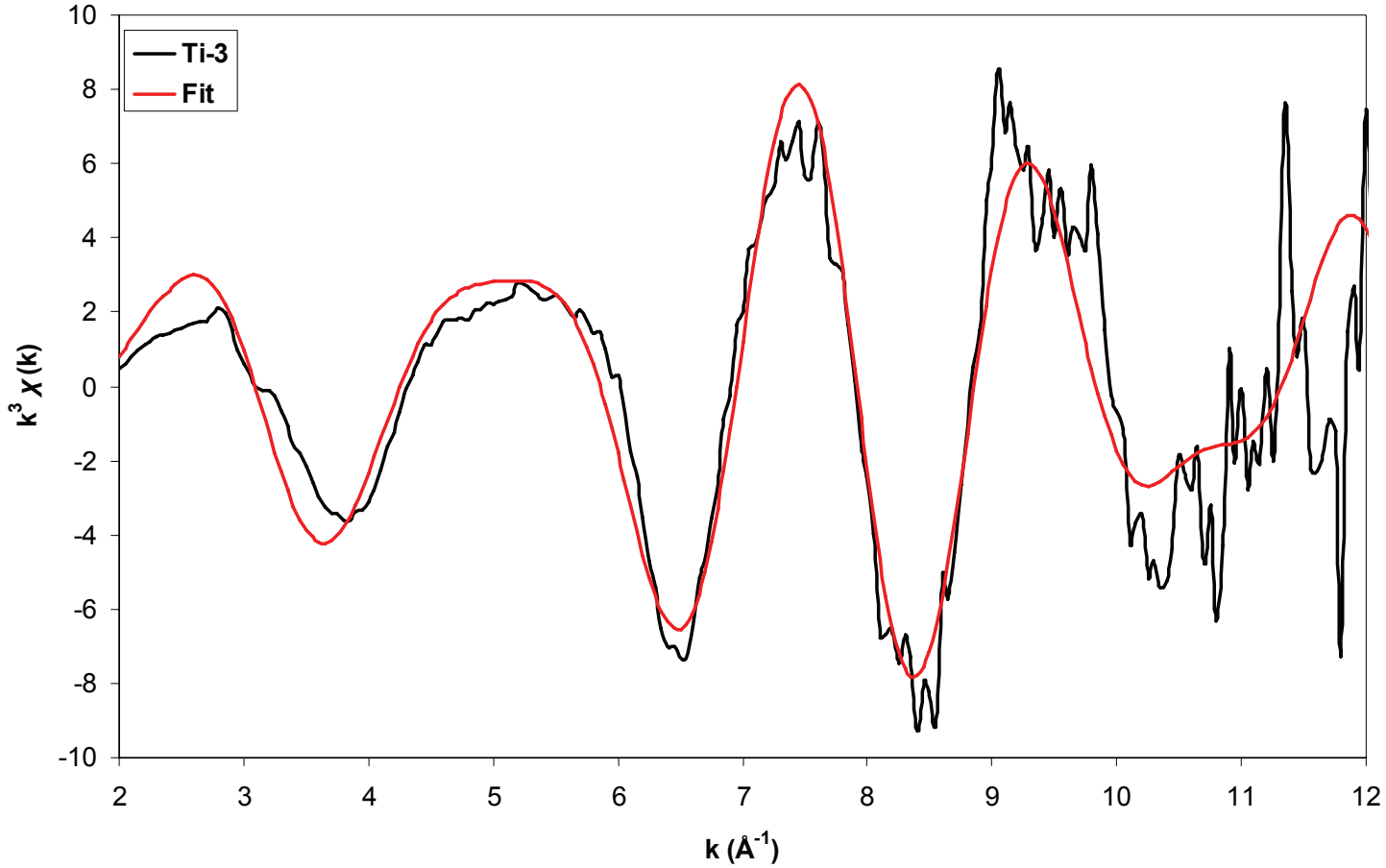

Figure 3-28. K^3 plot comparing the EXAFS data and the TiO_3Cl model fit for sample Ti-3.

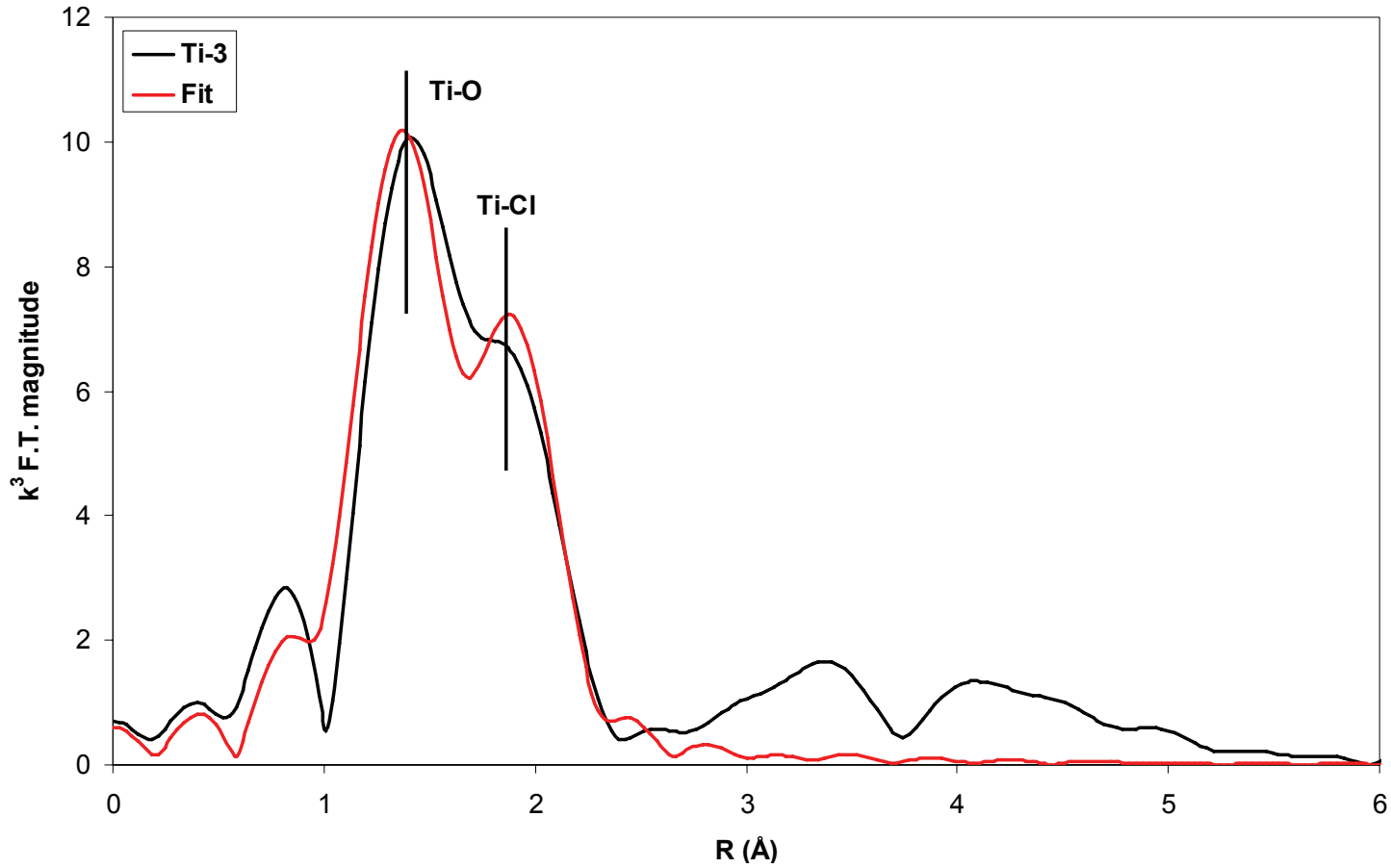

Figure 3-29. R-space plot comparing the EXAFS data and the TiO_3Cl model fit for sample Ti-3.

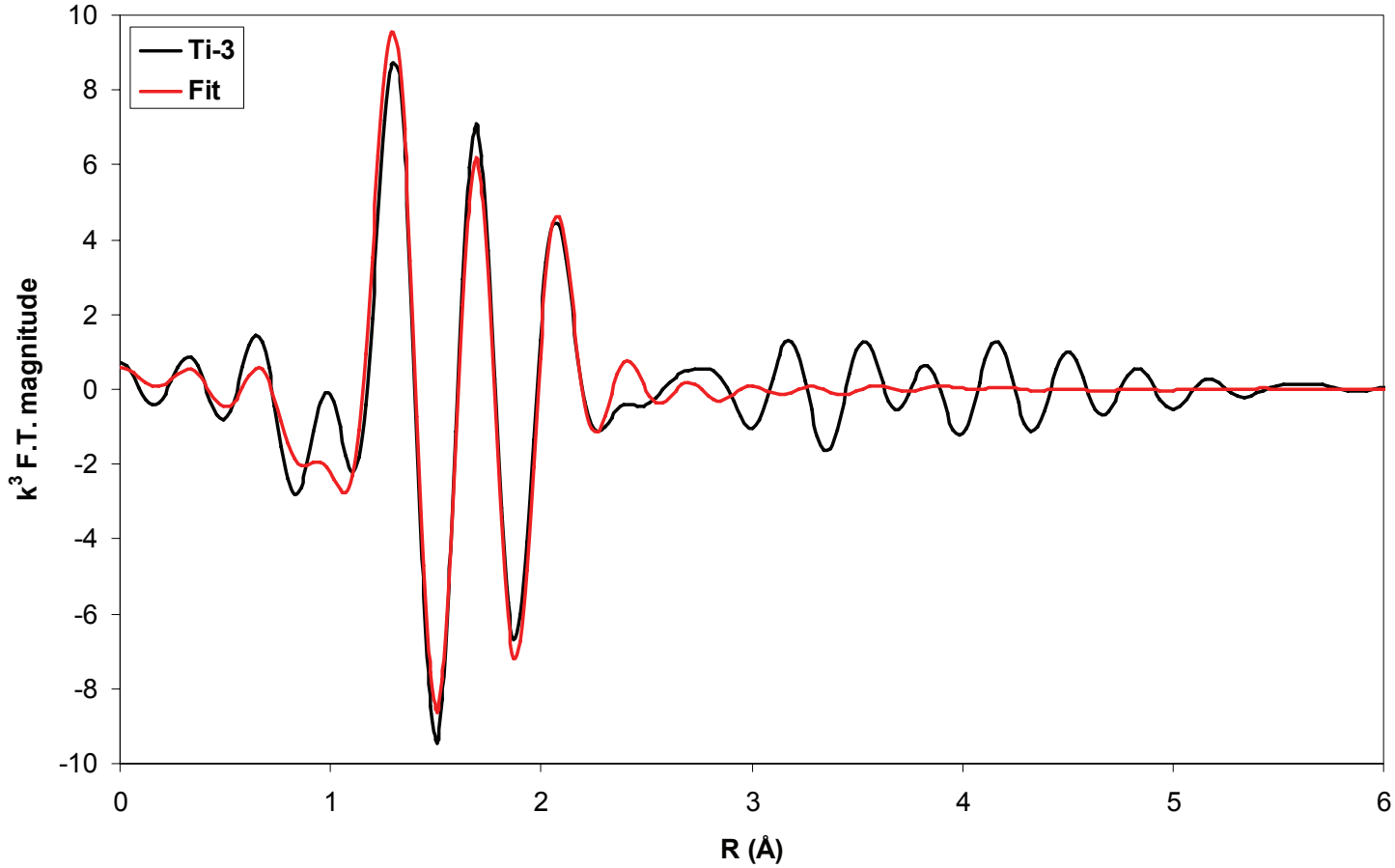

Figure 3-30. Plot of the real portion of the Fourier Transform comparing the EXAFS data and the TiO_3Cl model fit for sample Ti-3.

Table 3-9. Results of Ti-2 EXAFS fit.

Oxygen Coordination Number	2.4 ± 0.2
Ti-O Distance	1.81 ± 0.1 Å
Δr for Ti-O	0.00(8) ± 0.01
σ^2 for Ti-O	-0.0002 ± 0.001 Å^2
Chlorine Coordination Number	1.6 ± 0.2
Ti-Cl Distance	2.38 ± 0.1 Å
Δr for Ti-Cl	0.03 ± 0.01 Å
σ^2 for Ti-Cl	Set equal to Ti-O σ^2
S_0^2	0.829
ΔE_0	-1 ± 2
Reduced Chi-squared	107.9
R-factor	0.02

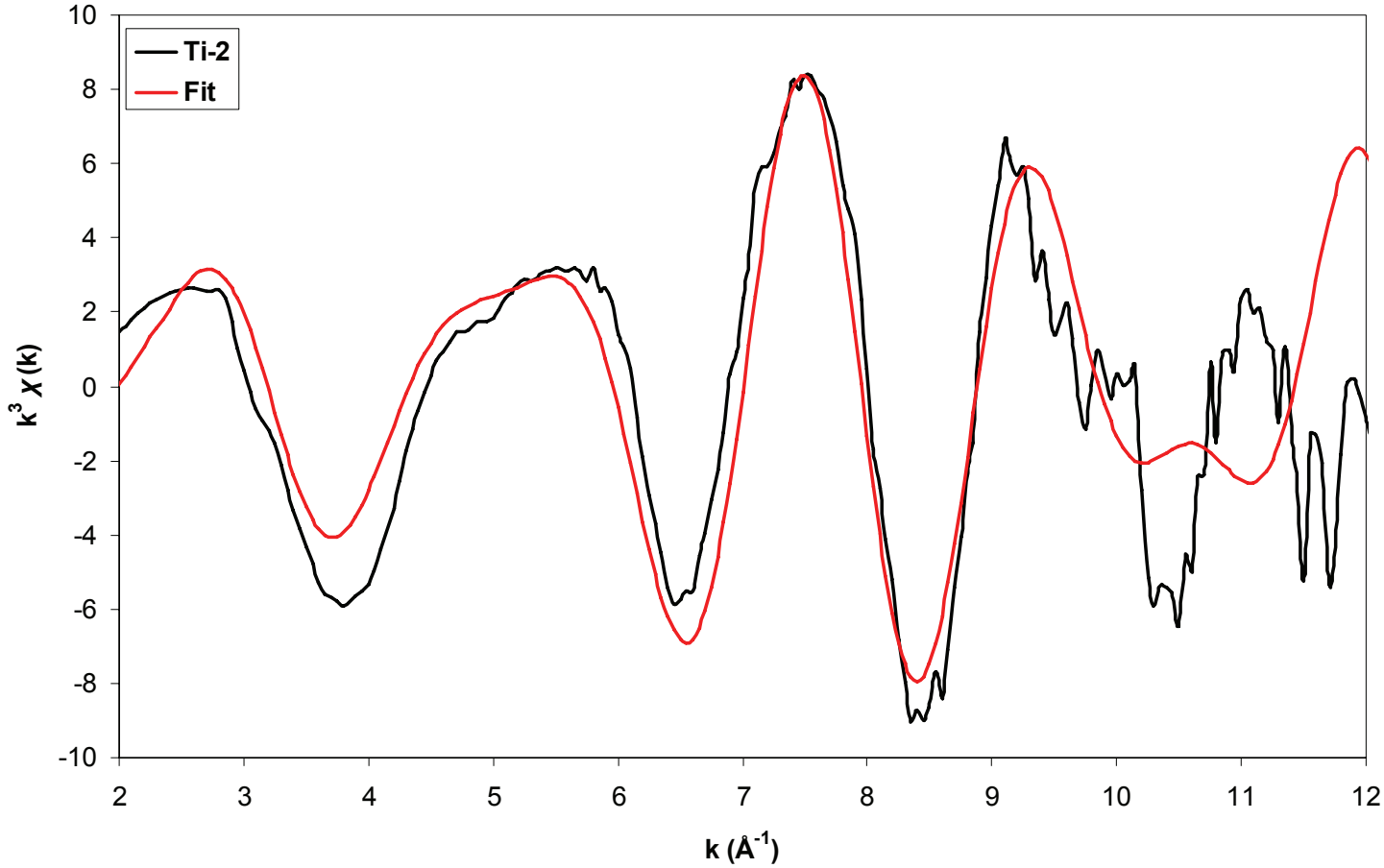

Figure 3-31. K^3 plot comparing the EXAFS data and the TiO_2Cl_2 model fit for sample Ti-2.

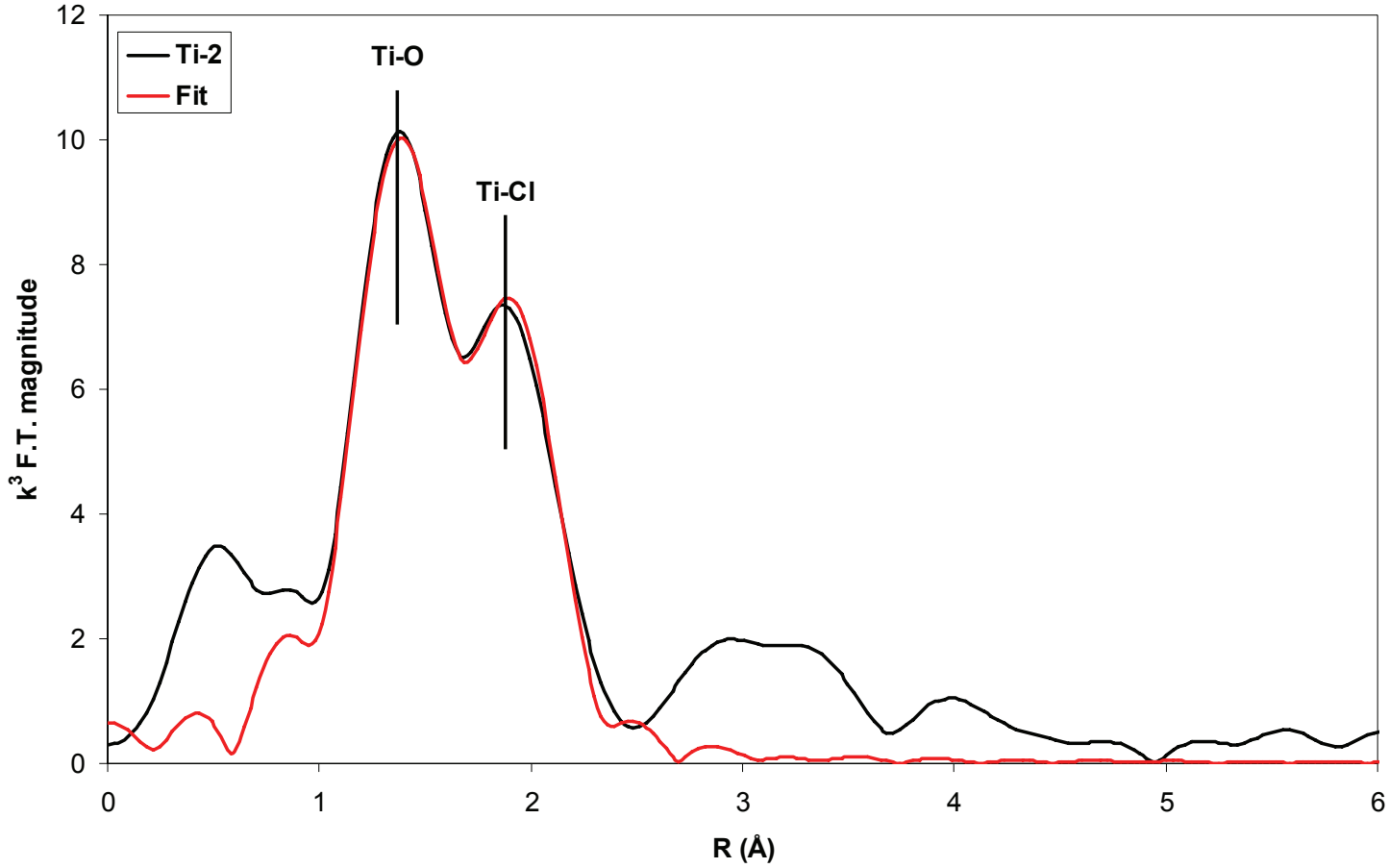

Figure 3-32. R-space plot comparing the EXAFS data and the TiO_2Cl_2 model fit for sample Ti-2.

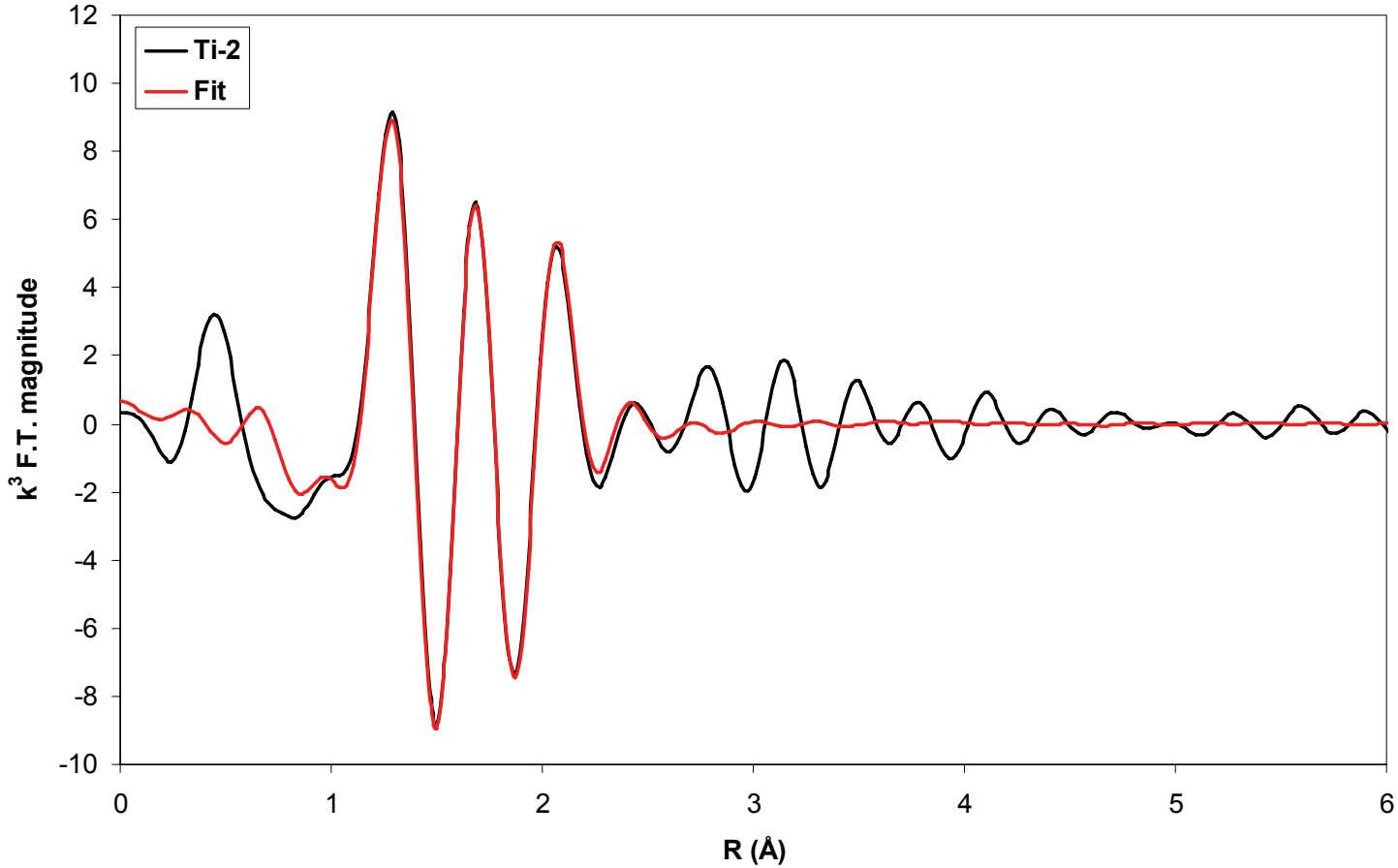

Figure 3-33. Plot of the real portion of the Fourier Transform comparing the EXAFS data and the TiO_2Cl_2 model fit for sample Ti-2.

Conclusion

Titanium containing silicate materials have been synthesized from $TiCl_4$ and $Si_8O_{20}(Sn^nBu_3)_8$ using the non-aqueous building block method. These materials were characterized using NMR, IR, Raman, XANES, and EXAFS spectroscopy. No direct evidence about the structure of the titanium centers was observed from SSNMR spectroscopy. Quantitative ^1H NMR spectroscopy allowed the amount of $ClSn^nBu_3$ by-product formed from the reaction of $TiCl_4$ with butyltin cube to be determined. The QNMR results were used to determine stoichiometric ratios of $TiCl_4$ to butyltin cube necessary to synthesize materials with titanium connectivity values of four, three, and two. The pre-edge features visible in the XANES spectra of the materials are evidence that the titanium centers have tetrahedral or pseudo-tetrahedral symmetry. Fits of the EXAFS data for the samples yielded information about the number of oxygen and chlorine atoms in the first coordination sphere of the titanium centers in the materials. The values obtained from the fits were consistent with the conclusions drawn from the QNMR studies. Table 3-10 summarizes the results of these structural characterization methods and shows the presumed structure of the titanium centers in the materials.

All of the materials showed bands near 950 cm^{-1} in their infrared spectra which are assigned to a Ti-O-Si vibrational mode. No bands from the anatase or rutile polymorphs of TiO_2 were visible in the Raman spectra of the materials either before or after calcination.

Table 3-10. Summary of structural results for titanium non-aqueous building block materials.

Sample Name	Stoichiometry $TiCl_4$ per tributyltin cube	QNMR Results $ClSn^nBu_3$ per $TiCl_4$	EXAFS Results CN O	EXAFS Results CN Cl	Presumed Structure
Ti-4	0.25	4.0	3.8 ± 0.2	Not modeled	$Ti(OSi\equiv)_4$
Ti-3	1	3.1	2.8 ± 0.1	1.2 ± 0.1	$Ti(OSi\equiv)_3Cl$
Ti-2	2	2.0	2.4 ± 0.2	1.6 ± 0.2	$Ti(OSi\equiv)_2Cl_2$

From the data presented herein, it is concluded that each of the non-aqueous building block materials containing titanium is structurally unique and, that they are effectively different catalysts when considered in the context of olefin epoxidation. The titanium centers in the Ti-4 material are bonded to 4 Si_8O_{20} building blocks. This structural determination is the most conclusive as the presence of other titanium centers with lower connectivity would give rise to an *average* connectivity value lower than four.

The data also shows that the average connectivity for titanium centers in the Ti-3 and Ti-2 materials is bonded to 3 and 2 Si_8O_{20} building blocks, respectively. Unlike the Ti-4 material it is possible that these materials contain titanium centers of different connectivities where their *average* value of connectivity happens to be an integral value. For example, if one-half of the titanium centers in a material had a connectivity of four and the other half had a connectivity of two the average connectivity of the titanium centers in the material would be three. That average value would also be reflected in the amount of by-product measured using ^{1}H QNMR, the XANES spectrum, and the EXAFS fits of the material. While it may be unlikely that the Ti-2 and Ti-3 materials both contain the correct amount of titanium centers with different connectivities to give an average value that is an integer, that possibility cannot be discounted.

In the future it may be possible to better characterize the Ti-3 and Ti-2 materials using techniques such as ^{17}O MAS NMR. Perhaps, resonance Raman techniques could be used to enhance bands from symmetric Ti-Cl stretching

modes that were not observable using conventional Raman techniques.[75,86] Until such experiments are performed, let us move on to compare the activity of these non-aqueous building block materials in the epoxidation of cyclohexene with *tert*-butylhydroperoxide.

Chapter 4. Effect of Active Site Structure on Olefin Epoxidation–A Review of Literature Catalysts and An Examination of Titanium Non-aqueous Building Block Catalysts

Epoxides are important intermediates in a number of chemical technologies. For example ethylene oxide, a commercially produced epoxide, is an intermediate in the manufacture of textiles, detergents, anti-freeze, solvents, and adhesive.[109] Propylene oxide, another commercially produced epoxide, is used widely in the manufacture of polyurethane foams. Epoxides of other olefins, although not produced on the scale of ethylene or propylene oxide, are important intermediates in the synthesis of fine chemicals and in the pharmaceutical industry.[43]

Ethylene oxide is produced industrially using a heterogeneous silver catalyst with oxygen as the oxidant. However, this method is not suitable for use with most olefins—especially those with allylic or other reactive C-H bonds.[43] The chlorohydrin method and the use of peroxyacids (peracids) as oxidants are two traditional “wet chemistry” means of synthesizing epoxides.[110] However, the costs associated with the handling of chlorine and chlorinated waste streams makes the use of the chlorohydrin method undesirable when scaled up. Likewise, the costs associated with the production and transportation of peracids makes their use less desirable than alternative oxidants that become available for use when catalysts are employed.

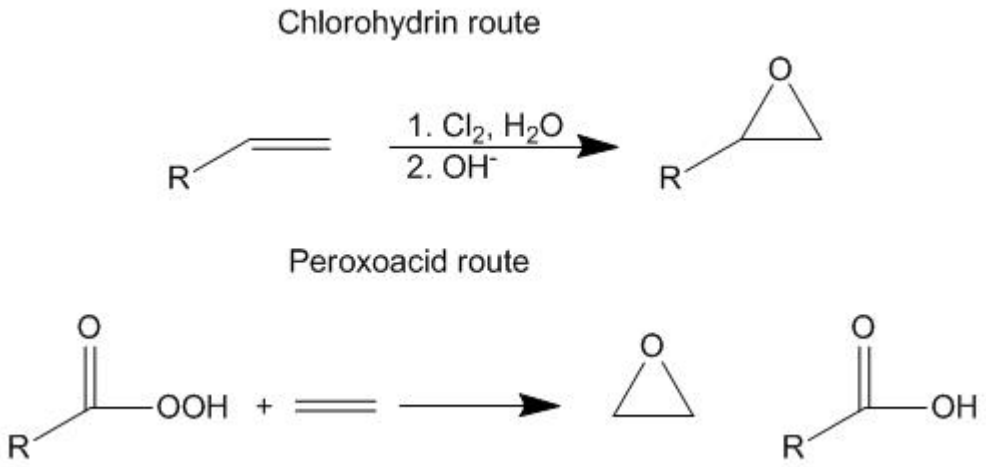

Scheme 4-1. Two common non-catalytic processes for epoxide synthesis.

Oxidants Made Available By Catalysts

"The ideal system for 'green' oxidation is the use of molecular oxygen as the primary oxidant together with recyclable catalysts in nontoxic solvents."[111] Increasing environmental regulation is a major incentive for the fine chemicals and pharmaceuticals industries to consider the use of catalytic processes in combination with "environmentally friendly" oxidants in the reactions they conduct. However, with the notable exception of ethylene, a suitable system for the catalytic epoxidation of olefins with molecular oxygen has not been discovered.

Hydrogen peroxide and *tert*-butylhydroperoxide (TBHP) are two leading "environmentally friendly" candidates for oxidants in catalytic epoxidation reactions. The reaction by-products for hydrogen peroxide and TBHP

epoxidations are water and *tert*-butanol respectively. Thus, hydrogen peroxide is touted as the "greenest" peroxide.

However, for non-radical, metal-catalyzed oxygenations of organics, TBHP is one of the best sources of oxygen atoms when one considers its combined advantages in economics, selectivity, and safety.[112] From the vantage point of safety, TBHP is less sensitive to decomposition from trace metals than hydrogen peroxide. From an economic standpoint aqueous solutions containing 30% hydrogen peroxide or 70% TBHP are shippable by rail giving them an enormous advantage over other peroxides which can only be shipped by truck. Finally, the ability to prepare non-aqueous solutions of TBHP provides an advantage in compatibility with some heterogeneous catalysts *vide infra*.

Thus, TBHP is a suitable alternative to oxygen and hydrogen peroxide in many catalytic oxidations.

Development of Catalytic Olefin Epoxidation

In the early 1960s employees of Halcon and Atlantic Richfield (ARCO) independently discovered and developed processes for the production of epoxides using an alkyl hydroperoxide in the presence of homogeneous transition metal catalysts.[43,113] Soluble compounds of molybdenum, vanadium, tungsten, and titanium were shown to be active catalysts, with molybdenum compounds having the best activities and selectivities.[43] Subsequently, Halcon and ARCO formed a joint venture called the Oxirane corporation to apply this

R = H or alkyl

Scheme 4-2. Catalytic expodiation of an olefin by a peroxide.

technology to the manufacture of propylene oxide. Roughly half of the propylene oxide produced annually worldwide is produced using the Oxirane process.[43]

Further investigation of these catalysts revealed that they contain the metal in its highest oxidation state. Metals with low oxidation potentials and high Lewis acidity in their highest oxidation states are superior catalysts, and the order of reactivity is: Mo(VI) > W(VI) > V(V) > Ti(IV). It was also found that strongly coordinating solvents, particularly, alcohols and water, severely retard the reaction by competitively binding to coordination sites on the catalyst. Thus, the co-product of the reaction causes the rate of reaction to decrease.[43,113]

About a decade later workers at Shell developed a heterogeneous titanium on silica (Ti(IV)/SiO_2) catalyst which exhibits selectivities comparable to homogeneous molybdenum epoxidation catalysts and high activities for a heterogeneous catalyst.[43,113,114] This catalyst was far superior to homogeneous Ti(IV) epoxidation catalysts. The superiority of the Shell catalyst has been attributed to two factors: 1) an increase in the Lewis acidity of the titanium center resulting from electron withdrawl through bonds to the silica surface and, 2) site isolation of discrete titanium centers on the silica surfaces which prevents

formation of what are thought to be unreactive μ-oxo species responsible for the poor performance of the homogeneous titanium catalysts.[43,113]

The Shell catalyst was the first truly heterogeneous epoxidation catalysts useful for continuous operation in the liquid phase.[43,113-115] This catalyst has become the basis of commercial propylene oxidation with ethylbenzene hydroperoxide, in which the co-product alcohol can be dehydrated to styrene.[113] Like the homogeneous catalysts, the Shell catalyst is deactivated by protic molecules with the severity of deactivation increasing as follows: *t*-BuOH < EtOH < MeOH < H_2O.[113] Thus, hydrogen peroxide is not a suitable oxidant for use with the Shell catalyst which in the presence of water deactivates quickly.[25]

Attempts have been made to synthesize silica supported heterogeneous catalysts containing molybdenum(VI), tungsten(VI), and V(V). However, these metals rapidly leach from the silica support under reaction conditions and, to this day a truly heterogeneous analog of the successful homogeneous molybdenum epoxidation catalyst has not been commercialized.[113]

TS-1

In 1983 TS-1, a synthetic titanium-containing zeolite with the MFI structure, was synthesized by Enichem.[41] TS-1 was revolutionary because it was found to be an active catalyst for a number of oxidation reactions, including epoxidation, when aqueous hydrogen peroxide is used as the oxidant. The failure of TS-1 to deactivate in the presence of water has been attributed to the hydrophobic nature of the microporous network in the support.[41]

Another important attribute of TS-1 is its ability to promote the ready epoxidation of relatively unreactive olefins such as propylene and allyl chloride at low temperatures (below 60 °C).[113] However, TS-1 is not without its shortcomings. Due to the size of its micropores, TS-1 is limited to the oxidation of substrates with kinetic diameters less than 5.5 Å.[43] TS-1 cannot, for example, catalyze the epoxidation of cyclohexene because of this size exclusion. The desire to carry out catalytic epoxidations on molecules having kinetic diameters greater than 5.5 Å helped cause a push to develop catalysts with larger pore structures.[44]

Mesoporous Epoxidation Catalysts

As the size of a pore in a material grows, the atomic scaffolding that defines that pore becomes less able to support the void volume in the material. In order to compensate for this the "walls" of a pore grow thicker as the size of the pore increases. As pore sizes transition from microporous to mesoporous, the walls must grow so thick that crystalline structure in the walls of the pore is lost. An important distinction between TS-1 and MCM-41 is that while both have ordered pore structures, only TS-1 has walls that are crystalline.

Following the 1992 report by Mobil scientists that they had synthesized a material with an ordered pore structure in the mesoporous size regime, a vast family of similar materials have been synthesized.[44] These mesoporous metal oxides, such as MCM-41 and SBA-15, are synthesized using a silica source and a structure directing agent (SDA) under hydrothermal conditions. The resulting

solid is then calcined to remove the SDA which leaves the surface of the resultant material covered with hydroxyl groups.

Two basic methods are available to researchers wishing to incorporate metals with catalytic potential into these materials. First, a metal source may be mixed in with the silica source prior to the synthesis. This results in the inclusion of the metal in the structure of the pore walls. Such materials are sometimes referred to as framework materials, as the metal is incorporated into the structural framework that defines the pores. The second method is a post-synthesis modification of the material where an appropriate metal reagent can be reacted with the hydroxyl groups on the surface of the mesoporous material. This method results in placement of the metal on the surface of the mesoporous material. Materials in this second class are often referred to as grafted materials to emphasize the surface location of the incorporated metal.

Of the mesoporous materials, MCM-41 containing titanium is the most well studied.[116] MCM-41 with framework titanium has been shown to be catalytically active in the epoxidation of olefins with TBHP, including bulky olefins such as norbornene and limonene.[116] Titanium grafted MCM-41 has been shown to be active in the epoxidation of cyclohexene and pinene when TBHP is used as the oxidant.[27]

MCM-41 and other mesoporous materials show a great deal of promise in the epoxidation of large substrates. However, when hydrogen peroxide is used as the oxidant they do not perform as well as TS-1. In general the rates of

reaction and the selectivity for the epoxide are low when hydrogen peroxide is used as the oxidant in titanium MCM-41 catalyzed reactions.[106,117-123]

Back to the Future?

Scott and Mayoral's groups revisited the technology used to develop the Shell catalyst in their recent work.[25,34,124-126] The Shell catalyst was prepared by treating silica with $TiCl_4$ or organotitanium compounds, followed by steam treatment and calcination.[43] In a method similar to that of Shell, these groups prepared their catalysts by treating partially dehydroxylated silica gels with titanium(IV) isopropoxide. The catalyst is then activated *in vacuo* at 140 °C. Steam treatment or calcination of the catalysts is not necessary. The catalysts are active in the epoxidation of bulky olefins with TBHP. Notably, both Scott and Mayoral report that the catalysts are much less sensitive to the presence of moisture than the Shell catalyst.[25,124]

Characterization of Titanium on Silica Epoxidation Catalysts

The ultimate goal of the work presented herein is to establish a relationship between the structure of titanium on silica epoxidation catalysts and their activity. Now that the major players have been introduced, let us examine the results of the structural studies of these materials and look for structural similarities between them.

TS-1

TS-1 is unique amongst the heterogeneous titanium-on-silica catalysts because it is the only one that is crystalline. Thus, it is not surprising that X-ray

diffraction (XRD) measurements of the material have been made. Attempts to precisely locate the sites at which titanium atoms substitute into the lattice have not been successful due to the low titanium loading, especially when considered in terms of atomic percentage.[41] The unit cell of TS-1 is observed to expand in direct proportion to the titanium content.[127] This has been taken as a sign of isomorphous substitution of a titanium atom for a silicon atom in the silicate structure.[41]

Vibrational spectroscopy has also been used to characterize TS-1. In the infrared (IR) spectrum a band at 960 cm^{-1} attributed to isolated tetrahedral $Ti(OSi)_4$ sites is present.[41,81] A discussion of the assignment of this 960 cm^{-1} band is provided in the third chapter of this work. A band in the Raman spectrum at 1125 cm^{-1} has been assigned to "a totally symmetric vibration of the TiO_4 tetrahedron, achieved through in-phase antisymmetric stretching of the four-connected Ti-O-Si bridges."[75] Put more simply, the band is assigned to a $Ti(OSi\equiv)_4$ unit.

X-ray absorption spectroscopy (XAS) has also been used to study TS-1. A strong pre-edge feature at 4967 eV in the XANES data indicates that the titanium in the sample is in a tetrahedral configuration (Figure 4-1).[41,75] EXAFS data indicates that the first coordination sphere of the titanium atoms contain four oxygen atoms at a distance of 1.79 – 1.81 Å.[41]

Diffuse reflectance UV-Visible spectroscopy (DRUV-Vis) has also been used to characterize TS-1. A band at 208 nm is observed.[75] This band is

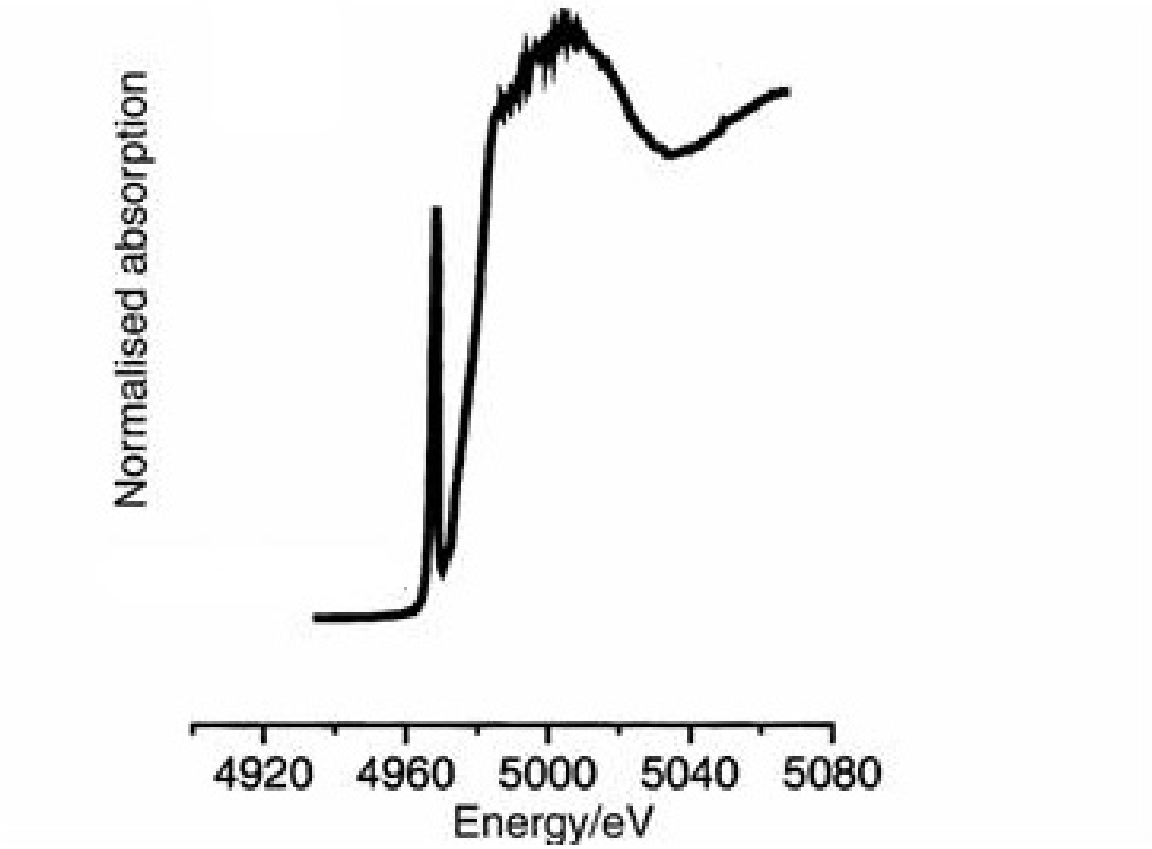

Figure 4-1. XANES spectrum typical of TS-1. (Modified from Gleeson, et. al. *Physical Chemistry Chemical Physics,* 20, *2*, 4812-4817 (2000), used with permission.)

assigned to a ligand-to-metal charge transfer (LMCT) band of an isolated tetrahedral TiO_4 unit.[41] If octahedral titanium oxides were present a band would be expected between 303 and 317 nm.[41]

Framework Ti-MCM-41

Infrared spectra of MCM-41 materials with titanium in the framework (Ti→MCM-41) show a band at 963 cm^{-1}.[82] This band is which is attributed to the presence of Ti-O-Si units. However, little Raman data has been presented, and to my knowledge there are no reports of a band located near 1125 cm^{-1} in the Raman spectrum similar to that reported in TS-1. The lack of Raman data may be due to the large fluorescence background of Ti→MCM-41 materials.[128]

XAS data supports the presence of a tetrahedral TiO_4 site. XANES data shows a significant, sharp pre-edge feature indicative of tetrahedral titanium at 4968 eV.[82,116] EXAFS data indicates that the first coordination sphere of the titanium atoms contain four oxygen atoms at a distance of 1.80 Å.[116]

Two reports of DRUV-Vis spectra of Ti→MCM-41 materials mention the presence of a strong LMCT band.[122,129] Eimer and co-workers report the location of the band as 210 nm, while Chaudhari and co-workers report it at 220 nm.

Grafted Ti-MCM-41

In 1995 J. M. Thomas and co-workers reported the structure of titanium centers grafted onto the surface of MCM-41 materials.[27] The synthetic scheme of the grafted material referred to as Ti↑MCM-41 is shown in Figure 4-2. This work is notable because the authors conclude that the structure of the active site

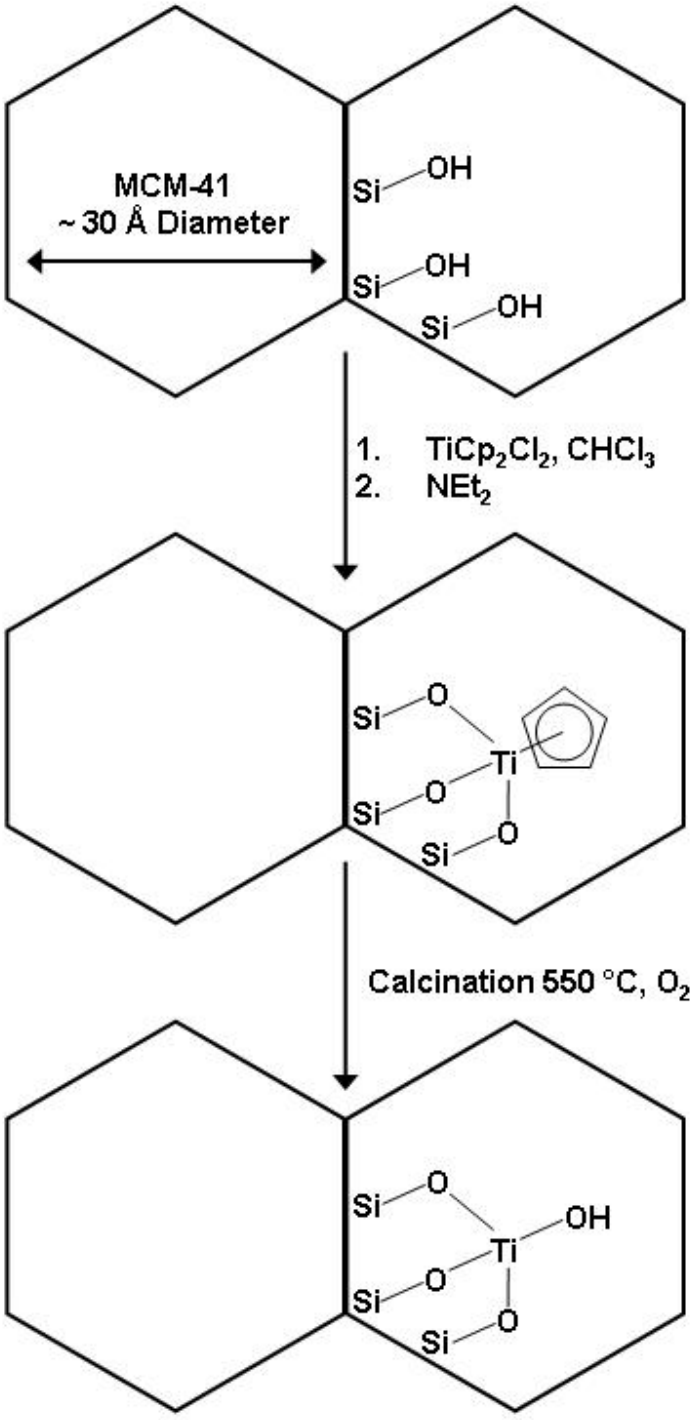

Figure 4-2. Synthetic scheme for titanium grafted MCM-41 (Ti↑MCM-41).

is $(\equiv SiO)_3TiOH$ and not $Ti(OSi\equiv)_4$ which is believed to be the active site in TS-1 and Ti→MCM-41.

XAS studies of Ti↑MCM-41 were somewhat more involved than those for other materials, as Thomas and co-workers chose to follow the reaction of titanocence dichloride ($TiCp_2Cl_2$) with MCM-41 using EXAFS.[27] Unlike the EXAFS results reported above, the researchers chose to model the first and second coordination spheres. The difficulty associated with accurately modeling the second coordination sphere and some concerns about the method used by Thomas and co-workers are discussed in detail in the third chapter of this work.

Thomas and co-workers report that after the chemical reaction between $TiCp_2Cl_2$ and MCM-41 is complete, the titanium species formed is $(\equiv SiO)_3TiCp$. This conclusion is based upon the presence of only five carbon atoms in the first coordination sphere of titanium in the structural model that best fit the EXAFS data. The model also includes three silicon atoms in the second coordination sphere of the titanium center. The conclusion that a $(\equiv SiO)_3TiCp$ species is formed is somewhat surprising as only the chloride ligands from the $TiCp_2Cl_2$ are expected to react and form bonds from the titanium center to the support.

The EXAFS results were surprising enough that computational studies were performed.[83] These studies indicate that the $(\equiv SiO)_3TiCp$ species is lower in energy (more stable) the the $(\equiv SiO)_2TiCp_2$ species and support the conclusions generated from fitting the EXAFS data.

Calcination of the material is reported to result in a catalyst with titanium centers of the structure $(\equiv SiO)_3TiOH$.[27] That conclusion is based upon evidence that only three silicon atoms are in the second coordination sphere of titanium as determined by fitting EXAFS data. A follow-up paper provided details of the method used to fit the second coordination sphere of the Ti↑MCM-41.[107] Specific concerns about the fitting procedure are given in the third chapter of this dissertation.

The strong pre-edge expected for tetrahedral titanium in the XANES spectrum is observed at about 4970 eV.[27]

Infrared spectra of MCM-41 materials with titanium grafted on the surface (Ti↑MCM-41) show a "very broad" band at 935 cm^{-1}.[130] Thomas and co-workers assign this band as a Ti-O-Si band even though its center is approximately 25 cm^{-1} from positions normally reported for such a band. In the same publication, the authors note a decrease in the intensity of the silanol band located at 3745 cm^{-1} of the MCM-41 materials following reaction with titanocene dichloride.[130] They argue that this decrease is evidence for successful chemical transformation of part of the surface ≡Si-OH groups to ≡Si-O-Ti≡ groups. Raman data for Ti↑MCM-41 has not been reported, presumably because of the high fluorescence background of these materials as noted above.

For Ti↑MCM-41 materials DRUV-Vis shows a band centered around 230 nm attributed to the LMCT band of isolated tetrahedral TiO_4 units.[130,131]

Ti(IV) on Silica Gel from $Ti(OR)_4$

Titanium grafted silica gel is produced by the reaction of silica gel with titanium(IV) isopropoxide, $Ti(O^iPr)_4$, under anhydrous conditions. Scott and co-workers used silica gel partially dehydroxylated at 200 °C (silica-200) in their studies, while Mayoral and co-workers used silica gel treated *in vacuo* at 140 °C in their research. In one article Scott and co-workers note the similarity between their work and that of Mayoral's group.[25] (The reader should note what while the materials are not rigorously the same, slightly different conditions very different loadings, they are reported together and may have active sites with similar structures.) Scott's group used gas chromatography to quantify the amount of propanol liberated during the reaction between silica-200 and $Ti(O^iPr)_4$ as shown in the equation below.[34] Somewhat surprisingly, propene was also observed as a product of the reaction. The amount of propene liberated during the course of the reaction was also quantified using gas chromatography.[34] The formation of propene during the reaction suggests that a reaction also occurs between two lone titanium centers which results in the formation of a Ti-O-Ti group. The condensed equation is shown below and an illustration of the reaction between two $Ti(O^iPr)_3$ groups on silica is shown in Figure 4-3.

$$\text{silica-200} + 2\ Ti(O^iPr)_4 \rightarrow [\equiv SiOTi(O^iPr)_2]_2O + 3\ ^iPrOH + C_3H_6$$

Quantitative FT-IR spectroscopy data was used to determine the amount of CO_2 liberated from calcination of the grafted products.[34] It was found that six moles of CO_2 were released per mole of titanium in the sample. The loss of the

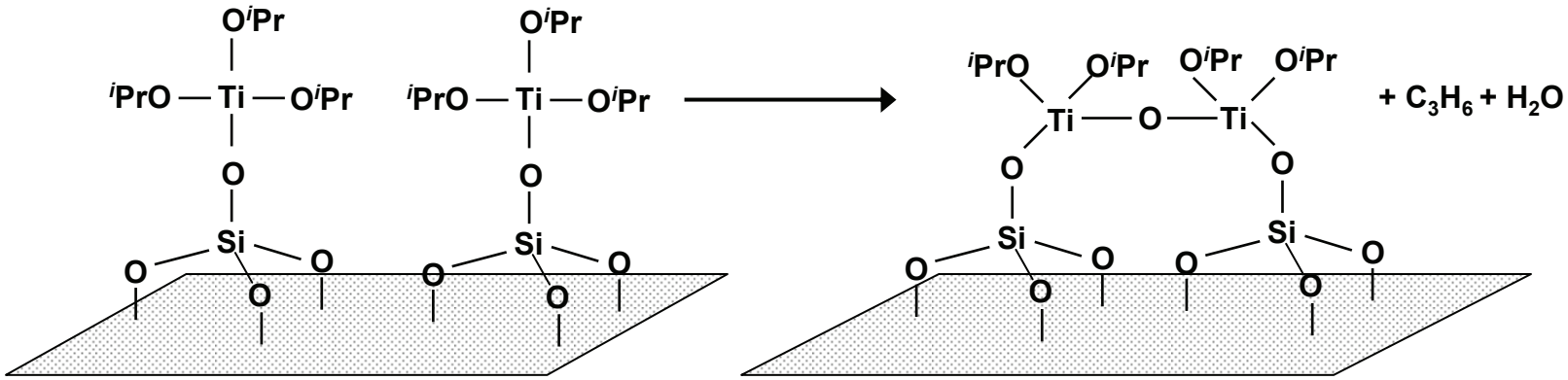

Figure 4-3. Schematic of the reaction between two Ti(O^{i}Pr)$_3$ groups on silica to form the Ti-O-Ti dimer proposed by Scott and co-workers.

silanol band 3747 cm^{-1} following the grafting reaction was taken as evidence of the formation of ≡Si-O-Ti≡ bonds.[25,34] A band at 680 cm^{-1} was also observed in the IR spectrum.[25] This band was assigned to a Ti-O-Ti vibration.

^{13}C cross-polarization MAS NMR of the product shows resonances at 25 (methyl) and 78 (methyne) ppm.[34] These resonances are assigned, respectively, to the methyl and methyne carbons of an isopropoxide group. From this data, Scott and co-workers concluded that the reaction of $Ti(O^{i}Pr)_4$ with the surface silanol groups of silica gel treated at 200 °C produces silica gel with dimeric μ-oxo titania species anchored to the surface. The structure of this species is shown in Figure 4-4.[34]

The catalysts synthesized by Mayoral's group were not as rigorously characterized as those of Scott's group. While, the procedure used to synthesize the materials is similar between the two groups there are two important procedural differences. First, Mayoral's group treats their silica gel at 140 °C which is lower than the pre-treatment temperature of Scott. This lower pre-treatment temperature may leave more silanol groups on the surface of the silica gel. Second, the loading of titanium placed on the silica gel support is much higher in the materials prepared by the Mayoral group (5.64 weight % Ti) as opposed to the low loadings used by the Scott group (0.2 weight % Ti). These differences prevent the assumption that the structures of the materials synthesized by the Scott and Mayoral groups are identical.

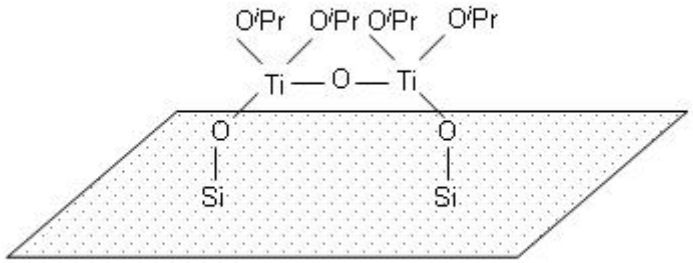

Figure 4-4. Structure of [≡SiOTi(O^{i}Pr)$_2$]$_2$O.

However, Mayoral's group is the only group to characterize materials prepared from the reaction of Ti(O^{i}Pr)$_4$ with silica gel using XAS.[125] Unfortunately, the publication indicates that no great care was taken to prevent exposing the material to moisture prior to or during XAS data collection. It is possible that the following information may be affected by the presence of water molecules in the titanium coordination sphere.

A weak pre-edge feature is observed at 4966 eV in the XANES spectrum.[125] The weakness of the feature may indicate the presence of water coordinated to the titanium sites.[132] A fit of the EXAFS data indicates the presence of 4.2 (±0.2) oxygen atoms in the first coordination sphere of titanium at a distance of 1.88 Å. (This bond length is 0.04 Å longer than the greatest Ti-O bond distance reported for tetrahedral titanium by Farges, et. al.[98]) While the comparison is not the most ideal, the coordination number determined by Mayoral's group for silica gel treated with Ti(O^{i}Pr)$_4$ can be said to be in agreement with the structure proposed by Scott's group.

Are There Common Structural Features between the Catalysts?

Is there a general consensus on structural features of the active site between these titanium-on-silica oxidation catalysts? A popular belief, possibly derived from the isomorphous substitution of titanium for silica in TS-1, is that atomically dispersed $Ti(OSi\equiv)_4$ sites are responsible for the catalytic activity. Yet, this level of structural detail is not supported by the results for the catalysts as described in the preceding text.

Although there is disagreement about the contents of the second coordination sphere of the active site, there is a clear consensus about the first coordination sphere of titanium. All the active sites proposed above consist of titanium in the oxidation state +4 surrounded by a tetrahedron of oxygen atoms with a Ti-O distance of approximately 1.8 Å.

Many researchers believe that there are either three or four silicon atoms in the second coordination sphere of the active site. These structures are represented respectively as $Ti(OSi\equiv)_3OH$ and $Ti(OSi\equiv)_4$. Although he champions the "tripodal" $Ti(OSi\equiv)_3OH$ active site in his work with Ti↑MCM-41, Thomas admits that "dipodal" $Ti(OSi\equiv)_2(OH)_2$ and possibly even "tetrapodal" $Ti(OSi\equiv)_4$ may also be present (Figure 4-5).[131] However, the work of Scott and co-workers with grafted titanium on silica gel suggests that titanium may be present in the second coordination sphere.

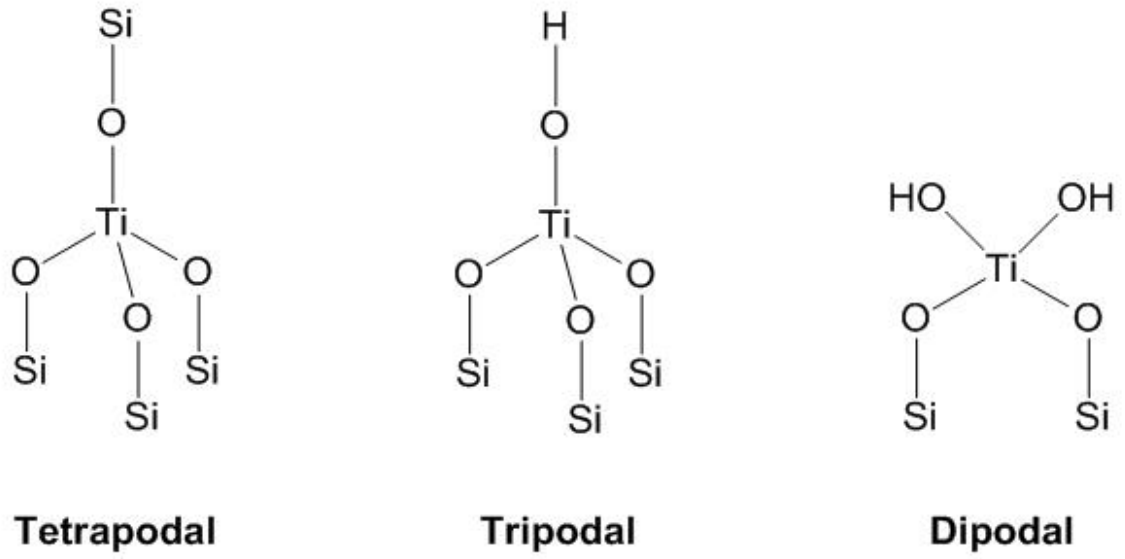

Figure 4-5. First and second coordination spheres of titanium sites described by Thomas.

The possibility of a titanium atom in the second coordination sphere is especially intriguing because it is widely believed that oligomerization of titanium species is responsible for the inactivity of homogeneous catalysts.[34,43,113] Yet, the structure of the active site that Scott proposes is a μ-oxo titanium dimer. In a single report, Yuan, et. al. argue that partially polymerized titania species are responsible for the catalytic activity of grafted Ti-MCM-41.[133] These species are similar to those proposed by Scott's group and are shown in Figure 4-6. (The reader should note that Yuan, et. al.[133] use the –podal terminology of J. M. Thomas, but apply it somewhat differently. The prefix indicates the number of silicon atoms in the second coordination sphere. Any second coordination sphere vacancies can be filled by OH or Ti.)

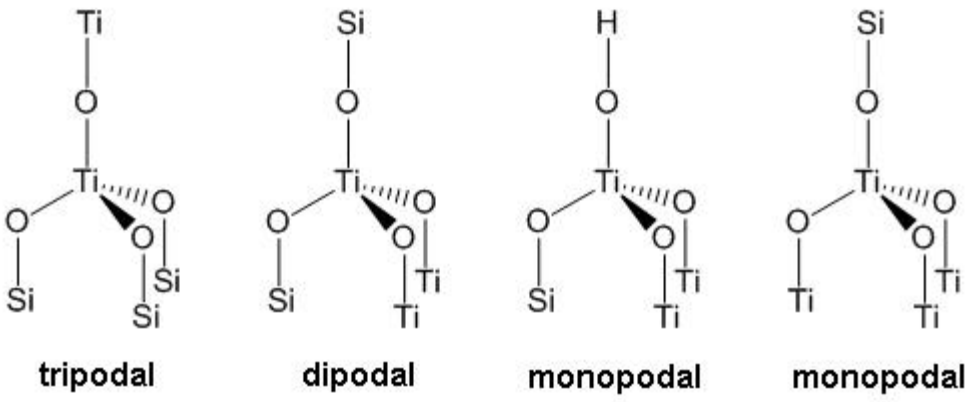

Figure 4-6. Oligomeric titanium sites proposed by Yuan, et. al.

A Challenge to the TiO_4 Active Site Structure

In a single report, Tuel and Hubert-Pfalzgraf suggest that small clusters of titanium atoms in octahedral coordination can be active catalysts for olefin epoxidation.[134] In their work they claim to graft the hexanuclear cluster $[Ti_6(\mu_3\text{-}O)_6(\mu\text{-}O_2CC_6H_4OPh)_6(OEt)_6]$ (shown in Figure 4-7), hereafter Ti_6 cluster, to the walls of SBA-15 (a mesoporous silica support). Following calcination, the material was found to be active in the epoxidation of cyclohexene with TBHP. Unfortunately, little structural characterization of the Ti_6 cluster on SBA-15 material is presented.

Clearly, there is a difference of opinion about the structure of the active site in titanium-on-silica catalysts for olefin epoxidation. These differences of opinion highlight the need for synthetic methods directed at the synthesis of single site catalysts which can be used to develop a clear the relationship between structure of the active sites and catalytic activity. The work of the Tuel,

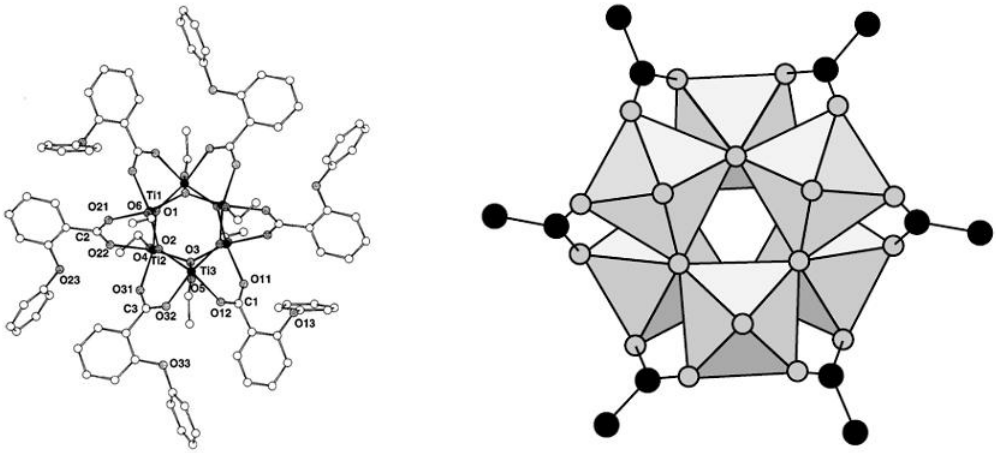

Figure 4-7. Ortep (left) and polyhedral (right) representations of the Ti-6 cluster. From Papiernik, et. al. *J. Chem. Soc., Dalton Trans.* 14, 2285-2287 (1998). – *Reproduced by permission of The Royal Society of Chemistry.*

Scott, and Mayoral groups provides evidence that the formation of μ-oxo bonds between titanium atoms may not be detrimental to activity in olefin epoxidation. It is known that bulk TiO_2 is detrimental to olefin epoxidations when hydrogen peroxide is used as the oxidant because it is an efficient catalyst for the decomposition of H_2O_2.[41] Perhaps, the key factor to the success of the Tuel, Scott, and Mayoral groups is that no TiO_2 particles large enough to display properties of bulk TiO_2 are produced using their synthetic methods.

Titanium non-aqueous building block (NABB) materials are well-suited for examining the relationship between the structure of the active site and its activity in olefin epoxidation. As shown in the third chapter of this work a series of Ti NABB materials containing Ti in a tetrahedral state with an oxidation number of positive four and four oxygen atoms in first coordination sphere have been

prepared. The difference between the materials is the average number of silicon atoms in the second coordination sphere. Furthermore, the Ti-4 material is a structurally well-characterized catalyst that contains only $Ti(OSi\equiv)_4$ sites and is a excellent material for examining the popular notion that $Ti(OSi\equiv)_4$ sites are the active sites in olefin epoxidation catalysts. Later in this chapter, a titanium NABB material that is proposed to contain a dimeric titanium site will be described. Before testing for a structure-activity relationship it important to examine issues encountered when comparing literature reports of catalytic activity to one another and the activity that will be reported for Ti NABB materials herein.

Comparing Ti(IV) on silica epoxidation catalysts

One of the difficulties encountered when comparing catalysts from various publications, especially between research groups, is the wide variety of catalyst preparations and reaction conditions that are often used. Catalyst pre-treatment procedures are not universal, and some pre-treatments such as calcination or reduction can alter the properties of a material significantly. A variety of choices are available for substrates and oxidants in epoxidation reactions. Likewise the choice of solvent, substrate-to-oxidant ratio, and temperature can impact the activity and selectivity observed in a reaction. When taken together the amount of variability between catalyst preparation and reaction conditions in the literature can make “apples to apples” comparisons of catalysts difficult.

In my opinion, the **best comparisons** between published catalyst results are made between reports with reactions that use the same substrate and

oxidants. Solvent choice does not necessarily have to be the same, although one should note if a protic solvent is used. As mentioned above, alcohols and water inhibit many heterogeneous epoxidation catalysts. Thus, comparisons between reports for a given set up substrates are best made if the solvents are either the same or aprotic. Substrate-to-oxidant ratio, reaction temperature, and duration should all be reported when comparing published catalyst results. Knowledge of these parameters allows the reader to assess if differences between catalysts can be explained by different reaction conditions or inherently different activities. For example, the use of different reaction temperatures might explain a difference in the rate or reaction reported for two catalysts.

In this work we will compare reports where cyclohexene was used as the substrate and TBHP was used as the oxidant. This reaction was chosen because data for it are often reported in the literature on heterogeneous epoxidation catalysts.

Prior to examining results for catalysts synthesized by the non-aqueous building block method, let us examine the results reported in the literature for some titanium on silica catalysts in the epoxidation of cyclohexene with TBHP as shown in Table 4-1. Cyclohexene (Cyc) conversion is given as percent converted of the theoretical maximum as shown in the equation below. In all cases, but one, the number of moles cyclohexene theoretically convertible

$$\text{Cyc conversion (\%)} = ([\text{Cyc}]_{\text{theoretical}} - [\text{Cyc}]_{\text{converted}})/[\text{Cyc}]_{\text{theoretical}} \times 100$$

Table 4-1. Selected results from the literature for the titanium-on-silica catalyzed epoxidation of cyclohexene with TBHP.

	Catalyst	Reported Structure	Ti Content (Wt. %)	Temp. (°C)	Cyc.:Ox.	Cyc. TON	Time (h)	Cyc. TOF[a]	Cyc. Conv. (%)	Epox. Sel. (%)
1	Ti→MCM-41[122]	$Ti(OSi)_4$	0.10	70	4:1	527	7	75	35	<28%
2	Ti→MCM-41[122]	$Ti(OSi)_4$	1.12	70	4:1	86	7	12	65	28%
3	Ti↑MCM-41[96]	$(SiO)_3TiOSiPh_3$	1.08	50	20:1	42	0.25	168	13	>95
4	Ti↑MCM-41[96]	$(SiO)_3TiOH$	1.08	50	20:1	48	0.25	192	14	>95
5	Ti↑MCM-41[27]	$(SiO)_3TiOH$	6.76	50	1:1.2	86	1	86	50	95
6	Ti→MCM-41[106]	$Ti(OSi)_4$	1.02	60	4:1	74	5	15	14	93
7	Ti/SiO_2[25]	$[\equiv SiOTi(O^iPr)_2]_2O$	0.20	50	1:1	980	16	62	98	100
8	Ti/SiO_2[124]	NR	5.64	25	1:1	9	1	35	87	98
9	Ti/SiO_2[124]	NR	5.64	15	2:1	35	7	9	57	98
10	Shell Ti/SiO_2[115]	NR	2.00	90	1:1	75	18	4	75	88

a) h^{-1}

to the epoxide is equal to the number of moles TBHP in the reaction. Epoxide selectivity is defined as the number of moles cyclohexene oxide (Cyc-ox) produced per mole cyclohexene converted. The turnover number, TON, is defined as the moles of

$$\text{Epoxide Selectivity (\%)} = [\text{Cyc-ox}]/[\text{Cyc}]_{\text{converted}} \times 100$$

cyclohexene converted per mole of titanium in the reaction. The turnover frequency, TOF, is defined as the turnover number divided by the reaction time in hours (h). TOF is a measurement of catalyst activity per unit time, it can be quite deceiving

$$\text{TON} = [\text{Cyc}]_{\text{converted}}/[\text{Ti}]$$

$$\text{TOF} = [\text{Cyc}]_{\text{converted}}/([\text{Ti}] \times \text{h})$$

as it can mask the fact that the activity of a catalyst can vary with time. For example, the Ti↑MCM-41 sample in the fifth entry in Table 4-1 shows a TOF of 86 h^{-1}. However, the reaction period over which the TOF is measured is rather short (one hour). Careful reading of the original report reveals that the catalyst deactivated after 90 minutes.[27] The reaction times for the preceding Ti↑MCM-41 entries are even shorter at 0.25 h. No explicit mention of deactivation is mentioned in this report, but given the short reaction times continued deactivation after 90 minutes would not be surprising.[96] At the same time, Ti↑MCM-41 is frequently cited in the literature as an excellent epoxidation catalyst.

The second entry in Table 4-1 Ti→MCM-41 shows a reasonable conversion of 65% but, the selectivity is poor. The selectivities of other entries

are high, but their conversions are generally low. Perhaps the best catalyst in the table is that of Scott and co-workers given in the seventh entry. The TOF and TON are reasonable, and the conversion and selectivity are both high. Indeed, that catalyst seems to slightly outperform the Shell catalyst in terms of conversion and selectivity.

Titanium Non-aqueous Building Block Epoxidation Catalysts

General Synthetic Method for Mononuclear Titanium Epoxidation Catalysts

The catalysts studied in this thesis were prepared in a manner similar to that described in the third chapter of this work. A typical reaction began with 8.00 g of $Si_8O_{20}(Sn^nBu_3)_8$ (butyltin cube). Following heating of the butyltin cube at 80 °C *in vacuo* for 18 hours to remove all water, 100 mL of hexanes was vapor transferred into the reaction vessel containing the butyl tin cube. Then magnetic stirring was started and an amount of $TiCl_4$ appropriate for the type of site desired (as determined in Chapter 3 and shown in Table 4-2) was added to the reaction vessel via vapor transfer at a temperature of -78 °C. The reaction was then allowed to warm to room temperature while being stirred and proceed for two hours. A yellow flocculant solid formed within minutes of removing the reaction vessel from the -78 °C bath.

After two hours had passed, the bis(pyridine) complex of silicon tetrachloride, $SiCl_4 \cdot py_2$, was added to the reaction vessel under a $N_2(g)$ purge. The number of moles added to the reaction was equal to the initial number of moles of tri-*n*-butyltin groups in the starting material less the number of moles of

Table 4-2. Stoichiometry used to prepared titanium non-aqueous building block catalysts.

Sample	$TiCl_4$:butyltin cube	$SiCl_4 \cdot py_2$:butyltin cube
Ti-4	0.25	7.75
Ti-3	1.0	7.0
Ti-2	2.0	6.0

$TiCl_4$ added. The reaction was allowed to proceed for 18 hours at room temperature.

Immediately following the addition of $SiCl_4 \cdot py_2$, both the yellow flocculant solid that had formed earlier and dense, white particles of $SiCl_4 \cdot py_2$ were visible in the reaction mixture. Over the course of 8 to 12 hours the amount of $SiCl_4 \cdot py_2$ particles visible diminished, and the amount of flocculant material increased while the color of the flocculant material changed from yellow to a white or light beige. At the end of the reaction a significant amount of the light beige flocculant material and clumpy, dense particles of $SiCl_4 \cdot py_2$ were visible.

Volatile liquids were then removed *in vacuo*. Excess $SiCl_4 \cdot py_2$ was removed using vacuum sublimation. Dry methanol or water was added to the solid product in the reaction vessel. The product was then collected on a fritted funnel, and washed until the pH of the filtrate (measured at the funnel stem) returned to the normal pH for that solvent. Presumably, this indicates that all chloride groups on the product have been converted to hydroxyl or methoxy

groups. The catalysts were activated by heating to 140 °C *in vacuo* for 12 hours prior to use.

The sample nomenclature remains the same as that used in the third chapter of this work. The only change in the structure of the active sites of the catalysts is presumed to be the exchange of chloride ligands on the titanium sites for hydroxide or methoxide ligands.

The final catalysts contain TiO_4 centers surrounded by Si_8O_{20} building blocks. The number of building blocks around the Ti site depends upon the stoichiometric ratio of $TiCl_4$ to butyltin cube used in the synthesis. The building blocks are further linked together by silicon atoms that have either hydroxy or methoxy groups attached depending upon the post synthesis treatment. In general terms, the catalyst consists of atomically dispersed TiO_4 in a silica building block matrix. The surface of the building block matrix is relatively hydrophilic if the material was treated water. The surface of the building block materials treated with methanol are less hydrophilic than those treated with water.

Synthetic Method for Dimeric Titanium Epoxidation Catalyst

The sample of the non-aqueous building block material containing the titanium dimer was prepared by Richard Mayes. The dimer, $[TiCl_2O_2C_5H_8]_2$ was prepared from the reaction of $TiCl_4$ and *cis*-1,2-cyclopentanediol in the method of Bachand and Wuest.[135] The proposed structure for the dimer is given in Figure 4-8 below.

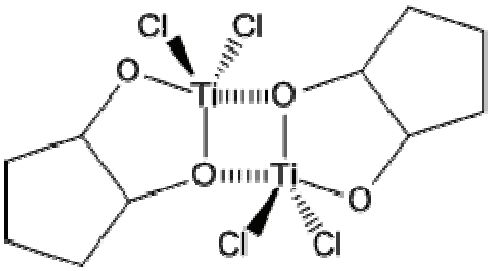

Figure 4-8. Structure of the titanium dimer, $[TiCl_2O_2C_5H_8]_2$.

Methyltin cube, $Si_8O_{20}(SnMe_3)_8$ was placed in a Schlenk vessel and dehydrated *in vacuo*. The dimer was added to the Schlenk vessel in a molar ratio of 0.53 dimer per methyltin cube. Dry toluene was then added to reaction vessel via vapor transfer at -78 °C to start the reaction. The reaction was heated to 80 °C and allowed to progress for 48 hours. After 48 hours had elapsed the reaction was cooled so that dichlorodimethylsilane, $SiMe_2Cl_2$, could be added to the reaction via vapor transfer. The molar ratio was 1.1 $SiMe_2Cl_2$ per mole of methyltin tin cube. The reaction was again heated to 80 °C and allowed to progress for 24 hours. After 24 hours volatiles were removed *in vacuo*, and the resulting solid was treated with an excess of trimethylchlorosilane, $ClSiMe_3$, in order to remove any residual trimethyltin groups.

Gravimetric analysis reveals that an average of 3.6 chlorides per dimer molecule reacted with the methyltin groups on the Si_8O_{20} cores. Thus, the active site in the resultant product is expected to consist mainly of dimers with a total of four Si_8O_{20} cores connected. However, structural characterization of the material

using EXAFS has not yet been completed. The sample is referred to as Ti-dimer catalyst.

Ti-dimer catalysts contain $[TiO_2C_5H_8]_2$ sites surrounded by Si_8O_{20} building blocks. The building blocks are further linked together by $SiMe_2$ groups, and un-reacted tin sites were removed using $ClSiMe_3$. The surface of the pristine catalyst is hydrophobic as the surface functionality consists of $=SiMe_2$ and $–SiMe_3$ groups. The surface of the calcined catalyst is hydrophilic and consists of Si-OH groups.

Figure 4-9 shows a schematic of the site and surface differences between the Ti-X (X = integer) series and the pristine Ti-dimer catalyst.

Catalytic Epoxidation Reaction Conditions

Cyclohexene (Aldrich, 99%), cyclohexene oxide (Aldrich, 98%), and mesitylene (Acros, 99%) were used as received. A solution of *tert*-butylhydroperoxide (TBHP) in toluene was made from a solution of 70% TBHP in water (Acros) using the method of Sharpless.[112] The concentration of the solution of TBHP in toluene was determined by iodometric titration.[136] A detailed procedure for iodometric titration is given in the appendix.

The epoxidation of cyclohexene using TBHP has been performed under batch-type conditions using glass vials sealed with Teflon® coated rubber septa. Vials were loaded with 18 mmol of cyclohexene (1.48 g), 16 mmol of TBHP (4.05 g of a 35.8% TBHP solution in toluene), 4.5 mmol of mesitylene (0.53 g, internal standard), and 40 mg of catalyst. The reaction was allowed to run for six hours

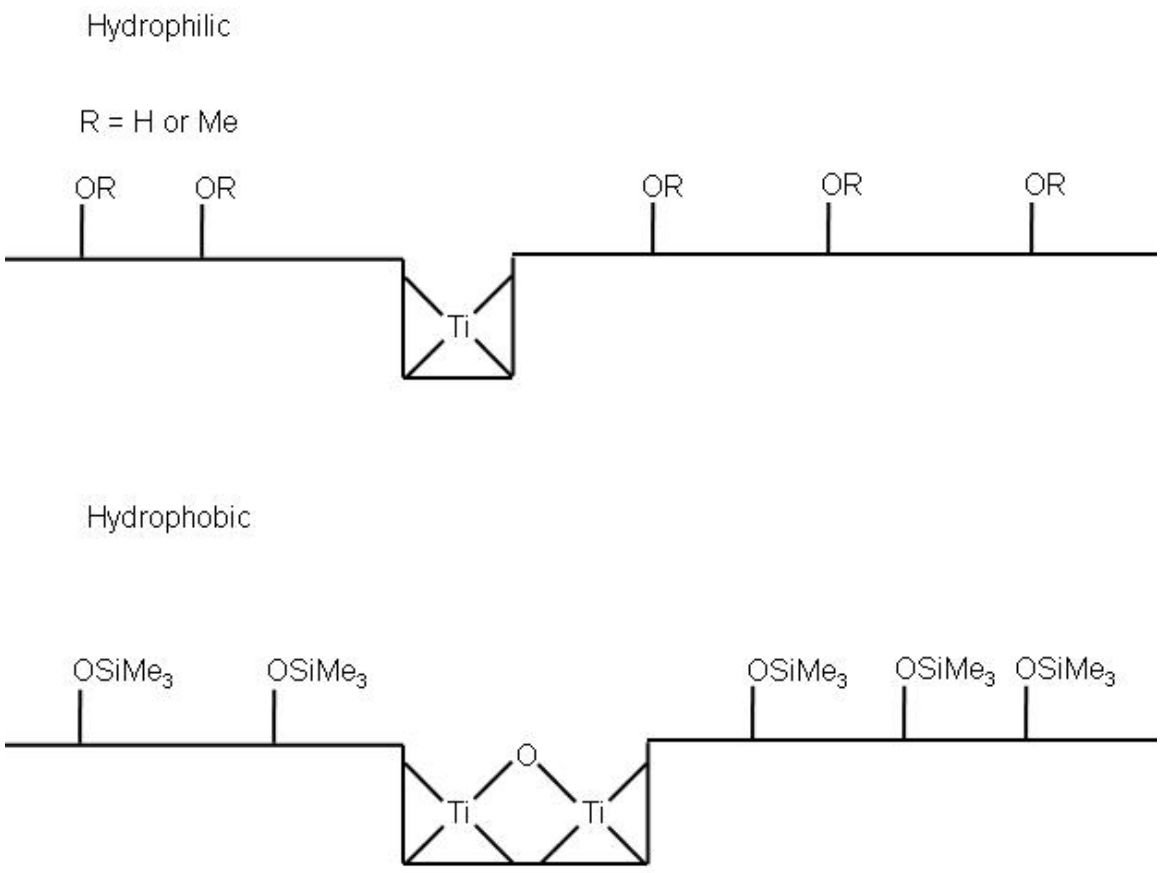

Figure 4-9. Schematic representations of the Ti-X series catalysts (top) and the Ti-dimer catalyst (bottom).

at 60 °C. A 0.1 mL aliquot was removed from the reaction vial using a syringe and diluted to 10 mL with ether.

A Hewlett Packard 5890A series gas chromatograph equipped with a standard 30 m (5% Phenyl)-95% methylpolysiloxane column and a flame ionization detector was used to quantify the amounts of cyclohexene and cyclohexene oxide in the aliquot. Helium (Ultra-high purity, Airgas) was used as the carrier gas. Response factors relative to mesitylene were determined to be: cyclohexene, 1.6; cyclohexene oxide 0.95. By-products of the reaction were identified using an Agilent 6890 series gas chromatograph equipped with a mass selective detector.

The results presented are an average of the results from three separate trials. The results of the individual trials for a given catalyst sample did not differ within experimental error from one another.

A blank run in which no catalyst was used showed cyclohexene conversion of two percent. The products of the blank reaction indicate that a free-radical reaction also occurs under the reaction conditions.[137] The amount of free-radical reaction products are not observed to increase when catalyst is present. The amount of cyclohexene consumed by the free-radical process is small, and the amount of epoxide produced by this process is within experimental reproducibility for non-radical epoxide formation. Thus, the effects of the free-radical process are not accounted for in the calculations of activity and selectivity.

Discussion of Results

Non-aqueous building block catalyst results

The catalysts produced by the non-aqueous building block method herein were found to be active in olefin epoxidation with a solution of TBHP in toluene. However, the catalysts were inactive when aqueous hydrogen peroxide was used as the oxidant. Preliminary results from extended reactions show that the mononuclear catalysts are sill active after 24 hours of continuous use under reaction conditions.

Several trends are apparent from the results of the catalytic epoxidation reactions presented in Table 4-3. First, for the mononuclear catalysts, the TON decreases with the connectivity of the titanium center. In other words the TON of the catalysts decreases as the number of silicon atoms in the second coordination sphere of titanium decreases. A second trend in the data for the mononuclear catalysts is that catalysts treated with methanol have higher activities than those treated with water. Similarly, the methanol treated catalysts are also more selective than their water treated counterparts. The greater activity of the methanol treated catalysts may due to the slightly more hydrophobic nature of these catalysts compared to those treated with water. The increased hydrophobicity reduces competitive coordination of the co-product alcohol and any water that may be present in the reaction mixture. The lower selectivity of the water treated catalysts can be explained by the Brønsted

Table 4-3. Results for the epoxidation of cyclohexene with TBHP in toluene using titanium non-aqueous building block catalysts.

Catalyst	Reported Structure	Ti Content (Wt. %)	Treatment	Cyc. Conv. (%) ± 5	Epox. Sel. (%)	Cyc. TON	Cyc. TOF
Blank	N/A	0.00	N/A	2[a]	27 ± 7	N/A	N/A
Ti-4	$Ti(OSi\equiv)_4$	0.90 ± .01	MeOH	52	44 ± 6	1114 ± 100	186 ± 17
Ti-4	$Ti(OSi\equiv)_4$	0.90 ± .01	H_2O	45	37 ± 5	885 ± 90	147 ± 15
Ti-3	$Ti(OSi\equiv)_3OMe$	3.45 ± .02	MeOH	44	37 ± 5	310 ± 40	52 ± 7
Ti-3	$Ti(OSi\equiv)_3OH$	3.45 ± .02	H_2O	31	27 ± 5	179 ± 30	30 ± 5
Ti-2	$Ti(OSi\equiv)_2(OMe)_2$	6.08 ± .02	MeOH	58	47 ± 6	153 ± 15	25 ± 2
Ti-2	$Ti(OSi\equiv)_2(OH)_2$	6.08 ± .02	H_2O	23	22 ± 5	97 ± 20	16 ± 3
Ti-dimer	$[TiO_2C_5H_8]_2Cl_{0.4}(OSi\equiv)_{3.6}$	5.18 ± .05	None	71	48 ± 4	246 ± 20	41 ± 3
Ti-dimer	Unknown	6.09 ± .05	550 °C	16	6 ± 2	46 ± 15	8 ± 2
Reference[124]	NR	3.85 ± .02	N/A	71	44 ± 4	244 ± 20	41 ± 3

a) ± 0.5

acidity of the hydroxyl groups on the catalyst. Hydroxyl groups can convert the epoxide to a diol through a ring-opening reaction.

Despite, the thorough characterization of the NABB series of catalysts, only the structure of the Ti-4 catalyst is known with a high degree of certainty. The possibility that the Ti-3 and Ti-2 materials, whose active sites were determined *on average* to be $Ti(OSi\equiv)_3OR$ and $Ti(OSi\equiv)_2OR_2$ (R = H, Me), contain $Ti(OSi\equiv)_4$ sites along with sites of lower connectivity cannot be excluded. Therefore, the observed activity *could possibly* be due to $Ti(OSi\equiv)_4$ sites in the material.

Quantitative ^1H NMR results indicate that $Ti(OSi\equiv)_4$ sites are formed with exclusivity up to about a one weight percent loading of titanium in the NABB catalysts. To examine the *possibility* that the activity of the Ti-3 and Ti-2 catalysts might be due to the presence of $Ti(OSi\equiv)_4$ sites, new TONs for the Ti-3 and Ti-2 samples were calculated. These calculations assume that the catalysts contain one weight percent titanium as $Ti(OSi\equiv)_4$ and that only $Ti(OSi\equiv)_4$ are active catalytic sites for olefin epoxidation. Using those assumptions, the TONs would be 1070 and 931 for the Ti-3 and Ti-2 catalysts respectively. Those TONs approach the TON of 1114 reported for the Ti-4 catalyst. These calculations show that the *possibility* that $Ti(OSi\equiv)_4$ sites are responsible for the activity observed in the Ti-3 and Ti-2 catalysts cannot be eliminated.

The turnover number for the pristine Ti-dimer material is 246. This is close to the level of the Ti-3 catalyst, but much lower than the TON of the Ti-4

catalyst. Readers should remember that the TON is calculated using the total amount of titanium in the material. If we normalize the TON to the number of sites, the TON doubles to 492. The 48% epoxide selectivity of the Ti-dimer catalyst is slightly better than the 44% selectivity of the Ti-4 catalyst. The high selectivity compared to that of the other NABB catalysts may be due to the lack of protons on the surface of the pristine Ti-dimer.

Calcination of the Ti-dimer material prior to use as a catalyst adversely effects the properties of the catalyst. The TON for the calcined Ti-dimer is less than 20% of the pristine material, and the selectivity for the epoxide falls to 6%. The structure of the sites in the calcined Ti-dimer have not been studied, but it is clear that calcination either destroys the majority of the active sites or prevents reagents from accessing them.

Comparison of non-aqueous building block catalysts with the literature

Table 4-4 collects results from some of the best non-aqueous building block epoxidation catalysts compared with some of the best epoxidation catalysts reported in the literature. The catalysts are ranked from first to eighth by turnover frequency. The eighth ranked catalyst is the heterogeneous Shell titanium-on-silica epoxidation catalyst which is a convenient point of reference. The Shell catalyst, which was commercialized, converts 75% of the cyclohexene in the reaction with 88% selectivity to the epoxide with a TOF of 4 h^{-1}. The high selectivity towards the epoxide allowed the catalyst to be commercialized despite it's low TOF.

Table 4-4. Selected literature and titanium non-aqueous building block epoxidation catalysts ranked by turnover frequency.

Rank	Catalyst	Reported Structure	Ti Content (Wt. %)	Temp. (°C)	Cyc:Ox	Time (h)	TOF	TON	Cyc. Conv. (%)	Epox. Sel. (%)
1	Ti↑MCM-41[96]	$(SiO)_3TiOH$	1.08	50	20:1	0.25	192	48	14	>95
2	Ti-4	$Ti(OSi)_4$	0.90	60	1.1:1	6	186	1114	52	44
3	Ti→MCM-41[122]	$Ti(OSi)_4$	0.10	70	4:1	7	75	527	35	<28
4	Ti/SiO_2[25]	$[\equiv SiOTi(O^iPr)_2]_2O$	0.20	50	1:1	16	62	980	98	100
5	Ti-3	$Ti(OSi)_3OMe$	3.45	60	1.1:1	6	52	310	44	47
6	Ti-dimer		5.18	60	1.1:1	6	41	246	71	48
7	Ti-2	$Ti(OSi)_2(OMe)_2$	6.08	60	1.1:1	6	25	153	58	47
8	Shell Ti/SiO_2[114]	NR	2.00	90	1:1	18	4	75	75	88

The first ranked catalyst, Ti↑MCM-41, has a selectivity of greater than 95% and a TOF of 192 h^{-1} which are both superior to the Shell catalyst. However, Ti↑MCM-41 deactivates following 90 minutes of use. The Ti-4 catalyst has a TOF of 186 h^{-1} which is comparable to Ti↑MCM-41, but Ti-4 still shows catalytic activity after 24 hours of use. The TOF and selectivity of Ti-4 are approximately twice that of the third ranked catalyst Ti→MCM-41.

The activity of Ti-4 is far superior to that of the original heterogeneous epoxidation catalyst developed by Shell. However, the selectivity of Ti-4 is half of the Shell catalyst. The catalyst fourth in terms of TOF has the highest selectivity for the epoxidation of cyclohexene with TBHP. This is the catalyst developed by Scott's group that is proposed to have dimeric titanium sites. The Scott catalyst has a TOF of 62 h^{-1}, converts nearly all the cyclohexene in the reaction after 16 hours, and exclusively forms the epoxide.

The selectivity of the non-aqueous building block catalysts are generally lower than those of the other catalysts presented in Table 4-4. The selecitivity of the NABB catalysts is better than the 28% selectivity given in one of the initial reports for Ti→MCM-41 as shown in the table, and it is important to remember that Ti NABB catalysts are in their first generation. Based upon the literature, it seems likely that fine-tuning the reaction conditions and parts of the structural hierarchy of the catalyst beyond the active site (see the first chapter of this work) should improve selectivity. It will be important to eliminate the free-radical process seen under the current reaction conditions in order to assure that the

presence of free-radicals does not negatively impact epoxide selectivity. Likewise, fine-tuning the surface properties of the catalysts by treating the surface of the catalysts with chlorotrimethylsilane or other silylating agents may result in increasing selectivity and activity of the Ti NABB epoxidation catalysts.

Conclusion

This work conclusively shows that isolated $Ti(OSi\equiv)_4$ sites in non-aqueous building block catalysts are highly active for the epoxidation of cyclohexene with *tert*-butylthydroperoxide in toluene. The structural characterization of the Ti-4 catalyst (third chapter of this work) shows evidence for the sole presence of isolated $Ti(OSi\equiv)_4$ through quantitative ^1H NMR, FT-IR, XANES, and EXAFS. Raman and XAS data indicate that the Ti-4 catalyst is free of TiO_2 domains.

The epoxidation TOF and TON figures of merit for methanol treated Ti-4 are both high. The activity of and selectivity of the titanium non-aqueous building block catalysts decrease as the connectivity of the titanium falls. These findings lend credence to literature reports that isolated $Ti(OSi\equiv)_4$ sites are responsible for the epoxidation activity of TS-1 and Ti→MCM-41 catalysts. The activity and selectivity of theTi-dimer catalyst suggest that di-nuclear titanium sites are also active for the epoxidation of cyclohexene with TBHP in toluene.

The Ti-4 and Ti-dimer materials both warrant further investigation for use as catalysts in olefin epoxidation. Despite their different proposed structures and the greater TON of Ti-4, both Ti-4 and the Ti-dimer are similar in selectivity for the epoxide. Further study of the structure of the active site in the Ti-dimer

material, and fine-tuning of the pore-structure and surface properties of both materials should help elucidate differences in the activity and selectivity of these two materials. The following chapter contains specific ideas for future research using the non-aqueous building block methods.

Chapter 5. Conclusions and Future Work

Conclusions

One of the fundamental challenges of heterogeneous catalysis is establishing a well-defined relationship between the structure of active sites in a catalyst and their activity. Understanding the structure-activity relationship should allow the synthesis of "next generation" catalysts with improved activities and selectivities. The first chapter of this work described traditional methods for the synthesis of heterogeneous catalysts. These traditional methods of synthesis often yield materials that have multiple types of active sites. Such materials can make the development of the relationship between the structure of a catalytically active site and its activity in a reaction very difficult. This had led to the development of synthetic methods designed specifically to produce single-site catalysts which can then be used to study structure-activity relationships.

The non-aqueous building block (NABB) method is one method being developed which is targeted at producing nanostructured single-site catalysts. When coupled with the *sequential additions* process explained in the first chapter of this work, the non-aqueous building block method should give rise to a series of catalysts each containing a unique and well-defined active site. This series of materials can then be studied to examine the impact of structural changes at the active site on the activity and selectivity of the catalyst. In this work the non-aqueous building block method was used to synthesize a series of titanium-on-silica catalysts that were used to study the effect of active site structure upon the

activity of the epoxidation of cyclohexene in toluene with *tert*-butylhydroperoxide (TBHP).

These titanium non-aqueous building block materials were synthesized from butyltin cube, $Si_8O_{20}(Sn^nBu_3)_8$. The butyltin cube was developed as an alternative to the methyltin cube used in much of the previous research developing the non-aqueous building block method. The butyltin cube is an important part of the non-aqueous building block method as the costs and toxicity of the reagents used in the synthesis of butyltin cube are lower than those for the reagents used in the synthesis of the methyltin cube. The synthesis of the butyltin cube and comparisons with the reagents used to synthesize the methyltin cube are found in the second chapter of this work.

In the third chapter of this work, the structure of the active site of each titanium-on-silica material synthesized using the non-aqueous building block method was characterized using quantitative ^{1}H NMR, infrared, Raman, XANES, and EXAFS. The results from those methods of characterization indicate that three materials with active sites of different average connectivity were prepared from the reaction of titanium tetrachloride with butyltin cube. Furthermore, the methods of structural characterization used indicate that the Ti-4 non-aqueous building block material is a single-site catalyst containing only atomically dispersed $Ti(OSi\equiv)_4$ active sites.

The catalytic activity for the epoxidation of cyclohexene with TBHP in toluene was measured for the three unique single-site catalysts synthesized from

the butyltin cube and a dimeric catalyst synthesized by Richard Mayes using the methyltin cube. The results of the batch-type epoxidation reactions show that the structure of the titanium center in the non-aqueous building block materials does affect the catalytic activity. The Ti-4 and Ti-dimer materials, which have high connectivities to the building block framework of the material, had the highest selectivity for the epoxide. The TOF and TON figures of merit are also high enough to warrant the further investigation of these materials, to see if the selectivity and activity of the materials can be improved. The Ti-3 and Ti-2 materials which have lower connectivities were not as active as the Ti-4 material and generally had low selectivity for the epoxide.

Future Work

Non-aqueous building block method in general

A large parameter space with respect to the non-aqueous building block method remains to be examined. There are many transition metal and main group elements of interest that could potentially be used in the non-aqueous building block method. To date only Si, Ti, V, and Al linking groups have been studied by the Barnes group. The linking chemistry of Cr, Sn, and W reagents are currently being studied, but many other metals have yet to be investigated.

In the future it may be desirable to substitute another functional group for the trialkyl tin functional groups on the methyltin and butyltin cubes. There are several reasons to do this. First, all trialkyl tin reagents are toxic to some degree. The use of a non-toxic substitute would eliminate exposure hazards and

potentially lead to lower waste disposal costs. Second, the use of functional groups other than trialkyl tin groups may improve the atom economy of the non-aqueous building block process. In the method currently used to produce methyl or butyltin cube, one-half of the trialkyl tin groups are converted to trialkyl tin hydride by-product as shown in Equation 1. Essentially, one-half of the trialkyl tin groups are converted to waste in the production of the trialkyl tin cubes essential to the non-aqueous building block method. Although procedures for recycling the trialkyl tin hydride by-product have been developed,[57] the use of a halide or alkoxy functionality on the Si_8O_{12} building block could lead to substantial gains in atom economy depending upon the method used to place those groups on the building block. In subsequent reactions of the trialkyl tin cube with a metal halide, shown schematically in Equation 2, the by-product is a chlorotrialkyl tin. While $ClSnMe_3$ can be converted to $O(SnMe_3)_2$ using bench top procedures by the Barnes group,[57] no such procedures are in place for $ClSn^nBu_3$. Finally, all trialkyl tin groups must be removed from a non-aqueous building block material in order to insure that the material is a single-site catalyst. Substitution of the trialkyl tin functionality for a catalytically inert functional group will obviate the procedures needed to ensure complete removal of trialkyl tin groups from the material.

$$Si_8O_{12}H_8 + 8\ O(SnR_3)_2 \rightarrow Si_8O_{20}(SnR_3)_8 + 8\ HSnR_3 \quad (1)$$

$$Si_8O_{20}(SnR_3)_8 + 8\ ClSiMe_3 \rightarrow Si_8O_{20}(SiMe_3)_8 + 8\ ClSnR_3 \quad (2)$$

Whatever functional group is chosen to replace the trialkyl tin group in the non-aqueous building block process, it is important to maintain the complimentary “A + B” functional group scheme. The “A + B” functional scheme is important in preventing the formation of metal oxide domains that so often plagues hydrothermal and sol-gel syntheses.

As mentioned is the first chapter, control of the structural morphology of catalysts is also important. While the Si_8O_{20} building block was picked with the thought that materials prepared from it using the non-aqueous building block method would have high surface areas, little work has been done with regard to controlling the pore structure of NABB materials. I conducted some experiments using block copolymers in a manner similar to that used by Kriesel and Tilley.[138] The initial trials were not successful, and the block copolymers that are most readily available are terminated with hydroxyl groups which are not compatible with the non-aqueous building block method used herein. A wide variety of surfactants are available for use as structure directing agents, and the use of these in the NABB method should be investigated.

Titanium non-aqueous building block materials

Future work for the titanium non-aqueous building block materials should include examining the use of reagents with blocking groups to prepare materials with titanium centers that have connectivities less than four. For example, titanocene dichloride could potentially be used to prepare a NABB material where the connectivity of the titanium centers in the material is two. The challenge

associated with the use of blocking groups may be finding routes to remove the blocking groups from the titanium center without changing the connectivity of the center.

The use of titanium clusters should also continue to be examined. An open question in the literature is what nuclearity is required at active catalyst sites. While it is widely believed that mononuclear sites are the only sites active for epoxidation reactions, the results for the Ti-dimer catalyst and the Ti_6 cluster of Tuel[134] suggest that this may not be the case. The inclusion of well-defined polynuclear clusters in non-aqueous building block studies may help clarify the answer to this important issue in catalysis.

Finally, the catalytic utility of titanium non-aqueous building block materials in other reactions should be explored. Transesterification is a reaction that should be explored. Clark performed some preliminary studies of transesterification activity using titanium NABB materials synthesized from the methyltin cube.[59] Given the importance of transesterification to the synthesis of biodiesel[139], the activity of titanium NABB materials in such reactions should definitely be explored.

Closing Remarks

The synthesis of single-site heterogeneous catalysts with nanostructured active sites is a fundamental challenge in the field of catalysis. The development of synthetic methods capable of producing such catalysts is important to allow

the study of structure-activity relationships. If scalable, those synthetic methods may be used to synthesize the next generation of catalysts used by industry.

This work is one part of a larger study of the non-aqueous building block method for the synthesis of nanostructured single-site heterogeneous catalysts. The whole body of work on the non-aqueous building block method is directed at showing that the method is broadly applicable to an array of catalytically interesting transition metal and main group elements, and that it is useful for making active and selective heterogeneous catalysts that can be used in industrially relevant chemical reactions.

This work has shown that titanium materials can be successfully synthesized using the non-aqueous building block method. These first generation titanium non-aqueous building block materials were used to study the structure-activity relationship of the titanium center in the epoxidation of cyclohexene with toluene. The results of these experiments have highlighted issues that deserve further study. Further success with other non-aqueous building block studies will allow this method to contribute to the body of fundamental knowledge regarding the effect of active site structure upon the activity of heterogeneous catalysts.

References

(1) Lu, Z.; Lindner, E.; Mayer, H. A. *Chem. Rev.* **2002**, *102*, 3543-3578.

(2) Armor, J. N. www.nacatsoc.org/who.asp

(3) Armor, J. N. *Applied Catalysis, A: General* **2001**, *222*, 407-426.

(4) Jenkinson, D. S. *Plant and Soil* **2001**, *228*, 3-15.

(5) Smith, B. E. *Science* **2002**, *297*, 1654.

(6) Laidler, K. J.; Meiser, J. H. *Physical Chemistry*; 3rd ed.; Houghton Mifflin Company: Boston, 1999.

(7) Arends, I. W. C. E. *Angewandte Chemie, International Edition* **2006**, *45*, 6250-6252.

(8) Li, C.; Zhang, H.; Jiang, D.; Yang, Q. *Chemical Communications (Cambridge, United Kingdom)* **2007**, 547-558.

(9) Beck, C.; Mallat, T.; Baiker, A. *New Journal of Chemistry* **2003**, *27*, 1284-1289.

(10) De Vos, D. E.; Sels, B. F.; Jacobs, P. A. *Advanced Synthesis & Catalysis* **2003**, *345*, 457-473.

(11) Armor, J. N. *Applied Catalysis, A: General* **2005**, *282*, 1-4.

(12) Somorjai, G. A.; McCrea, K. R.; Zhu, J. *Topics in Catalysis* **2002**, *18*, 157-166.

(13) Neurock, M. *Journal of Catalysis* **2003**, *216*, 73-88.

(14) Gladysz, J. A. *Chem. Rev.* **2002**, *102*, 3215-3216.

(15) Dupont, J.; de Souza, R. F.; Suarez, P. A. Z. *Chem. Rev.* **2002**, *102*, 3667-3692.

(16) Mason, A. F.; Coates, G. W. In *Macromolecular Engineering: Precise Synthesis, Materials Properties, Applications*; Matyjaszewski, K. G., Y.; Leibler, L., Ed.; Wiley-VCH: Weinheim, 2007.

(17) McKnight, A. L.; Waymouth, R. M. *Chemical Reviews* **1998**, *98*, 2587-2598.

(18) Song, C. E.; Lee, S. g. *Chem. Rev.* **2002**, *102*, 3495-3524.

(19) Fan, Q. H.; Li, Y. M.; Chan, A. S. C. *Chem. Rev.* **2002**, *102*, 3385-3466.

(20) Leadbeater, N. E.; Marco, M. *Chem. Rev.* **2002**, *102*, 3217-3274.

(21) Cole-Hamilton, D. J.; Tooze, R. P. In *Catalyst Separation, Recovery, and Recycling: Chemistry and Process Design*; Cole-Hamilton, D. J., Tooze, R. P., Eds.; Springer: The Netherlands, 2006; Vol. 30.

(22) Bryant, D. R. In *Catalyst Separation, Recovery, and Recycling: Chemistry and Process Design*; Cole-Hamilton, D. J., Tooze, R. P., Eds.; Springer: The Netherlands, 2006; Vol. 30.

(23) McNamara, C. A.; Dixon, M. J.; Bradley, M. *Chem. Rev.* **2002**, *102*, 3275-3300.

(24) Kakkar, A. K. *Chem. Rev.* **2002**, *102*, 3579-3588.

(25) Sensarma, S.; Bouh, A. O.; Scott, S. L.; Alper, H. *Journal of Molecular Catalysis A: Chemical* **2003**, *203*, 145-152.

(26) Turunen, J. P. J.; Pakkanen, T. T. *Journal of Applied Polymer Science* **2006**, *100*, 4632-4635.

(27) Maschmeyer, T.; Rey, F.; Sankar, G.; Thomas, J. M. *Nature (London)* **1995**, *378*, 159-62.

(28) Brown, G. E.; Henrich, V. E.; Casey, W. H.; Clark, D. L.; Eggleston, C.; Felmy, A.; Goodman, D. W.; Gratzel, M.; Maciel, G.; McCarthy, M. I.; Nealson, K. H.; Sverjensky, D. A.; Toney, M. F.; Zachara, J. M. *Chemical Reviews* **1999**, *99*, 77-174.

(29) Coperet, C.; Chabanas, M.; Saint-Arroman, R. P.; Basset, J.-M. *Angewandte Chemie, International Edition* **2003**, *42*, 156-181.

(30) Thomas, J. M.; Sankar, G. *Accounts of Chemical Research* **2001**, *34*, 571-581.

(31) Sankar, G.; Thomas, J. M.; Richard, C.; Catlow, A. *Topics in Catalysis* **2000**, *10*, 255-264.

(32) Rice, G. L.; Scott, S. L. *Langmuir* **1997**, *13*, 1545-1551.

(33) Deguns, E. W.; Taha, Z.; Meitzner, G. D.; Scott, S. L. *Journal of Physical Chemistry B* **2005**, *109*, 5005-5011.

(34) Bouh, A. O.; Rice, G. L.; Scott, S. L. *Journal of the American Chemical Society* **1999**, *121*, 7201-7210.

(35) Rocha, J.; Anderson, M. W. *European Journal of Inorganic Chemistry* **2000**, 801-818.

(36) Davis, M. E.; Lobo, R. F. *Chemistry of Materials* **1992**, *4*, 756-68.

(37) Rimer, J. D.; Fedeyko, J. M.; Vlachos, D. G.; Lobo, R. F. *Chemistry--A European Journal* **2006**, *12*, 2926-2934.

(38) Corma, A. *Chemical Reviews (Washington, D. C.)* **1997**, *97*, 2373-2419.

(39) Burton, A. W.; Zones, S. I.; Elomari, S. *Current Opinion in Colloid & Interface Science* **2005**, *10*, 211-219.

(40) Hartmann, M.; Kevan, L. *Research on Chemical Intermediates* **2002**, *28*, 625-695.

(41) Bordiga, S.; Damin, A.; Bonino, F.; Lamberti, C. *Topics in Organometallic Chemistry* **2005**, *16*, 37-68.

(42) Hartmann, M. *Angewandte Chemie, International Edition* **2004**, *43*, 5880-5882.

(43) Sheldon, R. A.; van Vliet, M. C. A. In *Fine Chemicals through Heterogeneous Catalysis*; Sheldon, R. A., Van Bekkum, H., Eds.; Wiley-VCH Verlag GmbH: Weinheim, Germany, 2001.

(44) Xiao, F.-S. *Topics in Catalysis* **2005**, *35*, 9-24.

(45) Livage, J. *Catalysis Today* **1998**, *41*, 3-19.

(46) Crayston, J. A. In *Fundamentals: Ligands, Complexes, Synthesis, Purification, and Structure*; Lever, A. B. P., Ed.; Elsevier Ltd.: Oxford, UK, 2004; Vol. 1.

(47) Schubert, U. In *From the Molecular to the Nanoscale: Synthesis, Structure, and Properties*; Fujita, M., Powell, A., Creutz, C. A., Eds.; Elsevier Ltd.: Oxford, U.K., 2004; Vol. 7.

(48) Wright, J. D.; Sommerdijk, N. A. J. M. *Sol-Gel Materials: Chemistry and Applications*; Gordon and Breach Science Publishers, 2001.

(49) Corriu, R.; Leclercq, D.; Lefevre, P.; Mutin, P. H.; Vioux, A. *Chemistry of Materials* **1992**, *4*, 961-3.

(50) Corriu, R. J. P.; Leclercq, D.; Lefevre, P.; Mutin, P. H.; Vioux, A. *Journal of Materials Chemistry* **1992**, *2*, 673-4.

(51) Lafond, V.; Mutin, P. H.; Vioux, A. *Chemistry of Materials* **2004**, *16*, 5380-5386.

(52) Brevett, C. S.; Cagle, P. C.; Klemperer, W. G.; Millar, D. M.; Ruben, G. C. *Journal of Inorganic and Organometallic Polymers* **1991**, *1*, 335-42.

(53) Acosta, S.; Corriu, R.; Leclercq, D.; Mutin, P. H.; Vioux, A. *Journal of Sol-Gel Science and Technology* **1994**, *2*, 25-8.

(54) Feher, F. J.; Weller, K. J. *Inorganic Chemistry* **1991**, *30*, 880-2.

(55) Feher, F. J.; Weller, K. J. *Chemistry of Materials* **1994**, *6*, 7-9.

(56) Clark, J. C.; Barnes, C. E. *Chemistry of Materials* **2007**, *19*, 3212-3218.

(57) Lee, M.-Y. Ph.D., University of Tennessee, 2007.

(58) Ghosh, N. N.; Clark, J. C.; Eldridge, G. T.; Barnes, C. E. *Chemical Communications (Cambridge, United Kingdom)* **2004**, 856-857.

(59) Clark, J. C. Ph.D., University of Tennessee, 2005.

(60) Clark, J. C.; Saengkerdsub, S.; Eldridge, G. T.; Campana, C.; Barnes, C. E. *Journal of Organometallic Chemistry* **2006**, *691*, 3213-3222.

(61) Saengkerdsub, S. Ph.D., University of Tennessee, 2002.

(62) *Metal Organics for Material & Polymer Technology, Supplement to the Gelest General Catalog: Silicon, Germanium & Tin Compounds, Metal*

Alkoxides Diketonates and Carboxylates; Arkles, B., Ed.; Gelest, Inc., 2001.

(63) Domazetis, G.; Magee, R. J.; James, B. D. *Journal of Organometallic Chemistry* **1978**, *148*, 339-53.

(64) Al-Allaf, T. A. K. *Journal of Organometallic Chemistry* **1986**, *306*, 337-46.

(65) Kuivila, H. G.; Considine, J. L.; Mynott, R. J.; Sarma, R. H. *Journal of Organometallic Chemistry* **1973**, *55*, C11-C14.

(66) Mitchell, T. N. *Journal of Organometallic Chemistry* **1973**, *59*, 189-97.

(67) Kriegsmann, H.; Hoffmann, H.; Geissler, H. *Zeitschrift fuer Anorganische und Allgemeine Chemie* **1965**, *341*, 24-35.

(68) Bornhauser, P.; Calzaferri, G. *Spectrochimica Acta, Part A: Molecular and Biomolecular Spectroscopy* **1990**, *46A*, 1045-56.

(69) Harrison, P. G.; Hall, C. *Main Group Metal Chemistry* **1997**, *20*, 515-529.

(70) Ribeiro do Carmo, D.; Dias Filho, N. L.; Stradiotto, N. R. *Materials Research (Sao Carlos, Brazil)* **2004**, *7*, 499-504.

(71) Marcolli, C.; Calzaferri, G. *Journal of Physical Chemistry B* **1997**, *101*, 4925-4933.

(72) Elliott, S. R. *Journal of Non-Crystalline Solids* **1990**, *123*, 149-64.

(73) Haw, J. F.; Nicholas, J. B.; Xu, T.; Beck, L. W.; Ferguson, D. B. *Accounts of Chemical Research* **1996**, *29*, 259-267.

(74) Busca, G. *Catalysis Today* **1996**, *27*, 323-52.

(75) Ricchiardi, G.; Damin, A.; Bordiga, S.; Lamberti, C.; Spano, G.; Rivetti, F.; Zecchina, A. *Journal of the American Chemical Society* **2001**, *123*, 11409-11419.

(76) Newville, M. *Journal of Synchrotron Radiation* **2001**, *8*, 322-324.

(77) Ravel, B.; Newville, M. *Journal of Synchrotron Radiation* **2005**, *12*, 537-541.

(78) Maniara, G.; Rajamoorthi, K.; Rajan, S.; Stockton, G. W. *Analytical Chemistry* **1998**, *70*, 4921-4928.

(79) Padro, D.; Howes, A. P.; Smith, M. E.; Dupree, R. *Solid State Nuclear Magnetic Resonance* **2000**, *15*, 231-236.

(80) Piper, T. S.; Rochow, E. G. *Journal of the American Chemical Society* **1954**, *76*, 4318-20.

(81) Astorino, E.; Peri, J. b.; Willey, R. J.; Busca, G. *Journal of Catalysis* **1995**, *157*, 482-500.

(82) Alba, M. D.; Luan, Z.; Klinowski, J. *Journal of Physical Chemistry* **1996**, *100*, 2178-82.

(83) Sinclair, P. E.; Sankar, G.; Catlow, C. R. A.; Thomas, J. M.; Maschmeyer, T. *Journal of Physical Chemistry B* **1997**, *101*, 4232-4237.

(84) Li, C.; Xiong, G.; Xin, Q.; Liu, J.-K.; Ying, P.-L.; Feng, Z.-C.; Li, J.; Yang, W.-B.; Wang, Y.-Z.; Wang, G.-R.; Liu, X.-Y.; Lin, M.; Wang, X.-Q.; Min, E.-Z. *Angewandte Chemie, International Edition* **1999**, *38*, 2220-2222.

(85) Soult, A. S.; Poore, D. D.; Mayo, E. I.; Stiegman, A. E. *Journal of Physical Chemistry B* **2001**, *105*, 2687-2693.

(86) Schrijnemakers, K.; Cool, P.; Vansant, E. F. *Journal of Physical Chemistry B* **2002**, *106*, 6248-6250.

(87) Arnal, P.; Corriu, R. J. P.; Leclercq, D.; Mutin, P. H.; Vioux, A. *Journal of Materials Chemistry* **1996**, *6*, 1925-1932.

(88) Zhang, J.; Li, M.; Feng, Z.; Chen, J.; Li, C. *Journal of Physical Chemistry B* **2006**, *110*, 927-935.

(89) Fujiwara, M.; Wessel, H.; Park, H. S.; Roesky, H. W. *Chemistry of Materials* **2002**, *14*, 4975-4981.

(90) Blasco, T.; Camblor, M. A.; Corma, A.; Esteve, P.; Guil, J. M.; Martinez, A.; Perdigon-Melon, J. A.; Valencia, S. *Journal of Physical Chemistry B* **1998**, *102*, 75-88.

(91) Dartt, C. B.; Khouw, C. B.; Li, H. X.; Davis, M. E. *Microporous Materials* **1994**, *2*, 425-37.

(92) Deo, G.; Turek, A. M.; Wachs, I. E.; Huybrechts, D. R. C.; Jacobs, P. A. *Zeolites* **1993**, *13*, 365-73.

(93) Kodre, A.; Arcon, I.; Gomilsek, J. P. *Acta Chimica Slovenica* **2004**, *51*, 1-10.

(94) Bare, S. R. http://cars9.uchicago.edu/xafs/APS_2005/Bare_XANES.pdf January 9, 2007

(95) Newville, M. http://cars9.uchicago.edu/xafs/xas_fun/xas_fundamentals.pdf

(96) Attfield, M. P.; Sankar, G.; Thomas, J. M. *Catalysis Letters* **2000**, *70*, 155-158.

(97) Ruiz-Lopez, M. F.; Munoz-Paez, A. *Journal of Physics: Condensed Matter* **1991**, *3*, 8981-90.

(98) Farges, F.; Brown, G. E.; Rehr, J. J. *Physical Review B* **1997**, *56*, 1809.

(99) George Serena, D.; Brant, P.; Solomon Edward, I. *Journal of the American Chemical Society* **2005**, *127*, 667-74.

(100) George, S. D.; Brant, P.; Solomon Edward, I. *Journal of the American Chemical Society* **2005**, *127*, 667-74.

(101) Bair, R. A.; Goddard, W. A., III *Physical Review B: Condensed Matter and Materials Physics* **1980**, *22*, 2767-76.

(102) Shadle, S. E.; Penner-Hahn, J. E.; Schugar, H. J.; Hedman, B.; Hodgson, K. O.; Solomon, E. I. *Journal of the American Chemical Society* **1993**, *115*, 767-76.

(103) Babonneau, F.; Doeuff, S.; Leaustic, A.; Sanchez, C.; Cartier, C.; Verdaguer, M. *Inorganic Chemistry* **1988**, *27*, 3166-72.

(104) Finnie, K. S.; Luca, V.; Moran, P. D.; Bartlett, J. R.; Woolfrey, J. L. *Journal of Materials Chemistry* **2000**, *10*, 409-418.

(105) Stern, E. pubweb.bnl.gov/users/frenkel/www/BNLworkshop2001/Stern/stern.html

(106) Blasco, T.; Corma, A.; Navarro, M. T.; Perez Pariente, J. *Journal of Catalysis* **1995**, *156*, 65-74.

(107) Gleeson, D.; Sankar, G.; Catlow, C. R. A.; Thomas, J. M.; Spano, G.; Bordiga, S.; Zecchina, A.; Lamberti, C. *Physical Chemistry Chemical Physics* **2000**, *2*, 4812-4817.

(108) Ankudinov, A. L.; Ravel, B.; Rehr, J. J.; Conradson, S. D. *Physical Review B: Condensed Matter and Materials Physics* **1998**, *58*, 7565-7576.

(109) www.epa.gov/ttn/hlthef/ethylene.html

(110) Wade, L. G. *Organic Chemsitry*; 3rd ed.; Prentice Hall, Inc., 1995.

(111) Punniyamurthy, T.; Velusamy, S.; Iqbal, J. *Chemical Reviews (Washington, DC, United States)* **2005**, *105*, 2329-2363.

(112) Sharpless, K. B.; Verhoven, T. R. *Aldrichimica Acta* **1979**, *12*, 63-74.

(113) Sheldon, R. A.; Arends, I. W. C. E.; Lempers, H. E. B. In *Supported Reagents and Catalysts in Chemistry (Royal Society Special Publication)*; Royal Society of Chemistry, 1998; Vol. 216.

(114) Sheldon, R. A. *Journal of Molecular Catalysis* **1980**, *7*, 107-26.

(115) Sheldon, R. A.; Van Doorn, J. A. *Journal of Catalysis* **1973**, *31*, 427-37.

(116) Rey, F.; Sankar, G.; Maschmeyer, T.; Thomas, J. M.; Bell, R. G. *Topics in Catalysis* **1996**, *3*, 121-134.

(117) Choi, J. S.; Kim, D. J.; Chang, S. H.; Ahn, W. S. *Applied Catalysis, A: General* **2003**, *254*, 225-237.

(118) Smet, P.; Riondato, J.; Pauwels, T.; Moens, L.; Verdonck, L. *Inorganic Chemistry Communications* **2000**, *3*, 557-562.

(119) Fraile, J. M.; Garcia, J. I.; Mayoral, J. A.; Vispe, E.; Brown, D. R.; Naderi, M. *Chemical Communications (Cambridge, United Kingdom)* **2001**, 1510-1511.

(120) Sankar, G.; Rey, F.; Thomas, J. M.; Greaves, G. N.; Corma, A.; Dobson, B. R.; Dent, A. J. *Journal of the Chemical Society, Chemical Communications* **1994**, 2279-80.

(121) Chen, L. Y.; Chuah, G. K.; Jaenicke, S. *Catalysis Letters* **1998**, *50*, 107-114.

(122) Eimer, G. A.; Casuscelli, S. G.; Ghione, G. E.; Crivello, M. E.; Herrero, E. R. *Applied Catalysis A: General* **2006**, *298*, 232-242.

(123) Bu, J.; Yun, S.-H.; Rhee, H.-K. *Korean Journal of Chemical Engineering* **2000**, *17*, 76-80.

(124) Cativiela, C.; Fraile, J. M.; Garcia, J. I.; Mayoral, J. A. *Journal of Molecular Catalysis A: Chemical* **1996**, *112*, 259-267.

(125) Fraile, J. M.; Garcia, J.; Mayoral, J. A.; Proietti, M. G.; Sanchez, M. C. *Journal of Physical Chemistry* **1996**, *100*, 19484-19488.

(126) Fraile, J. M.; Garcia, J. I.; Mayoral, J. A.; Vispe, E. *Journal of Catalysis* **2000**, *189*, 40-51.

(127) Lamberti, C.; Bordiga, S.; Zecchina, A.; Carati, A.; Fitch, A. N.; Artioli, G.; Petrini, G.; Salvalaggio, M.; Marra, G. L. *Journal of Catalysis* **1999**, *183*, 222-231.

(128) Luan, Z.; Meloni, P. A.; Czernuszewicz, R. S.; Kevan, L. *Journal of Physical Chemistry B* **1997**, *101*, 9046-9051.

(129) Chaudhari, K.; Bal, R.; Srinivas, D.; Chandwadkar, A. J.; Sivasanker, S. *Microporous and Mesoporous Materials* **2001**, *50*, 209-218.

(130) Marchese, L.; Gianotti, E.; Maschmeyer, T.; Martra, G.; Coluccia, S.; Thomas, J. M. *Nuovo Cimento della Societa Italiana di Fisica, D: Condensed Matter, Atomic, Molecular and Chemical Physics, Fluids, Plasmas, Biophysics* **1997**, *19D*, 1707-1718.

(131) Marchese, L.; Maschmeyer, T.; Gianotti, E.; Coluccia, S.; Thomas, J. M. *Journal of Physical Chemistry B* **1997**, *101*, 8836-8838.

(132) Bordiga, S.; Damin, A.; Bonino, F.; Zecchina, A.; Spano, G.; Rivetti, F.; Bolis, V.; Prestipino, C.; Lamberti, C. *Journal of Physical Chemistry B* **2002**, *106*, 9892-9905.

(133) Yuan, Q.; Hagen, A.; Roessner, F. *Applied Catalysis, A: General* **2006**, *303*, 81-87.

(134) Tuel, A.; Hubert-Pfalzgraf, L. G. *Journal of Catalysis* **2003**, *217*, 343-353.

(135) Bachand, B.; Wuest, J. D. *Organometallics* **1991**, *10*, 2015-25.

(136) Mair, R. D.; Graupner, A. J. *Anal. Chem.* **1964**, *36*, 194-204.

(137) Prasad, M. R.; Madhavi, G.; Rao, A. R.; Kulkarni, S. J.; Raghavan, K. V. *Journal of Porous Materials* **2006**, *13*, 81-94.

(138) Kriesel, J. W.; Sander, M. S.; Tilley, T. D. *Chemistry of Materials* **2001**, *13*, 3554-3563.

(139) Lopez, D. E.; Goodwin, J. G.; Bruce, D. A.; Lotero, E. *Applied Catalysis, A: General* **2005**, *295*, 97-105.

(140) Harris, D. C. *Quantitative Chemical Analysis. 4th Ed*, 1995.

Appendix

Determination of Peroxide Concentration via Iodimetric Titration

Introduction

Peroxides are used as the oxidant in the epoxidation of olefins. Due to the expense of organic peroxides used to enhance selectivity towards the epoxide product, an important consideration in determining the utility of a catalytic epoxidation reaction is the calculation of the percent of the peroxide converted to the peroxide. In order to perform this calculation one must accurately know the concentration of the peroxide solution used as the oxidant in the reaction.

The concentration of peroxides that are easily reduced can be readily determined through iodimetric titration. Such peroxides react readily with the iodide anion, I^-, to form the red-brown triiodide anion, I_3^-, under reflux conditions within five minutes (Equation 1). Triiodide then reacts with two equivalents of thiosulfate to yield iodide and render the solution colorless (Equation 2). The method given below is appropriate for use with peroxoacids, diacyl peroxides, and all hydroperoxides. This method is based largely upon the work of Mair and Graupner whose paper also includes methods for determining the concentration of peroxides that are easily reduced such as di-tert-butylperoxide.[136]

$$ROOH + 3\ I^- \leftrightarrow I_3^- + ROH + H_2O \qquad (1)$$

$$I_3^- + 2\ S_2O_3^{2-} \leftrightarrow 3\ I^- + S_4O_6^{2-} \qquad (2)$$

Preparation of Standard Sodium Thiosulfate[140]

Sodium thiosulfate, $Na_2S_2O_3$, is a widely used titrant for I_3^- and is the titrant used in this method. Thiosulfate solutions can be standardized with a fresh solution of I_3^- prepared from potassium iodate, KIO_3, and potassium iodide, KI, or a solution of I_3^- standardized with tetraarsenic hexoxide. Alternatively, one can use anhydrous $Na_2S_2O_3$, which is a suitable primary standard. Anhydrous $Na_2S_2O_3$ can be prepared from 21 g of $Na_2S_2O_3 \cdot 5H_2O$ by refluxing with 100 mL of methanol for 20 minutes. The anhydrous product is then filtered, washed with 20 mL of methanol, and dried at 70 °C for 30 minutes. This procedure is also suitable for restoring old anhydrous $Na_2S_2O_3$ to primary standard quality.

Thiosulfate solutions should be stored in the dark. The addition of 0.1 g of sodium carbonate per liter of solution maintains the pH in the optimum range for stability of the solution. If long-term storage is planned thee drops of chloroform should be added to the solution to inhibit bacterial growth.

Method of Iodimetric Titration

1. Pour 20-50 mL of an isopropanol solution that is 10% acetic acid by volume into a round bottomed flask equipped with a stir bar.
2. Add 2 g (13 mmol) of sodium iodide, NaI, and 10 mL of isopropanol to the round bottomed flask.
3. Dissolve the NaI completely with stirring.
4. Add up to 4 mmol of peroxide sample to the flask.
5. Reflux the sample for at least 5 minutes.

6. Add 5-10 mL of water.
7. Titrate with a standard $Na_2S_2O_3$ solution. Recommended concentration is between .4 and .8 M. Remember to add a few drops of 1% starch solution to enhance the remaining color as you approach the endpoint. Be aware that the reaction between the thiosulfate and triiodide is slow. I recommend waiting 30 seconds to 1 minute between additions of titrant near the end point to allow the solution time to go colorless between additions.

Vita

Geoffrey T. Eldridge was born in Valdosta, GA in February 1979. While growing up he lived in Valdosta, the Atlanta metro area, southern New Jersey, and central Texas. He attended Temple High School in Temple, TX and graduated in May 1997. Eldridge is a proud graduate of Texas Lutheran University where he studied chemistry. While at Texas Lutheran he completed a political science internship with the Alliance for Community Media in Washington, D.C., interned in the Research & Development division of Wilsonart International where he studied the application of acrylic overlays to high pressure decorative laminate, and researched phase transfer catalysis under the direction of Professor W. Preston Reeves. He graduated *cum laude* with a Bachelor of Science with a major in chemistry and minor in political science in May 2001 and was honored as the Outstanding Graduate for the College of Natural Sciences and Mathematics.

In June 2001 Eldridge enrolled in the University of Tennessee where he was the recipient of a Tennessee Advanced Materials Laboratory (TAML) Fellowship. His graduate studies were also generously funded by the Ralph Wilson Plastics Scholarship Committee. He worked under the supervision of Dr. Craig E. Barnes researching a method for the synthesis of nanostructured, single-site heterogeneous catalysts. Eldridge gained experience with the handling of air-sensitive materials, multinuclear NMR spectroscopy, gas

chromatography, and X-ray absorption spectroscopy. He completed the requirements for his Doctor of Philosophy Degree in April 2008. He currently plans to join the Naval Air Systems Command (NAVAIR) where he has been hired to serve as a chemist in the Power & Propulsion division.